## *Electron spin resonance in cadmium sulphide*

Brailsford, J.R.

# ELECTRON SPIN RESONANCE IN CADMIUM SULPHIDE

BY

J.R.BRAILSFORD B.Sc.

PRESENTED IN CANDITURE FOR THE DEGREE OF DOCTOR OF PHILOSOPHY IN THE UNIVERSITY OF DURHAM.

AUGUST 1967

## ACKNOWLEDGEMENTS

The author wishes to thank the Science Research Council for financial support during the course of this research, and Professor D.A.Wright for permitting the use of his Laboratory facilities.He is also deeply indebted to Dr. J.Woods for his excellent supervision and guidence.He would like to thank the other members of the CdS group for their assistance and interest;also Mr.D.E.Dugdale for many invaluable discussions.The assistance of the departmental workshop staff headed by Mr.F.Spence and the chief electronics technician Mr.D.Ellis in connection with the construction of the apparatus is acknowledged with gratitude.Finally he would like to acknowledge the encouragement and help of his wife Gwenda during the preparation of this thesis.

## ABSTRACT

For some time past there has been a need for a more positive identification of the nature of the defect centres which give rise to energy levels in the forbidden gap in cadmium sulphide. Electron spin resonance (e.s.r.) techniques have proved very useful in this type of investigation in other materials. Since little similar work on CdS has previously been reported, the purpose of the research described in this thesis, has been to examine the usefulness of the technique in studying CdS. Initially it was necesary to construct a sensitive x-band microwave spectrometer, which operates at temperatures down to 1.5°K and has provision for continual illumination of the samples. Electron spin resonance absorption signals have been detected in undoped single crystals of CdS which can be attributed to four different defect centres. The occurrence of the resonance signals can be correlated with the resistivities and edge luminescence spectra of the samples. This indicates that the centres responsible for the resonance absorption are important in determining the electrical and optical properties of CdS and are those which this work was initiated to study. Tentative models for the various defects have been proposed. The most important feature of the work reported in this thesis is the isolation of an e.s.r. signal which is thought to be associated with the class 2 centres which provide the photo-

conductive sensitisation and possibly act as I.R. emission centres in CdS.The model proposed for such centres is of compensated acceptor complexes with levels approximately 0.7eV above the valence band.A centre consists of four cadmium vacancies in nearest neighbour association. The models for the other three centres have not been discussed as fully as that mentioned above because of the lack of experimental data.However it is evident that e.s.r. techniques are a very valuable tool for investigating the nature of defect centres in CdS and that continuation of the work should prove invaluable in providing an unabiguous identification of the atomic structure of the defect complexes.

# INTRODUCTION

## 1) Outline of the problem

The chief problem in the development of the technology of cadmium sulphide lies in the lack of reproducibility of sample properties.This is attributed to the wide variation in the density of lattice defects from sample to sample.However at the present time the atomic natures of the defect centres is not known and until they are known control of sample properties will be very difficult to achieve.The measurements that have been carried out on CdS e.g. of thermally stimulated currents, photo-conductivity, Hall effect, luminescence etc. have been able to monitor the effects of the defects on the electrical and optical properties but have not provided an unambiguous determination of the nature of the defect centres.

## 2) Electron spin resonance as an experimental tool

The presence of defects produces an irregularity in the surroundings of the defect which may alter the pairing of the spins of the bonding electrons and thus introduce a paramagnetic character to the environment.Consequently electron spin resonance can be very useful in the study of defect centres.Resonance measurements are particularly

suitable in studying the environment of a defect in a solid and often in establishing, on an atomistic basis the role of the defect in the solid.The particular advantage of electron spin resonance is its ability to provide information concerning the nature of the defects, their symmetry and the nature of the surroundings.Moreover electron spin resonance measurements can be made on a single defect complex, even when many other types of defect centres are also present.

3) Aims of this work-

Since there was no previously reported work of this type in CdS the first aim of this work was to establish the usefulness of the electron spin resonance technique as a tool for the study of CdS.Then if this proved successful to begin a programme to investigate the nature of the defect centres in CdS.

As can be seen from the work reported in this thesis, these aims have been successfully fulfilled.

4) Layout of this thesis

As far as possible this thesis has been written in such a way as to be self contained and to provide a reference for future studies,since no report of comparable work is available at the present time.The first two chapters

give a brief review of the expected properties of ideal perfect CdS and then the experimentally observed properties with some indication of the role of defects and impurities in determining these properties, to provide an introduction to the nature of the defects in CdS.A chapter is included on the theory of electron spin resonance and one on the design and construction of the microwave spectrometer used in the work.Finally the electron spin resonance results are included with some conclusions concerning the nature of the defect centres responsible for some of the resonance lines observed.The rest of the resonance lines are attributed to isolated paramagnetic impurity ions and the results obtained on these ions are included separately.Many recommendations for future work are suggested.

# CONTENTS

# CHAPTER 1

# BAND STRUCTURE OF CADMIUM SULPHIDE

## 1-1 Band theory of semiconductors

### 1-1.1 Introduction

A knowledge of the electron energy band theory in solids is necessary for an understanding of their electrical and optical properties. Application of quantum mechanics to the motion of the electrons in the regular array of the charged ions in the solid shows that the discrete energy levels of the free ion become bands of closely spaced energy levels in the solid. A simplified treatment has been presented by several authors (see for example Ziman[1], Smith[2] and Cusack[3]) and will be outlined here.

### 1-1.2 Translational symmetry

We shall consider a crystalline solid with its atoms arranged in a lattice which is repeated regularly in all directions. Clearly this is an ideal situation. A real solid is bounded and contains imperfections which disturb the regularity of the ideal lattice. In addition we shall neglect the thermal vibrations of the atoms about their mean positions in the lattice. However the solutions obtained for the ideal lattice are fundamental to the problems of a real solid.

The existence of a regular crystal lattice is expressed

in the principle of translational symmetry, and leads to a simplification in the theory of the physical properties of a solid. The principle can be expressed by defining three vectors $a_1$ $a_2$ and $a_3$ such that the atomic structure of our ideal crystal remains invariant under translation by any vector (l) which is the sum of integral multiples of the vectors $a_1$ $a_2$ and $a_3$.

$$l = l_1 a_1 + l_2 a_2 + l_3 a_3 \qquad (1\text{-}1)$$

where $l_1$ $l_2$ and $l_3$ are integers.

The group of points generated by repeated application of the translational symmetry ~~are~~ is referred to as the space lattice. The points are the lattice sites and are defined by equation (1-1).

The translational invariance means that there must be an exactly similar arrangement of atoms about each lattice site. The simplest arrangement is when there is one atom situated at each site.

1-1.3 Periodic Functions

Any function f(r) of a solid which is determined by the symmetry of the lattice, for example, the wave function of

an electron ($\psi(r)$), must obey an equation of the form:-

$$f(r) = f(r + l) \qquad (1\text{-}2)$$

where l is a lattice translation as defined in equation (1-1). This periodic behaviour follows directly from the principle of translational symmetry.

The properties of periodic functions are easily described in one dimension. Equation 1-2 can be rewritten:-

$$f(x) = f(x + m) \qquad (1\text{-}3)$$

where $m = m_1 a$ and a is the period of the function and $m_1$ is an integer. Functions of this type can be expressed as Fourier series:-

$$f(x) = \sum A_n \exp.2\pi i n \frac{x}{a}$$

where n is an integer.

A more convenient form for our purposes is:-

$$f(x) = \sum_g A_g e^{igx} \qquad (1\text{-}4)$$

where $g = 2\pi \frac{n}{a}$ and is a real discrete function.

$$A_g = \frac{1}{a} \int_{\text{unit cell}} f(x) e^{-igx}$$

and is a periodic function.

Elementary manipulation shows that equation (1-4) is the same identity as equation (1-3) if:

$$e^{igm} = 1 \qquad (1\text{-}5)$$

for all translations m.

## 1-1.4 Bloch's Theorem

Bloch was able to show that the type of solution obtained above in equation (1-4) could be generalised to the three dimensional case. There is no simple proof of the theorem and the results will merely be quoted. Simplified proofs are available in references (1) and (2).

Bloch's theorem provides the starting point for the discussion of the motion of electrons in the three dimensional periodic potential of the ions at the lattice sites. If the ions are treated as point charges then the potential V(r) in which an electron moves in the lattice will be a periodic function with the periodicity of the lattice. For an infinite lattice as defined by equation (1-1)

$$V(r) = V(r + l_1 a_1 + l_2 a_2 + l_3 a_3) \qquad (1\text{-}6)$$

The wave functions $\psi(r)$ of the electrons in the solid are given by solutions of Schrodinger's equation, which using the potential function defined in equation (1-6) is:

$$\left(-\frac{h}{2m}\nabla^2 + V(r) - E\right)\psi(r) = 0$$

Bloch showed that the solutions for $\psi(r)$ were of the form:

$$\psi_{\underline{k}}(r) = e^{i\underline{k}r}\, U_{\underline{k}}(r) \qquad (1\text{-}7)$$

where $U_{\underline{k}}(r)$ is a periodic function of the form:

$$U_{\underline{k}}(r) = U_{\underline{k}}(r + l_1 a_1 + l_2 a_2 + l_3 a_3)$$

Equation (1-7) is clearly the generalisation to three dimensions of the one dimensional solution (1-4). These solutions are described as Bloch Waves and are in the form of plane travelling waves, modulated by the function $U_{\underline{k}}(r)$. Single waves of the form of equation (1-7) are appropriate to infinite crystals, but linear combinations

must be used to provide solutions for real crystals.

1-1.5 Brillouin Zones

The vector $\underline{K}$ is referred to as the wave vector of the Bloch wave. It is a vector defined in reciprocal lattice space. For simplicity let us consider the Bloch Wave in our one dimensional lattice, which has lattice spacing a. Then any Bloch wave which is defined by the wave vector g can be written:

$$\psi_g(x + m) = e^{igm}\psi(x) = \psi(x) \qquad \text{using equation (1-5)}$$

where $g = 2\pi\frac{n}{a}$ and is the lattice spacing in reciprocal lattice space.

Let the wave $\psi_{\underline{K}}(r)$ have the wave vector K such that

$$K = g + K'$$

K' is another reciprocal lattice vector.

Then $\psi_{\underline{K}}(x + m) = e^{iKm} \cdot \psi_{\underline{K}}(x) = e^{i(K' + g)m}\,\psi_{\underline{K}}(x)$

$= e^{iK'm}\,\psi_{\underline{K}}(x)$

i.e. The state is not uniquely defined by K, but can be

defined by any wave number in the set

$$K = 2\pi\frac{n}{a} + K' \qquad (1\text{-}8)$$

It is often convenient to choose (1K1) as small as possible and so we choose it to be in the range

$$-\frac{\pi}{a} < K \leqslant \frac{\pi}{a} \qquad (1\text{-}9)$$

The region of K- space defined by equation (1-9) is referred to as the <u>first Brillouin Zone</u> and $K = \pm\frac{\pi}{a}$ as the Zone boundaries.

The same procedure is adopted in three dimensions and the wave vector for a Bloch state is often chosen to lie in the first Brillouin Zone. This is commonly referred to as the <u>reduced Brillouin Zone scheme</u>. When the wave vector is allowed to take all the values available, as defined by equation (1-8), this is called the <u>extended Brillouin Zone scheme</u>. The first Brillouin Zone is defined by the Wigner-Seitz cell of the reciprocal lattice.

Fig. 1-1 shows the first Brillouin Zone for a rectangular two dimensional lattice and illustrates how any point in reciprocal space can be reduced to a point in the Zone.

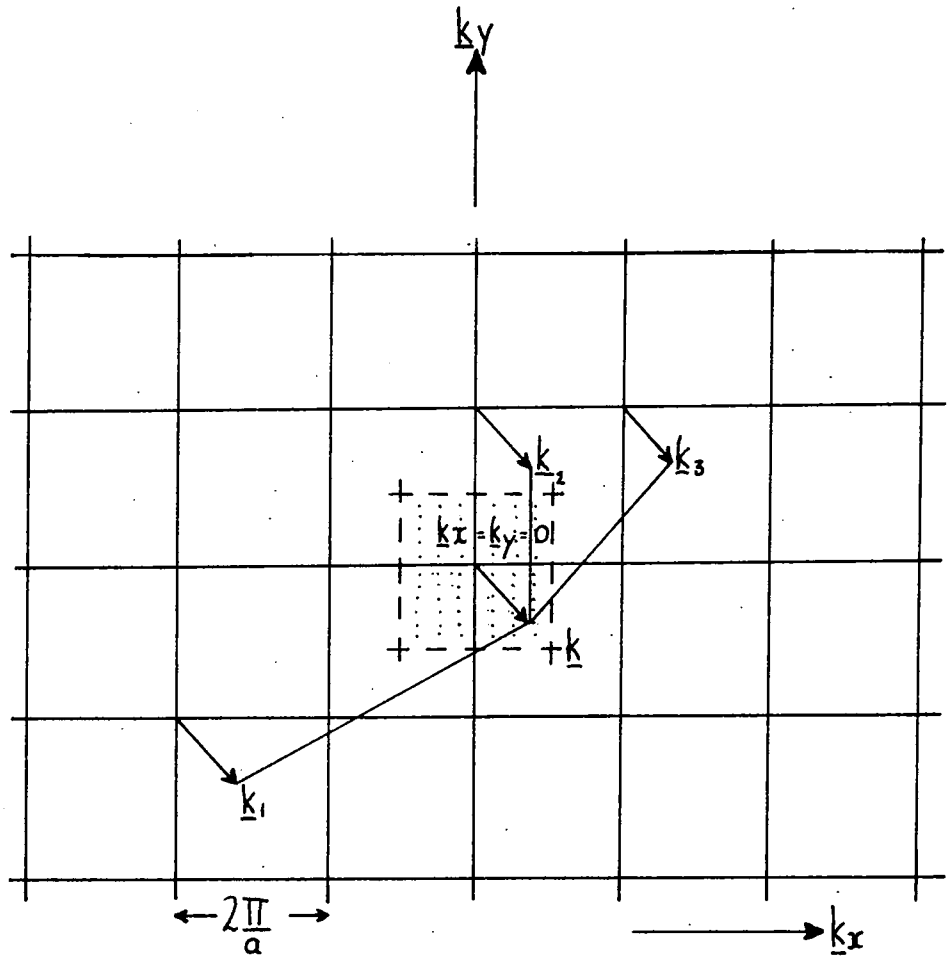


FIG.1-1. REDUCED BRILLOUIN SCHEME

The wave vectors $\underline{k}_n$ can all be reduced to $\underline{k}$ which lies in the first Brillouin Zone.

## 1-1.6 Electron states in crystals

The problem of determining the motion of all the electrons is far too complex to be solved by the methods available at present. The problem is simplified by adopting the one electron model, where the motion of a single electron only is considered in the field of all the atomic nuclei and of all the other electrons, averaged in some suitable way. The calculation now involves an estimation of the potential in which the electron moves and the solution of Schrodinger's equation for this potential function. More exact solutions are obtained by the use of a self consistent field method. With this method solutions are obtained for the initial approximation of the potential function. These solutions are fed back to calculate a correction to the original potential function. This process is repeated until self consistent solutions are obtained. This method of solution is similar to that of Hartree and Foch for determining the wave function of the electrons in an atom.

The potential in which the electron moves will have the same periodicity as the space lattice. However the potential will, in general, be a complicated function. For illustrative purposes, therefore, a simple function is

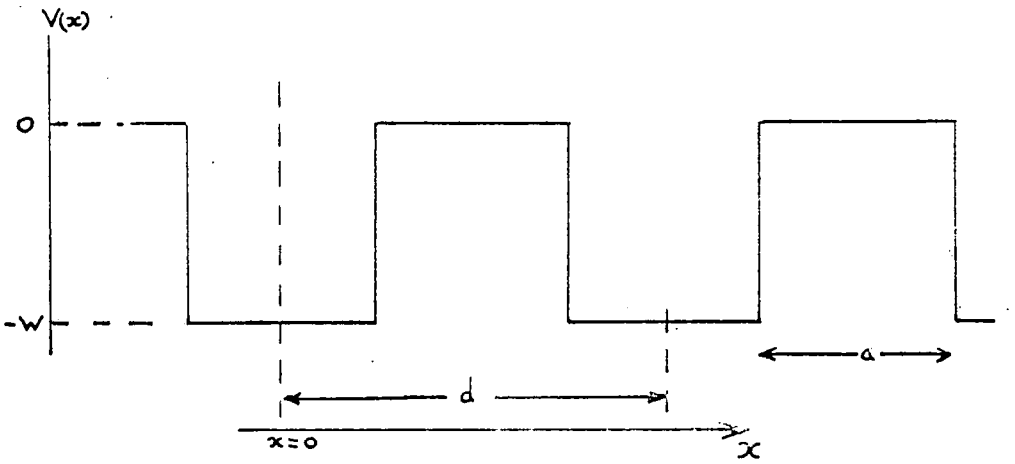


FIG.1-2 Periodic array of potential wells.

considered first. The simplest periodic potential that can be envisaged is a one dimensional array of potential wells, as shown in Fig. 1-2.

The allowed energies ($E_x$) for electrons in an isolated well of the form shown in Fig. 1-2 are:

$$E_x = \mathcal{E}_x - W$$

Where $\mathcal{E}$ are the allowed Kinetic energies for the electron. For $\mathcal{E} < W$ i.e. an electron trapped in the potential well

$$E_x = \frac{h^2}{2ma^2} N_x \text{ [illegible]} - W$$

where $N_x = 0, \pm 1, \pm 2, \ldots \ldots \ldots$

Kronig and Penney [4], by solving Schrödinger's equation for an array of such one dimensional wells, showed that each discrete level of the isolated well is broadened into a band of closely spaced levels, the number of levels per band being equal to the number of potential wells in the array. For an infinite array of wells the bands are a continuum of allowed energies for electrons, separated from each other by a band of energies which the electrons

are not allowed to occupy. In addition Kronig and Penney demonstrated that the wave function of the electrons in an allowed band was of the form required by Bloch's theorem and that electron waves could be propagated through an array of wells. Thus an individual electron can not be regarded as belonging to any single well. The width of the allowed band depends on the separation (d) of the wells if the other parameters are constant. For a large separation the bands become narrow approaching the limiting case of an isolated well. This is analogous to the behavior of the deep lying levels in atoms. The deep lying electrons are shielded from the surrounding nuclei by the outer electrons so that their energy levels are not appreciably broadened by interaction. Thus to a good approximation we may regard the deep lying electrons as having the same energies and wave functions as in an isolated atom. This provides some justification for the use of the one electron approach, where the motion of outer electrons only of the atom is considered and the inner (core) electrons are treated as being in the same configuration as in an isolated atom and are taken into account in the potential in which the outer electrons move.

In the Kronig-Penney model the treatment for small separation of the potential wells leads to the bands becoming very broad, so that the electrons can propagate very freely between the wells along a constant energy level in an allowed band. This is the analogue to the behavior of the outermost electrons in a crystal. Clearly this array of potential wells is a poor approximation to the potential which exists in a three dimensional crystal lattice. However it is a useful starting point in the calculation of the band structure of a solid. The model can be extended to compounds by considering different types of potential well for the different components. This has been attempted for the 3-5 class of semiconductors [5]. However the solutions must be treated with some caution in view of the poor approximation to the actual potential that exists. Solutions of Schrödinger's equation with a periodic potential which more closely resembles that which exists in a solid have been obtained by numerical methods. These lead to no new basic conclusions but clearly a better description of the motion of the electron is obtained.

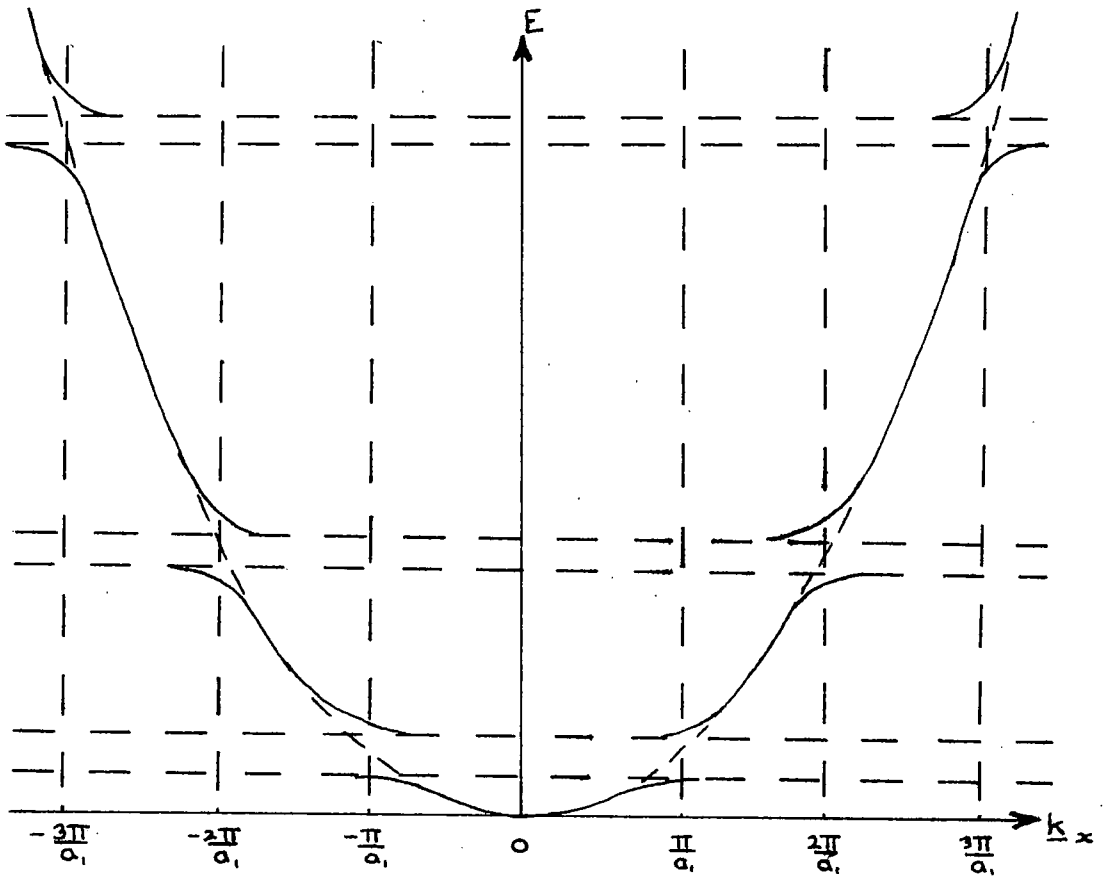


FIG.1-3. ENERGY BANDS FOR A SMALL PERIODIC POTENTIAL

The dotted curve represents the energy of free elec--trons.

The form of the energy bands in an ideal three dimensional solid is shown in Fig. 1-3. The potential is given by:

$$V(r) = Vo + v(r) \qquad (1\text{-}10)$$

Where Vo represents a constant term and v(r) is a small periodic term, which is symmetrical about $\underline{K} = 0$ and gives rise to isotropic bands.

The free electron case, indicated in Fig. 1-3, is obtained simply by putting v(r) = 0 in equation 1-10. The solution for the wave function is:

$$\psi = Ae^{i\underline{K}r}$$

where A is a constant.

These solutions are commonly referred to as Sommerfeld Waves. The solutions for the eigen states are given by:

$$E = -\frac{\hbar^2 \underline{k}^2}{2m}$$

The treatment outlined above shows that the existence of forbidden and allowed electronic energy bands is a consequence of the lattice periodicity and the principle of

translational symmetry of the lattice. More detailed calculations of the band structure can be obtained by using a better value of V(r) in equation 1-10 and taking into account the effects of electron-electron interactions. However exact solutions will only be obtained by the extension of the attempt already made to solve the many body problem. By making use of the symmetry of the space lattice, the calculations can be simplified by application of the methods of group theory.

1-1.7 Crystal Symmetry and Spin-orbit interactions

A knowledge of the symmetry of the crystal lattice of a particular solid enables simplifications to be made in the calculation of the electron band structure. These simplifications are brought about because it can be shown that the energy function of the electron in the Brillouin Zone has the full point group symmetry of the crystal, i.e. any symmetry operation which the crystal possesses is also possessed by the energy function ($E(\underline{K})$) of the band. The application of group theory allows one to make predictions concerning the nature of the wavefunction of the electrons and the shape of the energy bands, from the symmetry operations that the bands may or may not undergo.

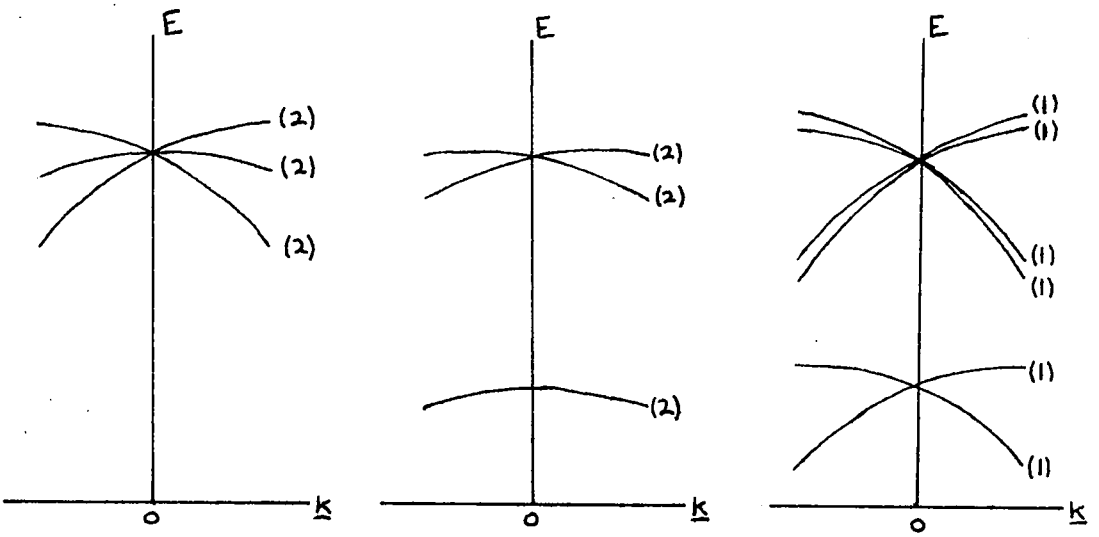


FIG.1-4. (a) (b) (c)

EFFECT OF SPIN-ORBIT INTERACTION ON A P-TYPE BAND NEAR THE CENTRE OF THE ZONE.

(a) 6 levels degenerate at centre of zone.

(b) Removal of some of the degeneracy at k=0 by spin orbit interaction, in a lattice with inversion symmetry. The states are still doubly degenerate.

(c) In the absence of inversion symmetry the twofold degeneracy is completely removed.

This knowledge is of great value in calculating the nature of the band structure, especially at points in the Brillouin Zone which have high symmetry.

The interpretation of spin-orbit interactions is also simplified by a knowledge of the symmetry of the energy function. In free atoms the spin-orbit interaction has the effect of removing the degeneracy between states with the same spatial wavefunction, but opposite electron spin. In the same way the spin-orbit interaction may remove some of the degeneracy between bands. At a general point in the Brillouin Zone, where the wavefunctions may not be degenerate, the spin-orbit interaction does not separate the states of opposite spin if the lattice has a centre of inversion. But with a lattice without a centre of inversion these states will be separated, (see Fig. 1-4). At points of high symmetry in the Brillouin Zone, the most interesting of which is usually the centre of the zone ($\underline{K} = 0$), the wave functions may be degenerate and the spin-orbit interaction may produce splittings.

Thus we can see how a knowledge of the symmetry of the lattice enables simplifications to be made in the calculations of band structure.

1-1.8 Direct gap and Indirect gap Semiconductors

Only the highest band containing electrons at $0^{o}K$ and the

lowest empty ones are important in the description of transport properties in a solid. A semiconducting solid has the highest band containing electrons completely filled at $0^{o}k$ and this is referred to as the valence band. The lowest empty band is referred to as the conduction band. The magnitude of the forbidden gap ($E_g$) separating these two bands determines the nature of the material. A material with $E_g < 2 eV$ is usually called a semiconductor and one with $E_g > 2 eV$ an insulator. Cadmium Sulphide has a forbidden gap $E_g \sim 2.5 eV$ at room temperature and is usually described as an insulator.

If the material absorbs a photon of light of energy greater than the forbidden gap then an electron can make a transition from the valence band to the conduction band. Thus accurate measurements of the absorption edge enable one to determine the position of the extrema of the band edges. When the material has an E-$\underline{K}$ relationship of the form of Fig. 1-5(a), then the electron can make the transition without co-operation of a phonon. The conservation of momentum for such a transition gives:

$$\underline{K}_{\text{initial}} = \underline{K}_{\text{final}} + \underline{K}_{L}$$

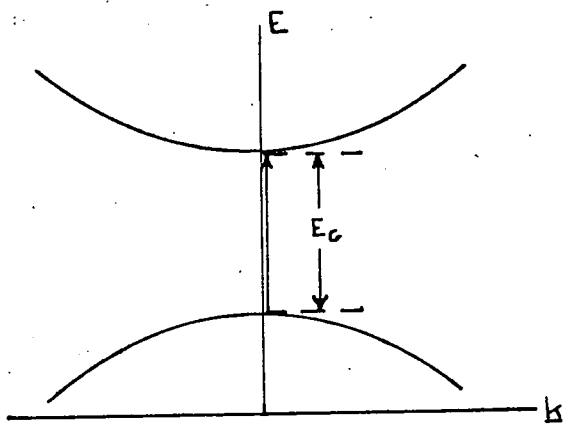


(a)

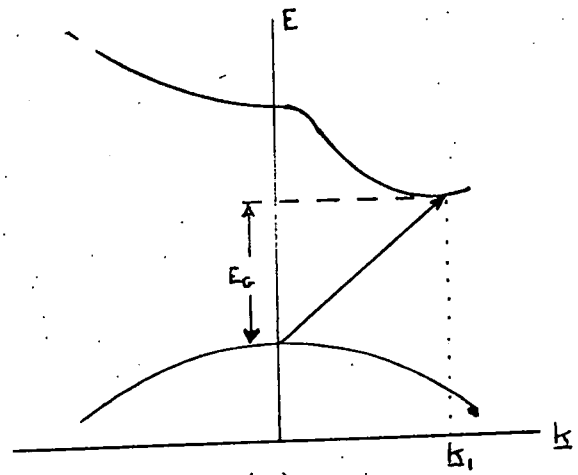


(b)

FIG.1-5.

(a) Direct gap semiconductor;direct transition indicated.

(b) Indirect gap semiconductor;indirect transition indicated.

Where $\underline{K}_L$ is the wave vector of the exciting photon. The magnitude of $\underline{K}_L$ is so small that to a good approximation:

$\underline{K}$ initial = $\underline{K}$ final

and the transition is vertical in $\underline{K}$-space. This type of semiconductor or insulator is said to have a 'direct' gap. When the E-$\underline{K}$ relationship is of the form 1-5(b), then the smallest vertical separation of the bands is larger than the minimum energy gap. It is then possible to observe optical transitions from the top of the valence band at $\underline{K}$ = 0 to the lowest valley of the conduction band at $\underline{K} = \underline{K}_1$. For conservation of momentum the co-operation of phonons is necessary. This is described as an 'indirect' gap semiconductor or insulator. The actual path of the transition may be via virtual intermediate states but energy conservation is unimportant for the virtual transitions. It is the overall energy conservation that is important. The probability of indirect transitions is much smaller than that for direct ones so that the indirect transition is in many cases detected only as a tail in the weak optical absorption on the lower energy side of the absorption edge due to the vertical transitions. Dutton[6] and Hopfield,

Thomas and Power[7] performed optical absorption measurements on Cadmium Sulphide and could not detect the presence of indirect transitions. They concluded that Cadmium Sulphide had a conduction band minimum at $\underline{K} = 0$, in agreement with the theoretical models proposed by other workers (see later), and that Cadmium Sulphide was a direct gap insulator.

1-1.9 Effective Mass

The Sommerfeld model of a free electron in a uniform potential (see section 1-1.6) gives the energy of an electron (E) as:

$$E = \frac{\hbar^2 \underline{K}^2}{2M} - W \qquad (1\text{-}11)$$

where W is the constant potential in which the electrons are supposed to move.

From equation (1-11) expressions can be obtained for the velocity ($\underline{V}$) and mass (M) of the electron:

$$\left.\begin{aligned} \underline{V} &= \hbar^{-1}\left(\frac{\partial E}{\partial \underline{K}}\right) \\ M &= \hbar^{2}\left(\frac{\partial^{2} E}{\partial \underline{K}^{2}}\right) \end{aligned}\right\} \qquad (1\text{-}12)$$

By analogy the effective mass ($M^*$) of an electron in the conduction band of a semiconductor can be defined:

$$M^* = \hbar^{2}\left(\frac{\partial^{2} E}{\partial \underline{K}^{2}}\right) \qquad (1\text{-}13)$$

In general $\frac{\partial^2 E}{\partial \underline{K}^2}$ is not constant and the value depends on the energetic position of the carrier in the band. The effective mass of a charge carrier is a function of band shape and in general is different in different regions of the band. Thus a determination of the value of effective mass of the charge carriers provides information about the shape of the bands. As we shall see later this approach has been very successful in the case of Cadmium Sulphide (see section 1-2). Cyclotron resonance at microwave frequencies provides the most direct and detailed measurement of the effective mass of charge carriers.

This technique has obvious applications to the treatment of electrons in the conduction band. However information

can be obtained about the shape of the valence bands. From Fig. 1-3 it can be seen that near the top of the band $\left(\frac{\partial^2 E}{\partial k^2}\right)$ and so $M^*$ is negative. The valence band of a semiconductor is filled at $0^o$k with electrons, and so near the top of the band there is an assembly of particles of negative mass and negative charge. Removal of one of these particles, leaves what is referred to as a 'hole', which behaves as a particle of positive mass and positive charge. Thus a 'hole' is capable of carrying electric current when an electric field is applied to the solid. The effective mass of the 'hole' will depend on its energetic position in the band and so measurement of its effective mass will provide information about the shape of the valence band.

## 1-2 Band structure of Cadmium Sulphide

The conduction band of Cadmium Sulphide originates from the 5s atomic levels of the cadmium ions and the valence band from the 3p atomic levels of the sulphur ions. A theoretical treatment of the nature of the bands began as an extension of the treatment by which knowledge of the band structure of zinc blende type materials was built up. For the zinc blende materials, Herman [8] developed a semi-empirical method to deduce their band structure from that of the diamond type materials Germanium and Silicon. A close correspondence between the band structure of the two types of material is to be expected since they have the same crystallographic lattice and in many cases are iso-electronic. This approach proved very useful [5] since the band structure of Germanium and Silicon was well understood. Since the lattices of the 2-6 Wurtzite and the Zinc blende material are closely related Birman[9] discussed the relationship of the band structure in the two classes of material. He concluded that parallel to the c-axis the electron states of the Wurtzite form may be regarded as perturbations of the Zinc blende states in the (111) direction if a small hexagonal crystal field perturbation

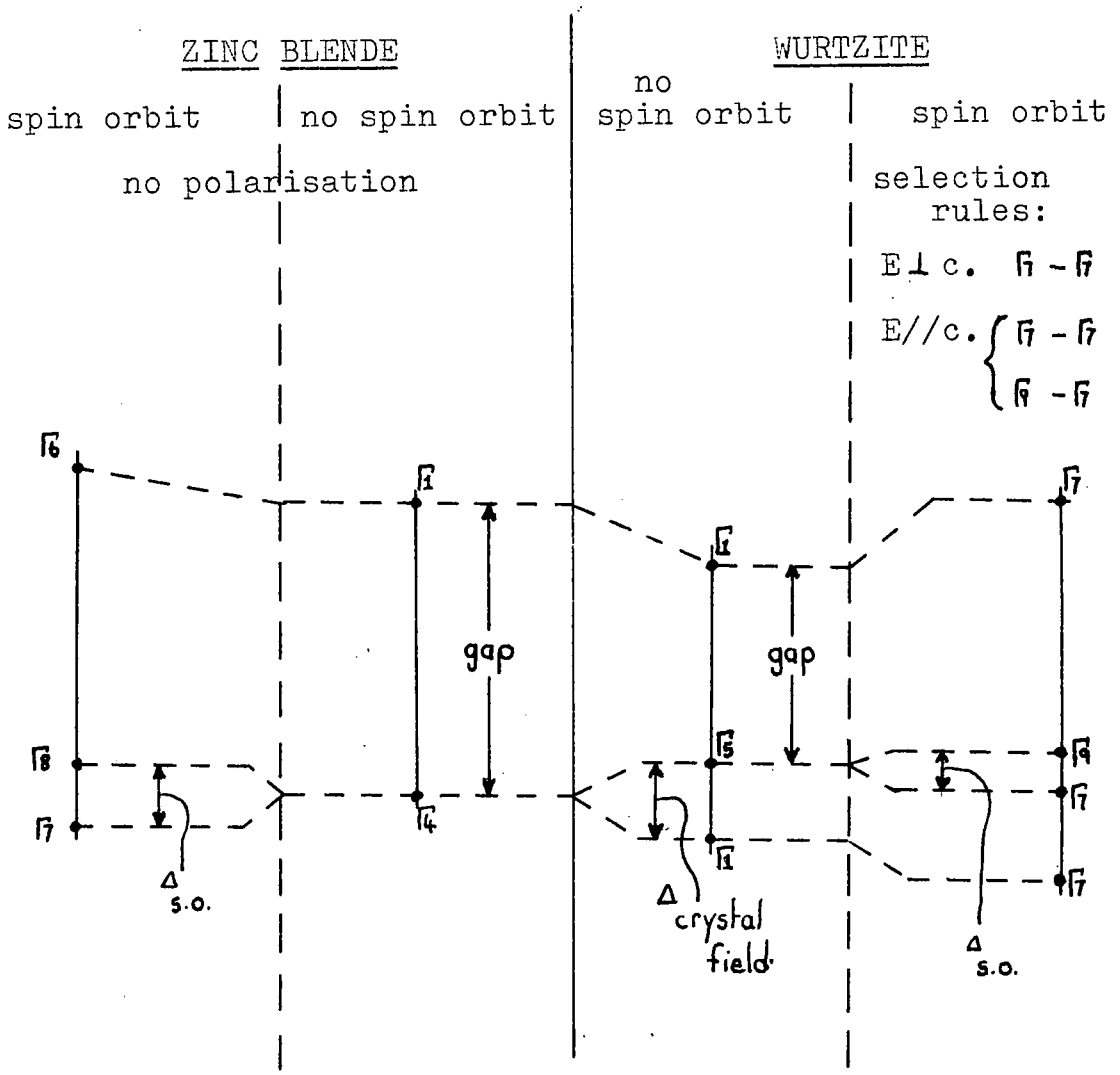


FIG.1-7. Band structure and selection rules for the Zinc blende and Wurtzite structures at k=0,0,0. The crystal field and spin orbit splittings are indicated schematically.Transitions which are allowed for the photon electric vector parallel and perpendicular to the c-axis are indicated.The selection rules are due to Dresselhaus. (13)

was added to the symmetry of the Zinc blende lattice. Subsequent work [10, 11] has shown that this approach is both valid and very useful in obtaining a detailed picture of the band structure of Wurtzite 2-6 compounds. However the earlier experimental work was directed towards a determination of the positions of the minimum of the conduction band and of the maxima of the valence band, since for most experimental conditions the carriers occupy these states. Birman[12] following the ideas of his earlier paper[9], gave a picture of the positions of the extrema of the valence and conduction bands at $\underline{K} = (0,0,0)$ which is illustrated in Fig. 1-7. Thomas and Hopfield[14] provided experimental evidence for the validity of this model in their measurements of the reflectance and luminescence spectra of hexagonal Cadmium Sulphide. They reported fine structure away from the fundamental edge which they assigned to exciton transitions. They identified three exciton series, which could be understood as arising from holes in the three valence bands at $\underline{K} = 0$ as derived by Birman (Fig. 1-7). They determined the energy splittings of the valence bands (see Fig. 1-8) (the values are in agreement with later measurements). Also they were able to verify the symmetry assignments of Birman by measurements with polarised light.

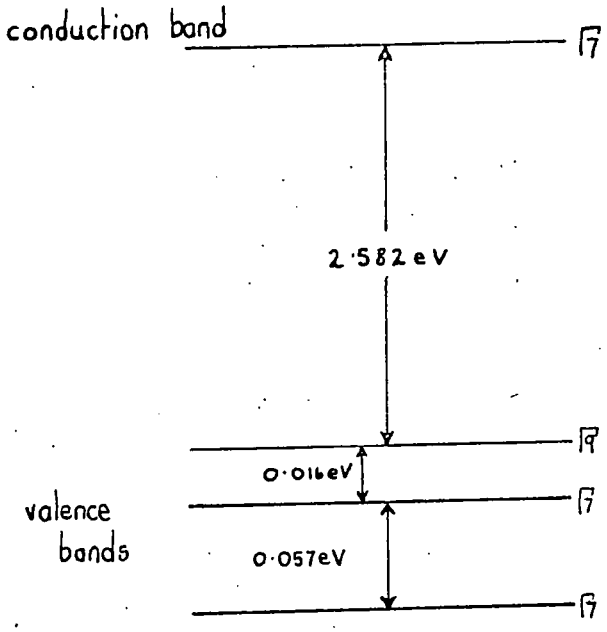


FIG.1-8. Energy bands for CdS at k=0,0,0, at 4.2°K as determined by Thomas and Hopfield[14].

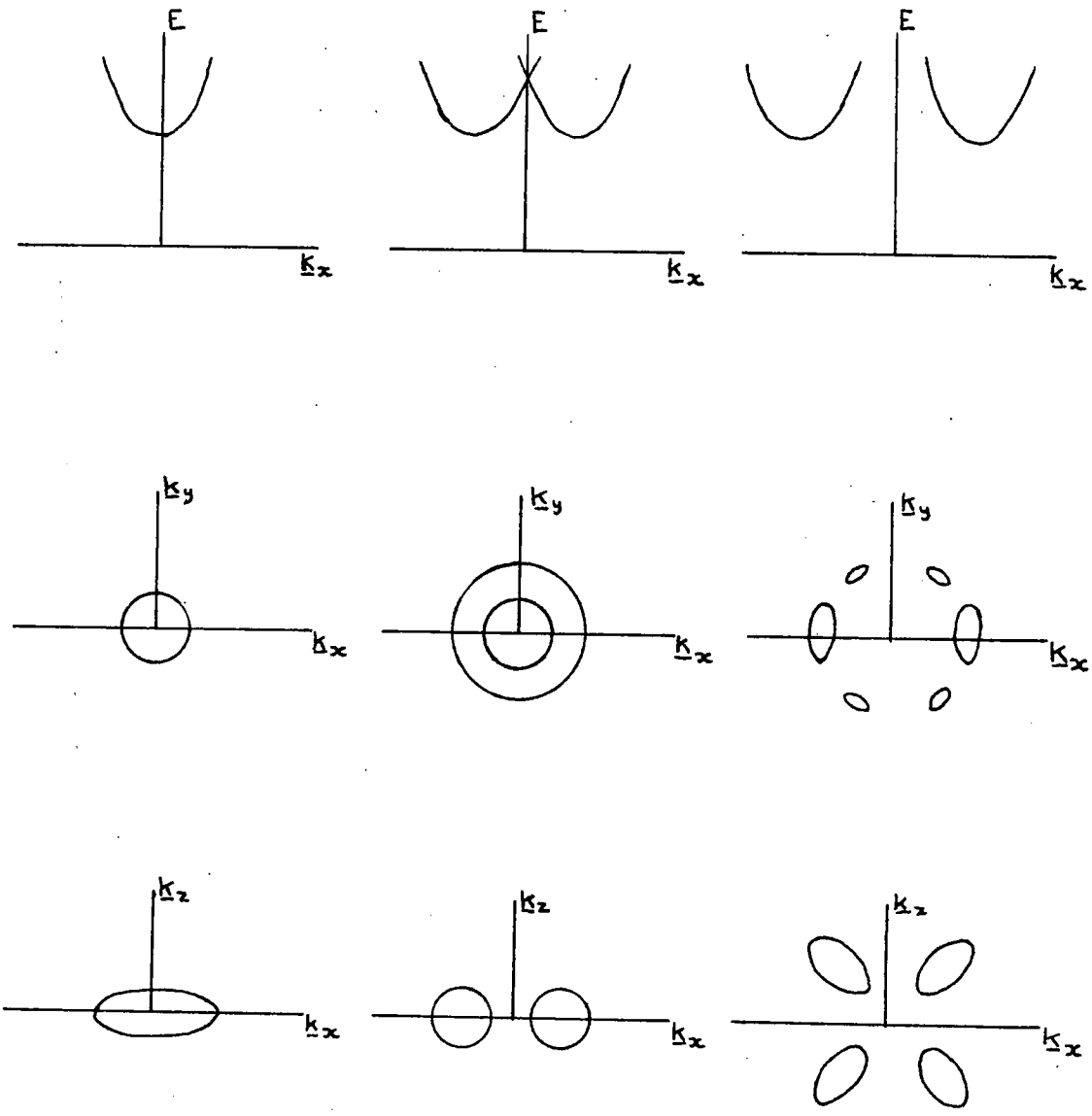


FIG.1-9. (a) (b) (c)

POSSIBLE BAND STRUCTURE IN WURTZITE TYPE CRYSTALS.

(a) Single ellipsoid. (b) Toroid. (c) Simple many valley.

The upper figures show the relationship between energy and wave number.The middle and lower ones show cross sections of constant energy.

However there was some disagreement over the shape of the energy bands away from $\underline{K} = 0$. The possible shape of the constant energy surfaces in the conduction band of Wurtzite type crystals had been discussed, using the principles of group theory, by several authors including Casella[15, 16], Balkanski and Des Cloiseaux[17], Hopfield[18] and Birman[9, 12]. They all showed that in the absence of spin-orbit coupling the conduction band should have a minimum at $\underline{K} = 0$, (Fig. 1-9(a)). But the inclusion of spin-orbit coupling may lead to three cases:

(1) Toroidal energy surfaces[16] Fig. 1-9(b)

(2) Many valley type of band structure[17] Fig. 1-9(c)

(3) Ellipsoidal energy surfaces Fig. 1-9(a)

Fig. 1-9 indicates three distinct possibilities, but it is possible in principle to have all three and/or intermediate cases in the same crystal, at different ranges of temperature. Consequently a great deal of experimental work was carried out to determine the situation in Cadmium Sulphide.

The position concerning the valence band was somewhat simpler. It was generally agreed that because of the lack of an inversion centre in the Wurtzite lattice, the valence band would show a single maximum at or near to

$\underline{K}$ = 0. Balkanski and Des Cloiseaux[17] showed from group theory that the maximum of the upper valence band should be at $\underline{K}$ = 0, but the two lower ones should have six maxima close to $\underline{K}$ = 0. The symmetry of the bands at $\underline{K}$ = 0 they showed to be the same as that calculated by Birman[12] and illustrated in Fig. 1-7. In all the experimental work mentioned below the workers assume the valence bands to have a maximum at $\underline{K}$ = 0, because this is the simplest case to consider and it did not invalidate their results. The problem then becamé one of establishing the shape of the conduction band extrema. Most of the experimental data favours the simple single ellipsoid model of Fig. 1-9(a). Dutton[6] and Thomas, Hopfield and Power[7] carried out absorption measurements on single crystals of Cadmium Sulphide. They found no evidence of indirect absorption processes. The data could be explained in terms of direct exciton plus phonon processes. In a further paper on the magneto-optical effects of the exciton spectrum, Hopfield and Thomas[20] provided additional data in support of the simple single ellipsoid model. However they did not rule out the possibility of two equivalent "direct band gaps" along a line from $\underline{K}$ = 0 to the centre of the hexagonal face of the Brillouin Zone. Balkanski and Des Cloiseaux[21]

claimed the existence of indirect transitions in the absorption spectra in support of their many valley band model[17] but Hopfield and Thomas[20] showed that this interpretation of the results of Balkanski and Des Cloiseaux was incorrect. At this stage only the results of Matsumi[19] suggested the existence of the many valley model. He observed longitudinal magnetoresistance parallel to the c-axis, a result which could not be explained by the single valley model.

In an attempt to clarify the position Zook and Dexter[22] undertook the measurement of all the independent components of the resistivity, Hall and magnetoresistance tensors in single crystals of n-type Cadmium Sulphide. The magnetoresistance in the three band models of Fig.1-9 should be quite different. In the single valley model (Fig. 1-9(a)) the magnetoresistance arises only from the spread in mobilities due to the dependence of the scattering of the electrons on their energy. The other two types of band models (Fig. 1-9(b)(c)) give rise to transverse currents at zero magnetic field and in the presence of the magnetic field a much larger transverse effect coupled with a longitudinal effect not found in the single valley model. Above 77°K their data was consistent with the

single valley band model, but below 77 K they could not exclude the possibility of Toroidal energy surfaces, with valleys close to the $\underline{K} = 0$ position. They were able to explain the results of Matsumi[19] as effects associated with their inhomogenous crystals and contact effects which Zook and Dexter observed themselves in some samples. Measurements of the effective mass of the electrons in Cadmium Sulphide provide strong evidence in support of the single valley model for the conduction band with the minimum at $\underline{K} = 0$. Piper and Halstead[23] obtained a value for the effective electron mass from measurements of the temperature dependence of Hall constant and Hall mobility. They used n-type material and interpreted their results in terms of a simple hydrogen-like model for the donor level, and obtained an effective mass of an electron in the donor level as 0.19 Me, where Me is the free electron mass. Hopfield and Thomas[20], from their measurements of the magneto-optical splittings of the exciton lines in the luminescence of Cadmium Sulphide, were able to obtain values for the effective mass of electrons in the conduction band ($Me^*$) and holes in the valence band ($M_h^*$).

$Me^* = (0.204 \pm 0.01)Me$ and is isotropic to within 5%

$$M_h^* \text{//c-axis} = 5 \pm 0.5 Me$$

$$M^*_{h\ \text{c-axis}} = 0.7 \pm 0.1 Me$$

Piper and Marple [24] measured the free electron contribution to the infra-red absorption spectrum of n-type Cadmium Sulphide to obtain a value for $Me^*$ of:

$$Me^*_{\text{average}} = (0.22 \pm 0.01) Me$$

They measured the anisotropy in the value parallel and perpendicular to the c-axis, in one sample at room temperature and found:

$$\frac{Me^*_\perp}{Me^*_{//}} = (1.08 \pm 0.04)$$

in agreement with that detected by Hopfield and Thomas. The values from the three measurements are all in good agreement.

Cyclotron resonance provides the most direct and detailed measurement of effective mass of charge carriers in a solid. Cyclotron resonance at microwave frequencies has been observed in Cadmium Sulphide by Baer and Dexter[25]

and Sawamotto[26]. Baer and Dexter observed only one resonance absorption at each orientation, which they attributed to electrons, and which is consistent with the single ellipsoid conduction band model. The (cyclotron) effective masses measured at 4.2°K with the crystal c-axis parallel ($Me^*_{//}$) and perpendicular ($Me^*_{\perp}$) to the magnetic field are:

$$Me^*_{//} = (0.171 \pm 0.003)Me$$

$$Me^*_{\perp} = (0.162 \pm 0.003)\ Me$$

As before there is some anisotropy, ~5%, indicating that the energy surfaces are not spherical but slightly oblate. The cyclotron masses are some 15% lower than those measured by the three methods mentioned above. This discrepancy can be accounted for in terms of an electron self energy correction resulting from the piezoelectric-phonon interaction found in Cadmium Sulphide[27]. Sawamotto measured the cyclotron mass at 1.7°K in single crystals, but made no attempt to measure any angular dependence. His value of 0.17 Me for the electron cyclotron mass is in agreement with that of Baer and Dexter and serves to accentuate the 15% difference

between the cyclotron mass and the effective mass as determined by other measurements. Sawamotto also observed another resonance absorption corresponding to a carrier with heavier effective mass which he attributed to holes. The value he obtained was:

$$M_h^* = 0.81Me$$

This value is in agreement with value of $M_{h_\perp}^*$ determined by Hopfield and Thomas[20].

Thus all the experimentally measured values of effective mass are in good agreement and they indicate a simple single valley model for the conduction band of Cadmium Sulphide. All the experimental data is in favour of this model. The accepted model for the band structure of Cadmium Sulphide is shown in Fig. 1-10, close to $\underline{K}=0$. As outlined at the beginning of this section the nature of the band structure away from $\underline{K}=0$ and of the bands higher and lower than those shown in Fig. 1-10 is obtained by comparison of the reflectivity data of wurtzite materials with that of the zinc blende type materials, where the band structure is well established. Measurements of this type have been performed by Cardona and Harbeke[11]

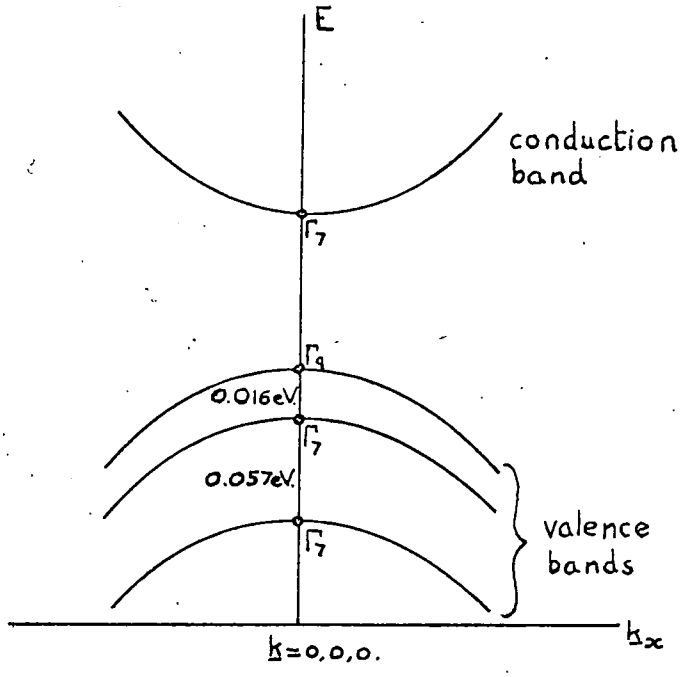


FIG.1-10.

Band structure of Cadmium Sulphide for the lowest conduction band and highest valence bands close to k=0,0,0.The splittings of the valence bands and the symmetry at k=0,0,0, are shown.(Not to scale).

$\Gamma_9$ valence bands only active for photon electric vector $\perp$ to c-axis.

$\Gamma_7$ bands active for all polarisations.

Initially they compared the reflectivity spectra of cubic Zinc Sulphide (zinc blende type) and hexagonal Zinc Sulphide (wurtzite type) far into the ultra-violet. In this way the differences in the spectra and hence the band structure in passing from the zinc blende to the wurtzite modification were established. They then obtained the reflectivity spectra of hexagonal Cadmium Sulphide and Cadmium Selenide. On the basis of the existing knowledge of the band structure of diamond and zinc blende materials they were able to predict the positions of the reflectivity peaks for the hypothetical zinc blende modifications of the hexagonal Cadmium Sulphide and Cadmium Selenide crystals. This was achieved using the perturbation method outlined by Birman[9]. The calculated peaks were identified with those found in the cubic Zinc Sulphide spectrum. Then the differences between the calculated peaks and those found in the wurtzite materials were analysed in terms of changes in band structure from the zinc blende to the wurtzite modification. In this way they obtained the band picture of Cadmium Sulphide along the c-axis as shown in Fig. 1-11. In principle the band picture along any direction can be obtained but this has not yet been accomplished.

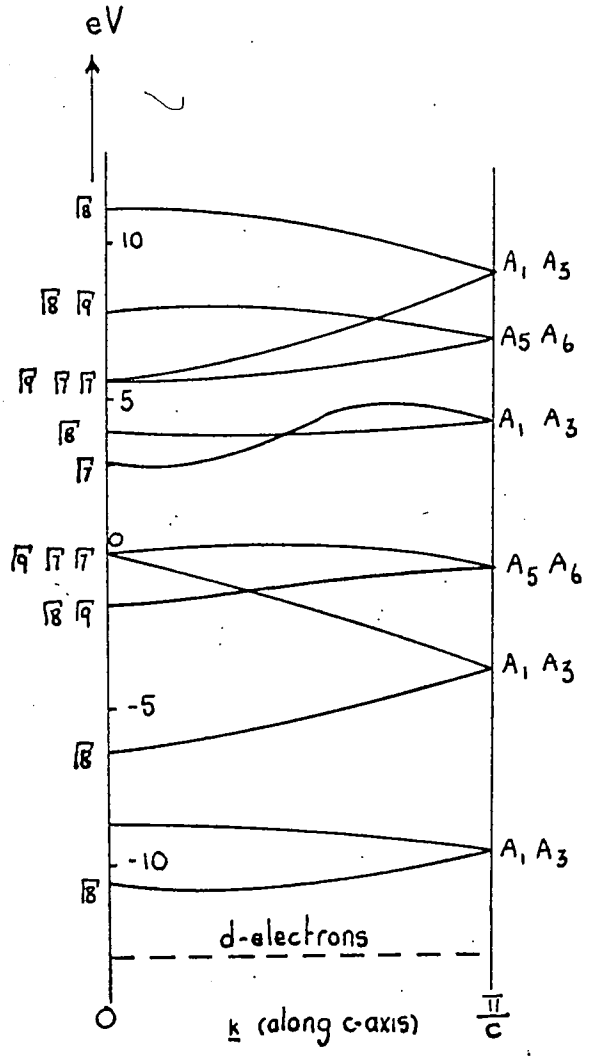


FIG.1-11. Band structure of cadmium sulphide along the hexagonal axis. Due to Cardona and Harbeke.(11)

Since the work of Cardona and Harbeke[11] there has been little published work concerning the band structure of Cadmium Sulphide. Balkanski, Amzallog and Langer[28] performed interband Faraday rotation measurements in a series of wurtzite 2-6 compounds. Their data was adequately described in terms of direct allowed transitions in the simple band structure scheme in Fig. 1-10. They obtained values for the effective mass of holes and electrons and their respective g-values in Cadmium Sulphide.

| | $M_e^*$ | $M_n^*$ | $g_e$ | $g_h$ |
|---|---|---|---|---|
| CdS | $0.2M_e$ (a) | $0.7M_e$ (c) | 1.78 (b) | 1.00 |

(a) See also [29]. This is in agreement with all the other measurements (20,23,24,25,26)

(b) In agreement with Hopfield and Thomas[20]

(c) In agreement with Hopfield and Thomas[20] and Sawamotto[26]

Recently Slagsvold and Schwerdfeger[29] measured the g-tensor for shallow donor levels in Iodine doped Cadmium Sulphide by means of electron spin resonance techniques. Roth[30] has shown that the g-value of an electron in

in a shallow trap in a semiconducting material can be calculated from a knowledge of the band structure (See also section 3-4.2 later). Slagsvold and Schwerdfeger calculated the g-value of donor electrons in Cadmium Sulphide using Roth's theory and assuming a band structure with extrema close to $\underline{K} = 0$ and with the conduction band formed completely from atomic s-states and the valence band from p-states. The g-value they calculated showed a large discrepancy from that determined experimentally. They showed that in order to obtain good agreement between the two values it was necessary to postulate a small admixture of s-type states into the highest valence band. The calculated g-value was very sensitive to the amount of admixture and they concluded that their method of determining the amount of mixing was rather arbitrary. A precise knowledge of the band states was necessary, and was not yet available to determine accurately the g-value of the donor electrons.

## 1-3 Conclusions

The band structure of Cadmium Sulphide has been well established from experimental measurements. The shape of the lowest conduction band and highest valence bands close to $\underline{K} = 0$ is shown in some detail in F.1-10. The structure of many of the bands is shown in Fig. 1-11 for the first Brillouin Zone in the direction of the

crystallographic c-axis. Recent advances in mathematical techniques have improved the theoretical calculations of band structure of wurtzite type materials[31]. However there are still large discrepancies with the experimentally determined model. Also the work of Slagsvold and Schwerdfeger[29] has underlined the need for a more precise knowledge of the nature of the band states. However for most experimental work our present knowledge of the band structure is adequate.

## REFERENCES

(1) J. M. Ziman - "Principles of the theory of solids". C.U.P. 1964

(2) R. A. Smith - "Wave Mechanics of solids". Chapman and Hall 1961

(3) D. Cusack - "Magnetic and electrical properties of solids". Longmans 1958

(4) R. DeL. Krönig and W. J. Penney - Proc. Roy. Soc. A130, 499 1930

(5) C. Hilsum and A. C. Rose-Innes - "Semiconducting 3-5 compounds". Pergammon Press 1961

(6) D. Dutton - Phys. Rev. 112, 785, 1958

(7) D. G. Thomas, J. J. Hopfield and M. Power - Phys. Rev. 119, 570, 1960

(8) F. Herman - J. Electronics 1, 103, 1955

(9) J. L. Birman - Phys. Rev. 155, 1493, 1959

(10) M. Cardona - Phys. Rev. 129, 1068, 1963

(11) M. Cardona and G. Harbeke - Phys. Rev. 137, A1467, 1963

(12) J. L. Birman - Phys. Rev. letts. 2, 157, 1959

(13) G. Dresselhaus - Phys. Rev. 100, 580, 1955

(14) D. G. Thomas and J. J. Hopfield - Phys. Rev. 116, 573, 1959

(15) R. C. Casella - Phys. Rev. 114, 1514, 1959

(16) R. C. Casella - Phys. Rev. letts. 5, 371, 1960

(17) M. Balkanski and J. Des Cloiseaux - J. Phys. Rad. 21 825, 1960

(18) J. J. Hopfield - J. Phys. Chem. Solids. 15, 97, 1960

(19) T. M. Masumi - J. Phys. Soc. Japan 14, 47, 1959

(20) J. J. Hopfield and D. G. Thomas - Phys. Rev. 122, 35, 1961

(21) M. Balkanski and J. Des Cloiseaux - Proc. Conf. on "Electronic Processes in Solids". Berlin 1960

(22) J. D. Zook and R. N. Dexter - Phys. Rev. 129, 1980, 1963

(23) W. W. Piper and R. E. Halstead - Proc. Int. Conf. on semiconductor physics. Prague 1960. Academic Press New York. 1961. P. 1046.

(24) W. W. Piper and D. F. T. Marple - J.A.P. 32, 2237, 1961

(25) W. S. Baer and R. N. Dexter - Phys. Rev. 135, A1388, 1964

(26) K. Sawamotto - J. Phys. Soc. Japan 19, 318, 1964

(27) G. D. Mahan and J. J. Hopfield - Phys. Rev. letts 12, 241, 1964

(28) M. Balkanski, E. Amzallag and D. Langer - J. Phys. Chem. Solids 27, 299, 1966

(29) B. Slagsvold and Schwerdtfeger - Can. J. Phys. 45, 127, 1967

(30) L. M. Roth - Phys. Rev. 118, 1534, 1960

(31) T. C. Collins, R. N. Euwema and J. S. Dewitt - Proc. Int. Conf. on the physics of semiconductors. Kyoto 1966 J. Phys. Soc. Japan 21 Supplement, 1966 p. 15.

# CHAPTER 2

# THE EFFECT OF IMPERFECTIONS ON THE PROPERTIES OF CADMIUM SULPHIDE

## 2-1 Introduction

In Chapter 1 the nature of the energy levels available to electrons in an ideal, perfect crystal was discussed. A detailed picture of the band structure of Cadmium Sulphide and an outline of some of the electrical and optical properties determined by the band structure was given. We now consider the effect on these properties resulting from the introduction of imperfections into the crystal lattice.

This discussion of imperfections will be mainly concerned with polar semiconducting materials since Cadmium Sulphide is in this class of compounds. (Curie[1] has discussed the available experimental evidence for determining the degree of ionicity in the bonding of Zinc Sulphide and Cadmium Sulphide and concludes that 75% ionic bonding contribution is the most probable value). Much of the treatment for the polar semiconducting materials is also applicable to metals and purely ionic solids. Only point defects will be discussed, since, as we shall see, these produce the dominant effect on the electrical and

optical properties of polar semiconducting materials and it is these properties with which we shall be most concerned. There will be no discussion of the effects of dislocations since these are small compared with those associated with point defects. For a more complete discussion of the imperfections in crystals the reader should consult references 2, 3, 4 and 5.

## 2-2 Point Defects in Polar Crystals

### 2-2.1 Types of point defect

The most common point defect is the vacancy, which occurs when an atom or ion is missing from a lattice site. Charge neutrality must be strictly fulfilled in the crystal. Since a vacancy in a polar crystal has an effective charge equal and opposite to that of the ion which should occupy the site, some charge compensation process is essential. In purely ionic crystals charge neutrality can be maintained by the production of equal numbers of positive and negative ion vacancies (Schottky defects), by the introduction of foreign atoms with a valency differing from that of the ions of the crystal, or by a combination of the two processes. In semiconductor type materials a further process is available where charge neutrality is achieved by the introduction (or removal) of free charge carriers.

The other simple point defect is the interstitial and this

is formed when an ion or atom is present in a crystal at a site which is not a lattice site. If the interstitial is a charged ion then charge compensation is again essential and can be achieved in a number of ways. The most common methods are the simultaneous production of vacancies at lattice sites where the ion has the same charge as the interstitial (Frenkel defects), or by the introduction of foreign atoms of suitable valency. Once again free charge carrier compensation is possible in semiconductor type materials. The formation of interstitials is also governed by considerations of size. There must be sufficient volume at the interstitial site to accommodate the atom or ion. Thus in close packed metal structures interstitials are a rare occurrence, whereas in the more open non-metallic structure interstitials can occur more readily.

These two simple point defects frequently associate into pairs or larger clusters. This association may come about because of the effective charge of the defects or because the relaxation of the lattice around such a cluster favours the association.

In a polar semiconductor the point defects possess an effective charge. Thus a free electron or hole is capable of being 'trapped' into a localised orbit in the vicinity of the defect, depending on the sign of the effective

charge of defect. In terms of the band structure picture of Chapter 1, this means that the defects produce trapping levels in the forbidden gap. Defects can in certain cases trap both a hole and free electron and so act as recombination centres at which free holes and electrons can recombine. Clearly a wide variety of traps and recombination centres are possible depending on the defects and clusters present in the lattice and these can give rise to structure sensitive properties which are dependent on the history of the sample.

This situation occurs in Cadmium Sulphide and accounts for much of the difficulty in interpretation of the experimentally observed characteristics of Cadmium Sulphide. A brief outline of the main properties of Cadmium Sulphide associated with the presence of the imperfections will be presented in section 2-3.

2-2.2 Equilibrium concentrations of defects

The presence of lattice defects might be expected to increase the energy of a crystal since they destroy the periodicity of the lattice and require energy for their formation. However, once the energy has been supplied to form a defect, usually of the order of a few eV, the lattice will relax around the defect and in doing so

compensate for most of the energy of formation.
Calculations have been performed to estimate the energy changes during the formation of a point defect in polar and metallic materials. These calculations are somewhat unreliable, but they do indicate that from energy considerations alone, a certain concentration of defects is to be expected in a solid.
The existence of defects can also be justified from thermo-dynamic principles. By introducing a vacancy or interstitial into a perfect lattice the possible number of distinguishable arrangments of atoms increases from unity to a very large number of the order of $10^{23}$ / $cm^3$. i.e. the introduction of point defects increases the configurational entropy of the lattice and, at sufficiently high temperatures, this compensates for the energy of formation of the defect. This point can be emphasised by defining the Helmholtz free energy (F) of a solid[6], in thermodynamic equilibrium, as:

$$F = U - T.S. \qquad (2\text{-}1)$$

where U is the total internal energy of the solid, T is absolute temperature and S is entropy of the solid.

The introduction of n point defects into the lattice, increases the internal energy by an amount nW, where W is the energy of formation. The increase ($\Delta S$) in entropy due to these defects is given by the Boltzmann expression for configurational entropy:

$$\Delta S = K \log_e P$$

where K is Boltzmann's constant and P is the number of ways in which the defects can be arranged.
Thus the change in free energy ($\Delta F$) due to the defects is:

$$\Delta F = nW - K\log_e P \qquad (2\text{-}2)$$

Then by minimising $\Delta F$ with respect to n, the thermal equilibrium concentration of defects (n) required to minimise the free energy of the solid can be calculated.
Note - strictly one should minimise the Gibb's free energy but use of the Helmholtz energy is an adequate approximation. This calculation can be improved by taking account of the fact that near a point defect the vibrational frequencies of the neighbouring ions is modified and also that the

internal energy of the lattice and the energy of formation of the defects are temperature dependent functions. Thus we see that far from being non-equilibrium states in the lattice, the point defects must be present in order to reduce the free energy of the solid.

2-2.3 Non-equilibrium concentrations of defects

The thermal equilibrium concentrations of point defects usually only reach values sufficient to produce noticeable effects on the properties of materials at temperatures approaching the melting point. In practice, however, at temperatures much below the melting point concentrations are frequently encountered which are many orders of magnitude larger than the corresponding equilibrium values. These large concentrations have a major effect on the properties of the material. This is the case in Cadmium Sulphide. Such situations can arise in a variety of ways: for example,

(1) By rapid quenching of the material from a temperature close to its melting point. Clearly this is a non-equilibrium process and the defect concentration corresponding to the high temperature is 'frozen-in' into the lattice at the low temperature where the rate of the diffusion of the defects is low. In practice it is

usually difficult to cool a material sufficiently slowly to maintain equilibrium conditions over the range from near the melting point to room temperature. This is the case with Cadmium Sulphide, which is grown by vapour phase techniques at temperatures of the order of $1000^{0}C$.

(2) Via large concentrations of dislocations and hence point defects. Since intersecting and climbing dislocations are sources of point defects, the latter can be introduced into a solid by strain. This strain can be produced during cooling from a high temperature e.g. during growth.

(3) The concentrations of defects can be controlled by the presence of charged impurities. The defects provide the charge compensation mechanism for the impurities. Since the defects and impurity must be of opposite charge polarity for charge neutrality they frequently occur as associated pairs e.g. the Zinc Sulphide A centre[8] which is composed of a halogen impurity substituting for Sulphur associated with a Zinc ion vacancy. Clearly a similar type of defect impurity pair might occur in Cadmium Sulphide, but no direct evidence for its existence has yet been obtained.

(4) Non-stoichiometry can develop during the growth of compounds and obviously lead to large non-equilibrium concentrations of defects. This is thought to be the process chiefly responsible for the production of defects in

Cadmium Sulphide, especially as the crystals are grown from the vapour phase where control of the correct vapour pressures for stoichiometric growth is very difficult. Clearly it is possible for non-equilibrium concentrations of defects to be present in solids. The processes described above are frequently difficult to control during the growth and subsequent handling of the samples so that for materials whose properties are very dependent on the concentrations of point defects, e.g. Cadmium Sulphide, the control and reproducibility of properties from sample to sample is impossible unless the atomic composition of the defects can be identified.

2-2.4 Point defects in polar semiconductors in equilibrium with their surroundin gs

We have discussed in section 2-2.2 the equilibrium concentration of defects in a solid, without reference to the interactions with their surroundings. Kröger and Vink[4] have described the formation and equilibrium conditions for point defects in divalent, diatomic compounds. The basis of their method is to describe the formation of defects in terms of quasi-chemical equations. As an example let us consider the formation of $\delta$ isolated Frenkel defects in the diatomic compound MX. This process can be

represented by the reaction equation:

$$MX \rightleftharpoons M_{1-\delta} + (Vm)_{\delta} + (Mi)_{\delta} + X \qquad (2\text{-}3)$$

Where Vm represents a metal ion vacancy and Mi a metal ion at an interstitial site. Since this is a thermodynamically reversible process then the principle of chemical equilibrium, often referred to as the law of mass action[9], can be applied. According to this principle the products of the concentrations of reaction components are related through a reaction constant. For the reaction (3) the concentrations of the components can be expressed by the relation:

$$[Vm] \cdot [Mi] = K_F \qquad (2\text{-}4)$$

where $K_F$ is the reaction constant. Here we shall assume $\delta << 1$ so that the concentration of the atoms occupying proper lattice sites does not change appreciably. This is valid for the concentrations of defects usually found in practice, so that the law of mass action deals only with the concentrations of the defects. Relationships of the form of equation (2-4) can be obtained for all the processes which lead to departures from the perfect crystal by the formation of defects. The effect of the external atmos-

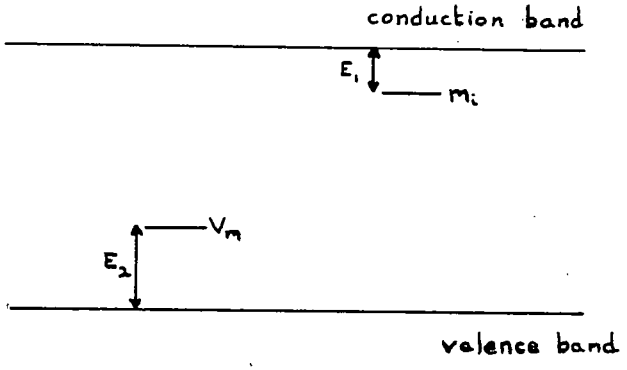


FIG.2÷1. Possible energy level scheme for the solid MX with Frenkel disorder.

phere can be treated in a similar manner. The method becomes extremely powerful when applied to a compound in equilibrium with its vapour. For illustrative purposes let us treat a specific example. Consider departures from stoichiometry in the compound MX due to formation of metal ion interstitials ($M_i$) by diffusion of metal ions ($M_g$) from the vapour into the solid and that the deviations from stoichiometry are accommodated by the formation of Frenkel defects. A possible band scheme for the system, containing metal ion interstitials and vacancies, is shown in Fig. 2-1.

The production of the metal ion interstitials can be expressed by the pseudo-chemical equation:

$$MX + M_g = MX + M_i \qquad (2\text{-}5)$$

The rate of reaction for this process is governed by the law of mass action in the normal way, leading to the relation:

$$\frac{[M_i]}{Pm} = K_1 \qquad (2\text{-}6)$$

Where Pm is the partial pressure of the metal vapour. This automatically defines the partial pressure ~~of the~~

of the component X, in the vapour. $K_1$ is the appropriate reaction constant.

From equation (2-4) the concentrations of the components of the Frenkel defects are related by:

$$[Vm] \quad [M_i] \quad = \quad K_F \qquad (2\text{-}7)$$

Another pair of equations are obtained by considering the electron transitions from the metal interstitial donor levels to the conduction band and hole transitions from the vacancy levels to the valence band:

$$M_i \quad + \quad E_1^{\cdot} \longrightarrow \quad M_i^{\cdot} \quad + \ominus \qquad (2\text{-}8)$$

where $M_i^{\cdot}$ is an ionised donor and $\ominus$ is a free electron in the conduction band.

$$Vm \quad + \quad E_2 \longrightarrow \quad Vm^1 \quad + \quad \oplus \qquad (2\text{-}9)$$

where $Vm^1$ is a vacancy minus a hole and $\oplus$ is a free hole in the valence band.

Applying the law of mass action in the normal way the following relationships are obtained:

From (2-8) $$\frac{N\,[M_i^{\cdot}]}{[M_i]} = K_2 \qquad (2\text{-}10)$$

From (2-9) $$\frac{P\,[Vm^{1}]}{[Vm]} = K_3 \qquad (2\text{-}11)$$

where n and p are the free electron and free hole concentrations respectively.

For any semiconductor the product of the free electron concentration and free hole concentration is a constant.

i.e. $$n.p. = K_4 \qquad (2\text{-}12)$$

~~Including~~ The condition of charge neutrality provides one further relation:

$$n + [Vm^{1}] = P + [M_i^{\cdot}] \qquad (2\text{-}13)$$

Clearly there are now sufficient equations to obtain relationships for the concentrations of the defects and the free carriers in terms of the reaction constants, the external vapour pressure and the temperature.

An approximate method of solution has been devised by Brouwer[10], which consists of taking logarithms of both sides of the equations (2-6), (2-7), (2-10), (2-11), (2-12)

and (2-13) to provide a set of simultaneous equations. The form of equation (2-13) is not suitable for this method and so its form is simplified by considering different regimes of the partial pressure (Pm) of the metal vapour. For example, at extremely high values of Pm the formation of metal interstitials is favoured relative to the formation of vacancies and so $[M_i] \gg [Vm]$.
Clearly in this case equation (2-13) can be rewritten:

$$n \rightleftharpoons [M_i^{\cdot}] \qquad (2\text{-}14)$$

and solutions for $[M_i]$, $[M_i^{\cdot}]$, $[V_i][Vm^{-1}]$, n and p can be easily obtained using the method of Brouwer[10]. The form of equation (2-13) is then considered in different regimes of the partial pressure Pm and solutions for the defect and free carrier concentrations obtained in each regime. These separate solutions can then be fitted together to provide a solution over the complete range of vapour pressure.
The extension of this method to other types of defect disorder situations can be obtained in an obvious manner from the above example. The more complicated situation which arises when foreign atoms are incorporated into the solid can also be treated by an extension of this

method. A further set of relationships which includes the effects of the impurity atoms can be obtained. A sufficient set of equations can always be obtained so that Brouwer's method can be applied. For a thorough review of the method outlined above the reader should consult references (4) and (5).

Thus in principle the concentration of defects which will be produced by heating a compound MX in the vapour of one or both of its constituents can be evaluated. If the effect on the properties by the heat treatment can be measured and related to the changes in the defect concentrations predicted by the techniques described above one can determine the defects which dominate the properties of the compound. This technique has been applied with a limited degree of success to Lead Sulphide, Cadmium Telluride and Cadmium Sulphide. However many inconsistencies remain to be explained, especially in the case of Cadmium Sulphide.

2-3 Point Defects in Cadmium Sulphide

Many of the potentially commercially important electrical and optical properties of semiconductors and insulators like Cadmium Sulphide, such as their photoconductivity and luminescence, are associated with the presence of impurities and imperfections in the lattice. The expected influence of such imperfections on the photo-

electronic properties is known, and so it is possible to use the measurement of these properties to investigate the nature of the imperfections. An account of the more important techniques that have been applied to study the photoelectronic processes in Cadmium Sulphide is given below:

2-3.1 Effects due to imperfections

The introduction of imperfections may have one or more of the following effects on the properties of Cadmium Sulphide:

(1) Change the dark conductivity. Donor imperfections increase the conductivity and acceptors decrease it since Cadmium Sulphide of present impurity is always n-type (see below).

(2) Alter the photosensitivity. Imperfections which act as recombination centres decrease the sensitivity. On the other hand, imperfections which have a large cross section for capturing photoexcited holes, but a small one for capturing photoexcited electrons after capturing holes may increase the sensitivity by increasing the free electron lifetime when the electrons are the majority carriers (see also section 2-3.4).

(3) The imperfections can influence the speed of response of the photoconductivity. The speed of response decreases when imperfections trap the free carriers, until they are

thermally freed i.e. they effectively reduce the carrier mobility. However this may increase the carrier lifetime before recombination and so may increase the sensitivity. This may lead to conflicting requirements.

(4) They will extend the spectral response of the photoconductivity to the long wavelength side of the absorption edge, since direct excitation from an imperfect centre with its level lying in the forbidden gap requires less energy than excitation across the band gap.

(5) They may provide radiative recombination paths. Emission of photons with energy less than the band gap becomes possible via recombination centres in the forbidden gap.

2-3.2 Imperfection levels in Cadmium Sulphide

The general pattern for imperfection behaviour in Cadmium Sulphide (and all 2-6 compounds) is that group 3 and group 7 impurities and anion vacancies act as donors. While group 1 and group 5 impurities and cation vacancies act as acceptors. The energy levels of these imperfections are largely determined by the host lattice[11]. The ionisation energies of all the donors is of the order of 0.03eV and of all the acceptors in the range 0.8-1.0eV. The presence of the deep lying acceptors is responsible for the fact that Cadmium Sulphide can only be made n-type and not p-type. Also the concentration of donors always

apparently exceeds that of the acceptors in material of present purity so that the acceptors are always completely compensated. Woodbury[12] has measured the self diffusion of Cadmium in Cadmium Sulphide and concluded that the main deviations from stoichiometry are accommodated in the lattice by Schottky defects. He also concluded that under all conditions the concentration of Sulphur vacancies (Vs) exceeded that of the Cadmium vacancies (Vcd). If donor impurities are present the formation of Cadmium vacancies will be favoured by compensation. In material of present purity Woodbury concludes that the concentration of Cadmium vacancies is always determined by the donor impurity concentration, but that [Vs] > [Vcd] still and the Cadmium vacancies are compensated by the donors.

2-3.3 Investigation of the trapping spectrum

The majority of this work has been centred on electron rather than hole traps, since the nature of the traps has usually been inferred from their observed effects on the transport properties, which are dominated by the majority carriers, the electrons.

Woods and Nicholas [13, 14] used the technique of thermally stimulated currents to investigate the trapping spectrum of levels in the upper half of the forbidden gap. They found

levels at depths of 0.05eV, 0.15eV, 0.25eV, 0.41eV, 0.63eV and 0.83eV below the conduction band.

They proposed the following tentative assignment of the levels:

0.05eV), 0.15eV) - associated with isolated Sulphur vacancies

0.25eV - A complex of associated Sulphur vacancies.

0.41eV - A complex of associated Cadmium and Sulphur vacancies in nearest neighbour sites.

0.63eV - A complex of associated Cadmium vacancies.

0.83eV - A complex of associated Cadmium and Sulphur vacancies in nearest neighbour sites.

No one crystal contained all six levels and they found that the 0.05eV, 0.41eV, 0.63eV and 0.83eV traps showed photochemical effects during cooling to 77$^{o}$K while under illumination. Recently Woods and Cowell (to be published) using the same technique have observed a trap at 0.33eV below the conduction band. A trap at this depth has been observed by several workers, but was not observed by Woods and Nicholas[13, 14]. By using a slower heating rate Woods and Cowell have shown that the thermally stimulated current peak corresponding to this trap is a super position of two closely spaced peaks corresponding to trap depth of 0.38eV and 0.42eV.

Nicholas and Woods[14] compared their results with several other authors, who between them have used a wide variety of methods. The table is reproduced in table 1. Clearly there is a large measure of agreement, concerning the trap depths and their capture cross sections.

One cannot rule out the possibility that some, or all, of these traps may be due to surface states. Sawamotto and Toyoda[15] studied the surface states of Cadmium Sulphide using a transverse D.C. field effect technique[16] with the samples in vacuo. They observed the presence of six trapping levels at 0.043eV, 0.08eV, 0.13eV, 0.43eV, 0.6eV and 0.82eV below the conduction band. The correspondence between these values and those obtained by Woods and Nicholas[14] indicates that the two experiments are possibly looking at the same trapping centres. Also Itakura and Toyoda[17] have shown that the surface states on Cadmium Sulphide are affected by the degree of crystal perfection, the ambient atmosphere and the surface treatment in a similar manner to the photochemical effects observed by Woods and Nicholas. Also Mark[18] has observed substantial reversible changes in the photoconductive gain and response in insulating Cadmium Sulphide as a result of varying the partial pressure of an electronegative ambient ($O_2$ or $I_2$ vapour) above the Cadmium Sulphide. He explains the

TABLE 1.

| Reported by; | Method of measurement. | | Comparison of values of trap energy depths. | | | | | | | |
|---|---|---|---|---|---|---|---|---|---|---|
| Woods & Nicholas. | T.S.C. Photodecay | E<br>T* | 0.051<br>150 | 0.14<br>190 | 0.25<br>295 | – | 0.41<br>300 | – | 0.63<br>330 | 0.83<br>290 |
| Woods & Wright. | Bube | E<br>T* | 0.24<br>120 | – | 0.32<br>170 | 0.38<br>220 | 0.5<br>270 | – | 0.59<br>320 | – |
| Niekisch. | alternating light | E<br>E | – | 0.12<br>– | 0.22<br>– | 0.31<br>– | 0.4<br>0.45 | – | 0.55<br>0.66 | 0.7<br>0.8 |
| Brophy et. al. | Noise | E | – | – | – | 0.36 | 0.43 | – | 0.6 | – |
| Bube & Barton. | Bube | E<br>T* | 0.2<br>100 | 0.25<br>135 | 0.41<br>180 | 0.44<br>220 | 0.51<br>270 | 0.58<br>305 | 0.63<br>350 | – |
| Sokol'skaya. | S.C.L. Currents | E | 0.09 | 0.12 | 0.22 | – | – | – | 0.66 | – |
| Broser et. al. | T.S.C. Photo decay | E<br>E | – | – | – | 0.34<br>– | 0.43<br>0.48 | – | – | – |
| Broser. | T.S.C. | E | – | – | 0.22 | 0.31 | – | – | – | – |
| Bube & Macdonald. | Photohall | E | – | – | – | 0.35 | 0.46 | 0.54 | – | – |
| Franks & Keating. | Franks & Keating | E | 0.053 | – | – | – | – | – | – | – |
| Driver & Wright. | Primary T.S.C. | E | – | – | – | – | 0.41 | – | – | – |
| Marlor & Woods. | S.C.L. Currents | E | – | – | – | – | – | – | 0.61 | – |
| Tanaka & Tanaka. | — | E | – | – | – | – | 0.4 | – | – | – |
| Clayton et. al. | Grossweiner | E | 0.09 | 0.13 | – | – | – | – | – | – |
| Smith. | S.C.L. Current | E | – | – | – | – | – | – | – | 0.8 |
| Trofimenko et. al. | Photo decay activation energy | E | 0.045 | | 0.23 | – | – | 0.5 | – | – |
| Unger. | Photo/glow | E | – | – | 0.26 | 0.32 | 0.41 | – | 0.58 | – |
| Lappe. | — | E | – | – | – | – | 0.41 | – | – | – |

E in eV. T.S.C. ≡ Thermally Stimulated Currents.

T* in °K. S.C.L. ≡ Space charge Limited.

effects in terms of a photoassisted chemisorption process for the adsorption of gas ions on the surface.

The recent work of Böer er al[19] has somewhat clarified the position. They carried out measurements of photoconductivity and thermally stimulated currents on undoped single crystals of Cadmium Sulphide after heat treatment between 370°K and 620°K in ultra-high vacuum ($10^{-11}$ Torr). The very large changes usually associated with heat treatment in high vacuum ($10^{-6}$ Torr) were not observed and so they concluded that these must be due to changes in a surface layer and possible interaction with the gas ambient. However they did find reproducible changes of smaller magnitude than those usually observed after vacuum heat treatment, which they interpreted in terms of a dissociation of a large bulk defect associated complex containing Cadmium vacancies to produce single Cadmium vacancies and Cadmium vacancy pairs. Thus they concluded that both surface and bulk effects were important in determining the mechanism of the photoelectronic processes in Cadmium Sulphide.

Clearly the picture of the trapping spectrum is confused and more experimental work is required. Furthermore there is little reported work on the trapping spectrum associated with the bottom half of the forbidden gap. This information is required before a complete understanding of the properties of Cadmium Sulphide can be obtained.

## 2-3.4 Investigation of the recombination centres

Information concerning the behaviour of the recombination centres has been obtained in several ways.

### Photoconductivity

Photoconductivity is of great interest in Cadmium Sulphide since Cadmium Sulphide can show large photoconductive gains in the visible region. The photoconductivity (G) of a material is defined as the number of excess charge carriers passing between electrodes at each end of the sample per second per photon absorbed. Thus if $\Delta I$ is the photocurrent and F is the number of electron-hole pairs created per second, then:

$$G = \frac{\Delta I}{eF} \qquad (2\text{-}15)$$

where e is the electronic charge.

Since in Cadmium Sulphide the current is carried almost solely by the electrons then equation (2-15) can be rewritten:

$$G = \frac{\tau_n}{t_n} \qquad (2\text{-}16)$$

where $\tau_n$ is the electron lifetime and tn the electron transit time. In practice the value of $\tau_n$ is governed by the recombination centres present in the forbidden gap. Rose [20] has produced the following nomenclature, which is in common usage

~~usage~~ for the different types of recombination centre:

| | |
|---|---|
| Class 1 | $S_n \approx S_p$ |
| Class 2 | $S_n \ll S_p$ |
| Class 3 | $S_n \gg S_p$ |

where $S_n$ and $S_p$ are the capture cross sections of the centres for electrons and holes respectively. In Cadmium Sulphide class 1 centres provide a fast recombination path for the electrons, leading to a low electron lifetime, and these always seem to be present. The introduction of class 2 centres can increase the electron lifetime by trapping the holes liberated by the excitation. Now since there are very few free holes the class 1 centres that have trapped electrons will remain filled and thus not permit the conduction electrons to recombine. The holes will tend to accumulate in the class 2 centres. In this way the class 2 centres increase the electron lifetime and consequently the photo-conductive gain.

Sample containing class 2 centres show a variation of photocurrent with a power of light intensity greater than unity over a limited range of light intensities. This is referred to as <u>superlinearity</u> and occurs when the class 2 centres are beginning to provide their sensitising effect

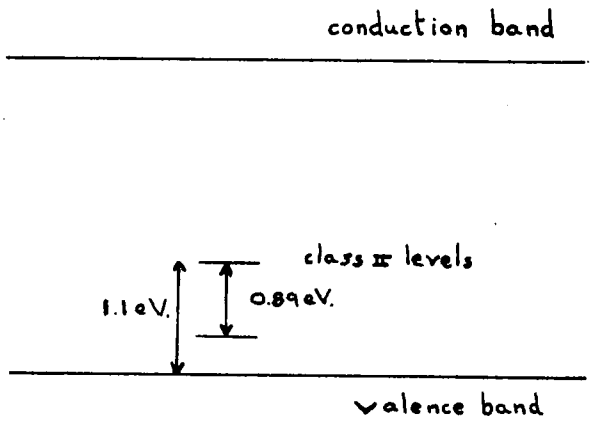


FIG.2-2. The energy level scheme for the infrared quenching of photoconductivity in CdS.

with shifting steady state Fermi level.

Quenching of the photoconductivity can be achieved by simultaneous irradiation with infra-red and the pumping excitation. Under these conditions the infra-red radiation raises electrons from the valence band to the class 2 centres thereby releasing free holes in the valence band. The free holes can then recombine with the conduction band electrons via the class 1 centres, so that the photocurrent is reduced. In Cadmium Sulphide at ~~R.T.~~ 300°K the infra-red quenching can be produced by light in two spectral bands with maximum at wavelength 0.92 microns and 1.45 microns. The 1.45 micron band is not present at 77°K, implying that there is a thermal step in this process. The proposed energy level scheme[1] for the infra-red quenching is shown in Fig. 2-2.

The spectral response of the photoconductivity of a typical undoped single crystal of Cadmium Sulphide is shown in Fig. 2-3.

Edge emission

The green edge emission of Cadmium Sulphide appears when it is irradiated at temperatures below about 100°K with light of photon energy greater than the band gap. The emission consists of a series of overlapping bands, the maxima of which are equally spaced 300 $cm^{-1}$ (0.033eV)

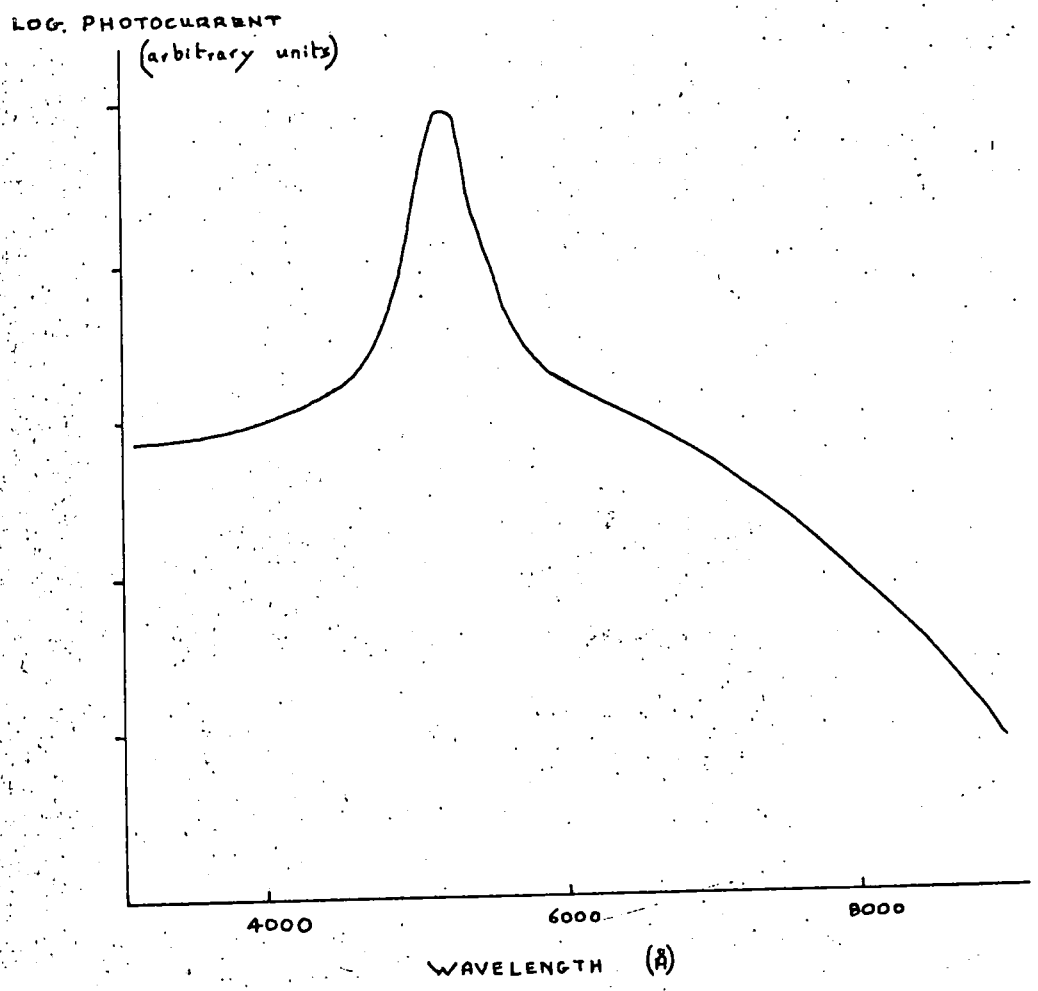


FIG.2-3. Spectral sensitivity of photocurrent in undoped CdS.

apart. The first of these bands corresponds to an energy close to, but less than, that of the fundamental absorption edge. The series has been established as being due to emission via some recombination centres with the co-operation of n longitudinal optical phonons (where n = 0, 1,2,3,---). Various models have been proposed to explain the emission, but the problems are complex and have not yet been resolved. The difficulties are increased because of the existence of two series of emission peaks, a high energy series dominant at liquid Nitrogen temperatures with the zero phonon peak corresponding to 2.415eV and a low energy series dominant at liquid Helium temperatures with the zero phonon peak at 2.395eV.

Hopfield[21] has shown theoretically that the shape of the phonon peaks can only be understood if the mechanism of recombination involves trapped carriers. Lambe et al[22] have proposed the model that electrons trapped at levels close to the conduction band recombine with free holes. Whereas Collins[25] has proposed a free electron to bound hole recombination process, where the holes are trapped at levels close to the valence band. But neither of these models have been completely consistent with experimentally observed data.

Recently Thomas et al(26), from their measurements of the spectral change of the emission during its decay, have indicated that the edge emission series dominant at $4^{o}K$ is a bound electron to bound hole process. A bound to bound recombination mechanism has been established in GaP by Thomas et al[27]. In addition to the broad spectrum, which is similar to the edge emission in CdS, this material shows a number of narrow emission lines which definitely identify the spectrum as recombination between two trapped carriers at a donor-acceptor pair. The series of narrow lines arises because the different separation of pairs leads to different recombination energies. The broad spectrum occurs when there are a large number of overlapping narrow lines due to a statistically large number of pairs of almost equal separation. Such a fine structure has not yet been observed in CdS, but the recent work of Maeda[28], Colbow [29], Yee and Condas[30] and Goede and Gutsche[31] indicate that the bound to bound model for the recombination radiation in CdS may be the correct one.

The edge emission of an undoped single crystal of CdS is shown in Fig. 2-4.

At liquid Helium temperatures, a series of sharp lines appears at high energy than the edge emission. These are

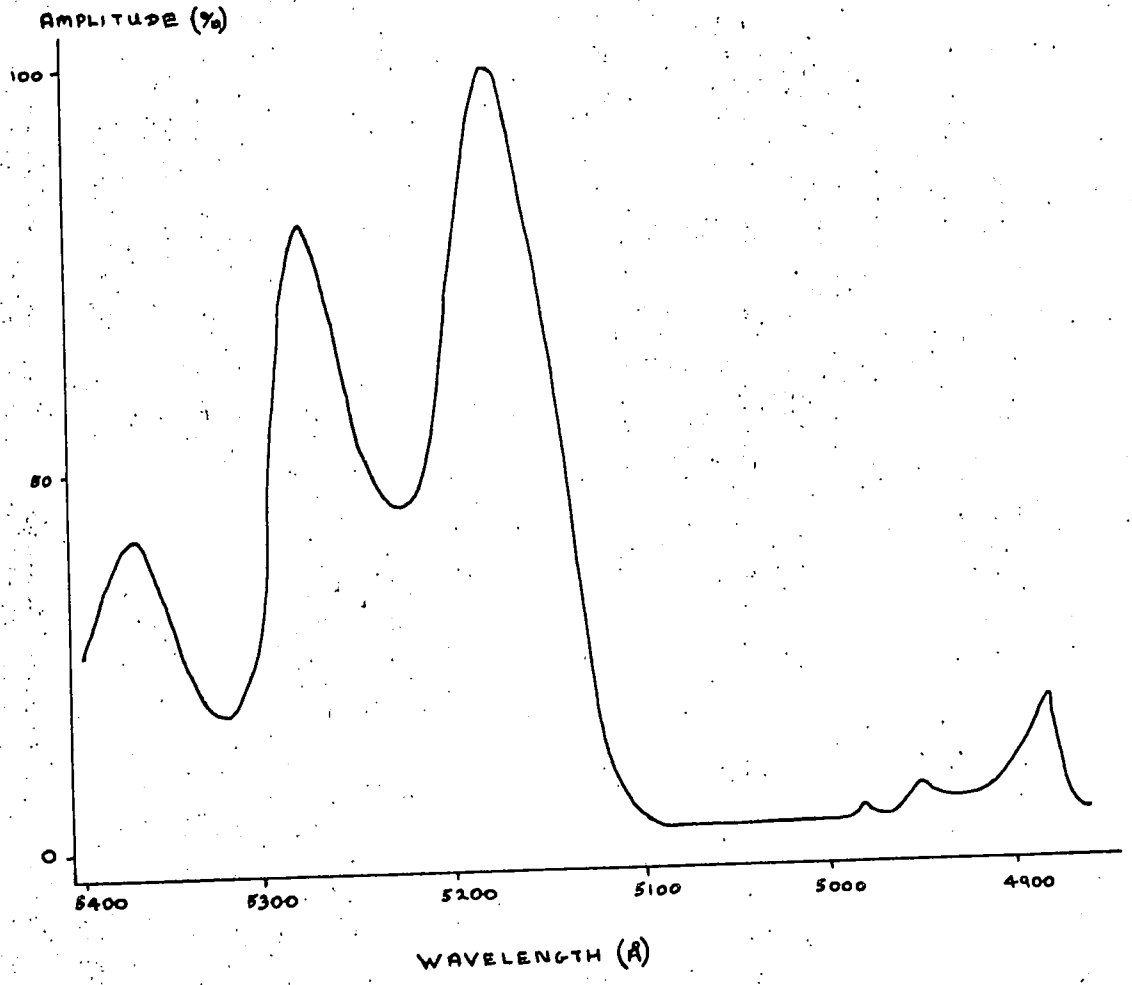


-FIG.2-4. Edge emission from undoped CdS, at 4.2°K.

the so called exciton lines. The origin of most of these lines, many of which are due to excitons bound to imperfections, has been established. The reader is referred to the comprehensive review article of Reynolds et al[32].

Infra-red Emission

The nature of the recombination centres can also be studied via the infra-red emission. The edge emission is concerned with levels close to the band edges. However luminescent processes involving levels in the middle of the forbidden gap can occur and give rise to infra-red emission. Bryant and Cox[33] observed banded emission in the range 1.5 microns to 2.3 microns, with three bands centred on 1.6, 1.8 and 2.05 microns. They were able to explain their results and most of the other published work in terms of an unoccupied centre with an energy level 0.83eV above the highest valence band. The banded emission occurs when an electron excited to this level returns to the p-state valence band, which is split into three components (see Fig. 1-8), where the occupied centre lies 0.7eV above the highest valence band. Bryant and Cox[34] have also observed two further emission bands centred on 0.75 and 1.05 microns. These two bands require band gap irradiation to excite them, whereas the three former bands could not be excited by band

gap light but by light in range 0.6 - 1.05 microns or 1.3 - 1.65 microns. Thus Bryant and Cox concluded that the emission at 0.75 microns occurs when an electron moves from the conduction band (or a state near to it) to the unoccupied centre and that the 1.05 micron emission occurs when an electron moves to the unoccupied centre from some level which must lie 0.49eV below the conduction band. From their observations of the changes in the emission when the samples were heated in the range 300°K to 550°K in broad band illumination they concluded that the centre contains a ground state which is common to the 0.75 and 1.05 micron emission and which is the excited state of the bands in the range 1.5 - 2.2 microns. The centre was thought to be a complex association of defects. These conclusions are in general agreement with those obtained by Cowell and Woods[35]. However these authors observed that the 1.05 micron emission was not present in some samples and so concluded that the centres responsible for this emission and that in the range 1.5 - 2.2 microns to be separate entities, but closely associated with one another in space.

2-3.5 Paramagnetic resonance

Clearly an explanation of many of the effects outlined above would be simplified if the atomic nature of defects

present were known. The more direct measurements of the paramagnetic resonance of carriers trapped at the defect sites may provide this information. This technique has been applied successfully to other types of materials e.g. alkali halides.

## REFERENCES

(1) D. Curie - "Luminescence in Crystals" Methuen. London. 1953, p.111.

(2) F. Seitz - Advances in Physics 1, 43, 1952.

(3) H. G. VanBueren - "Imperfections in Crystals". North Holland Publ. Co. Amsterdam. 1960.

(4) F. A. Kroger and H. J. Vink - Solid State Physics. 3, 307, 1955.

(5) F. A. Kroger - "The Chemistry of Improper Solids". North Holland Publ. Co. Amsterdam. 1963.

(6) J. K. Roberts and A. R. Miller - "Heat and Thermodynamics" edition 5, Blackie and Son Ltd. London. 1960. p.385.

(7) N. F. Mott and R. W. Gurney - "Electronic Processes in Ionic Crystals" Oxford Univ. Press. 1948.

(8) P. H. Kasai and Y. Otomo - J. Chem. Phys. 37, 1263, 1962.

(9) S. Glasstone and D. Lewis - "Elements of Physical Chemistry" MacMillan and Co. Ltd. London. 1960 p.293.

(10) G. Brouwer - Philips Res. Reports 9, 366, 1954.

(11) W. Kohn and J. M. Luttinger - Phys. Rev. 99, 1903, 1955.

(12) H. H. Woodbury - Phys. Rev. A134, 492, 1964.

(13) J. Woods and K. H. Nicholas - B.J.A.P. 15, 1361, 1964.

(14) K. H. Nicholas and J. Woods - B.J.A.P. 15, 783, 1964.

(15) K. Sawamotto and H. Toyoda - Rev. Electrical Communication Lab. 14, 177, 1966.

(16) R. H. Kingstone and F. Neustadter - J.A.P. 26, 718, 1955.

(17) M. Itikura and H. Toyoda - Jap.J.A.P. 3, 197, 1964.

(18) P. Mark - J. Phys. Chem. Sols. 25, 911, 1964.

(19) K. W. Boer and C. A. Kennedy - Phys. Stat. Sol. 19, 203, 1967.

(20) A. Rose - Prog. in Semiconductors 2, 1, 1957.

(21) J. J. Hopfield - J. Phys. Chem. Sols. 10, 110, 1959.

(22) J. J. Lambe, C.C.Klick and D. L. Dexter - Phys. Rev. 103, 1715, 1956.

(23) G. A. Marlor and J. Woods - B.J.A.P. 16, 797, 1965.

(24) W. E. Spear and G. W. Bradbury - Phys. Stat. Sol. 8, 649, 1965.

(25) R. J. Collins - J.A.P. 30, 1135, 1959.

(26) D. G. Thomas, J. J. Hopfield and K. Colbow - Int. Conf. on Semiconductors, Paris, 1964.

(27) D. G. Thomas, M. Gershenzon and F. A. Trumbore - Phys. Rev. A133, 269, 1964.

(28) K. Maeda - J. Phys. Chem. Sols. 26, 1419, 1965.

(29) K. Colbow - Phys. Rev. 141, 2, 1966.

(30) J. H. Yee and G. A. Condas - App. Phys. Letts. 9, 186, 1966.

(31) O. Goede and E. Gutche - Phys. Stat. Sol. 17, 911, 1966.

(32) D. C. Reynolds, C. W. Litton and T. C. Collins - Phys. Stat. Sol. 9, 645, 1965.

(33) F. J. Bryant and A. F. J. Cox - B.J.A.P. 16, 463, 1965.

(34) F. J. Bryant and A. F. J. Cox - B.J.A.P. 16, 1065, 1965.

(35) T. A. T. Cowell and J. Woods - Admiralty Contract C.P. 11339/63 Research on CdS. RU 15-2 Annual Report 1965-66.

# CHAPTER 3

# PRINCIPLES OF THE THEORY OF ELECTRON SPIN RESONANCE

## 3-1 Introduction

Paramagnetism in a solid can arise because some or all of the atoms or defects in the solid possess unpaired electrons. Typical examples are, the transition elements, free radicals possessing unpaired electrons and defect sites in the lattice which have trapped holes or electrons. In semiconductors the conduction electrons and holes can make a contribution to the paramagnetic susceptibility. In all these cases, transitions between Zeeman levels produced by an external magnetic field can be observed, under the correct experimental conditions. The usual theories of paramagnetism in solids treat the magnetic properties in terms of the permanent magnetic dipoles associated with the unpaired electrons and are, therefore, concerned with the calculation of the dipole moments.

The most commonly studied paramagnetic systems are those of the 3d transition and rare earth group ions. The theory of electron spin resonance (e.s.r.) of these ions is concerned with the modifications of the energy levels of the free ion, which result from the interaction of the ion with the crystal lattice. With defect centres this

approach must be modified since there is no 'free-ion' analogue, as is shown in section 3-4.3.

3-2 The resonance condition

Consider a free ion, with a resultant total electronic angular momentum J, placed in a magnetic field H. The Zeeman energy levels are given by:

$$W = g\beta H.m$$

where g is the Landé g-factor $= 1 + \frac{J(J+1) + S(S+1) - L(L+1)}{2J(J+1)}$

$\beta$ is the Bohr magneton.

L and S are the orbital and spin angular momentum vectors respectively, and m is the component of J in the direction of the magnetic field and can take the values J, J-1, --- -J + 1, -J.

If an alternating magnetic field of frequency $\nu$ is applied perpendicular to H, then magnetic dipole transitions are induced according to the selection rule $\Delta m = \pm 1$

The magnetic field $H_R$ required for a given frequency with a quantum energy ($h\nu$) is given by:

$$h\nu = g\beta H_R$$

where h is Planck's constant.

The simplest case that can be envisaged is that of a single unpaired electron with zero orbital angular momentum, L = 0. The Landé g-factor is then 2 (strictly 2.0023). In a system in thermal equilibrium, the lower electronic energy states have a higher probability of occupation so that power is absorbed from the alternating magnetic field. Some mechanism must be present whereby the absorbed energy can be dissipated from the spin system to maintain the Boltzmann population distribution and allow the e.s.r. to be observed. The most important of these mechanisms is transfer of spin energy to the lattice via the spin-orbit interaction. This is the well-known spin-lattice relaxation process. The relaxation processes will not be discussed further, but it should be remembered that they must be present to allow observations of the e.s.r. absorption. The value of the spin-lattice relaxation time influences the choice of the experimental conditions for observation of an e.s.r. transition. For a transition where the spin-lattice relaxation is $<10^{-6}$ seconds the absorption is very broad and is usually unobservable. The spin-lattice relaxation time increases with decreasing temperature and so low temperatures are frequently necessary for the observation

of e.s.r. signals e.g. the e.s.r. due to the $Cr^{2+}$ ions in Cadmium Sulphide can only be observed at temperatures below about $10^{o}K$. For transitions where the relaxation time is $>10^{-2}$ seconds the absorption becomes 'saturated' at incident power levels greater than about a few m. watts. In these conditions the absorbed energy is not dissipated sufficiently rapidly from the spim system and the Boltzman population distribution is disturbed. The population of the higher lying state begins to approach that of the lower state and so the intensity of the e.s.r. absorption line is reduced and in the limit of very high power disappears altogether. Under these conditions broadening of the e.s.r. line is frequently observed. Consequently the experimental operating conditions must be chosen taking these considerations into account. Considerations of sensitivity, as we shall see in chapter 4 show that it is preferable to employ an a.c. magnetic field of the highest possible frequency. In practice r.f. microwave power in the frequency range 1,000 - 30,000 Mc/s. is used, which, since $h\nu = g\beta H_R$, necessitates d.c. magnetic fields ($H_R$) between 1 and 25 Kgauss.

3-2 Paramagnetic Ions in solids

The interactions between a paramagnetic ion and the surrounding ions in a solid are of two types:-

(a) Interactions between the paramagnetic ion and the

neighbouring diamagnetic ions in the lattice.

(b) Interactions between the magnetic dipoles of the paramagnetic ions in the solid.

In this discussion we will assume that the paramagnetic ions are present as impurity atoms in a diamagnetic solid. Further we will assume that the concentration of the paramagnetic impurity is low ($< 0.1\%$) and so interactions of the type (b) will be neglected. The vast majority of experimental work has been performed on such magnetically dilute systems.

The interactions of the paramagnetic centres with the surrounding diamagnetic ions can be treated using the simple concept of the crystal electric field originated by Van Vleck[1]. The paramagnetic ion is treated as a free ion which is situated in an external static electric field of the surrounding diamagnetic ions. The symmetry of the crystal field is determined by the arrangement of the diamagnetic ions around the paramagnetic site. This method is capable of explaining, in a qualitative way, the structure of the lowest energy levels of a paramagnetic ion.

The Hamiltonian of a paramagnetic ion in a solid can be expressed in the following form:-

$$\mathcal{H} = \mathcal{H}_0 + \mathcal{H}_c + \lambda \underline{L} \cdot \underline{S} + \beta(\underline{L} + 2\underline{S}) \cdot H \qquad (3\text{-}1)$$

where $\mathcal{H}_o$ is the Hamiltonian of the free ion. This formulation ignores spin-orbit interaction of the free ion. $\mathcal{H}_c$ represents the interaction with the crystal electric field, which can be written:-

$$\mathcal{H}_c = \sum_i eVc\ (x_i, y_i, z_i)$$

The summation is carried out over all the surrounding ions. $V_c$ is the crystal electric field potential. $\lambda \underline{L}.\underline{S}$ is the spin-orbit interaction. Where $\lambda$ is a constant $\beta\ (\underline{L} + 2\underline{S}).H$ is the interaction with the applied magnetic field. $\underline{L}$, $\underline{S}$ refer to the operators of total orbital and spin angular momentum as usual.

Dipolar and exchange interactions between the paramagnetic ions are neglected since the system is magnetically dilute.

The Hamiltonians of most free ions ($\mathcal{H}_o$) have been calculated for use in the field of atomic optical spectroscopy. For a full discussion the reader is referred to the text by Condon and Shortley[2]. With free ions the most important interaction is due to coulomb forces. The self consistent field (s.c.f.) method considers a simplified coulomb interaction where the electrons move independently of each other within the restrictions of the exclusion principle. The resultant eigenstates are referred to as

'configurations' in which the individual electron orbits are specified, e.g. $3d^3$, $3d^{10}4s^1$ etc. Account is next taken of the correlation between the electrons, which the s.c.f. method does not deal with fully, and at the same time terms are included to represent spin-spin and orbit-orbit interactions. The result is that the configurations are split into 'Terms', i.e. into levels which are specified by total orbital and spin moments, e.g. $^4F$. This represents the case of Russell - Saunders coupling which is applicable to the lighter atoms on which most of the e.s.r. work to date has been performed. Finally, in the case of a free ion, the spin orbit interaction is included. This removes some of the Term degeneracy and couples the orbital ($\underline{L}$) and spin ($\underline{S}$) moments to give states of well defined ($\underline{J}$), where $\underline{J} = \underline{L} + \underline{S}$.

A possible energy level scheme for a free ion is shown in Fig. 3-1, where the Term splittings and the effect of the spin-orbit interactions are indicated.

It follows from this discussion that the term $\mathcal{H}_o$ in the Hamiltonian (3-1) represents the Hamiltonian for the Term states of the free ion. The other interactions in equation (3-1) can now be considered as perturbations on $\mathcal{H}_o$. We will consider two common cases:-

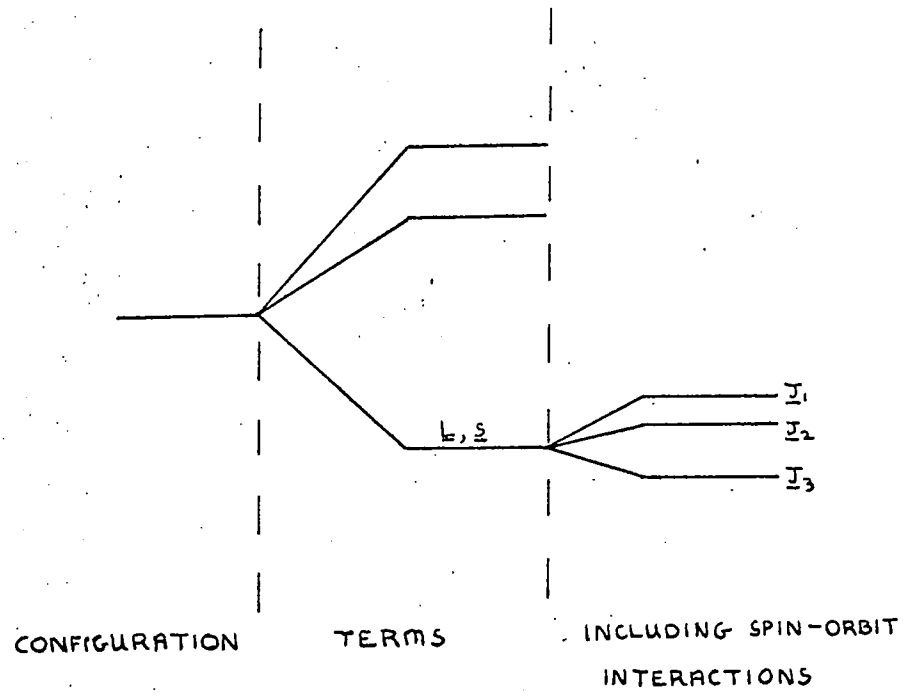


FIG. 3-1 Energy level scheme for a free ion.

(a)'Medium' crystal fields. Where the magnitudes of the interactions are:-

$$\mathcal{H}_o > \mathcal{H}_c > \mathcal{H}_{\text{spin-orbit}}$$

this applies for most of the iron group (3d) ions.

(b) 'Weak' crystal field. Where:-

$$\mathcal{H}_o > \mathcal{H}_{\text{spin-orbit}} > \mathcal{H}_c$$

this applies for the rare earth (4f) group ions.

3-3.1 Iron group

By far the largest term in the perturbation is the crystal field interaction. The 'magnetic' electrons of an atom of the iron group, which belongs to the 3d atomic orbital shell, are strongly exposed to this field. We only consider the effect of the crystal field on the ground state Term since this is the only state populated at room temperature. The Term splittings are usually sufficiently large for interactions between the excited and ground Terms to be ignored and the perturbation is only taken to first order. The crystal field potential (Vc) is assumed to satisfy Laplace's equation so that it can be expressed as a sum of spherical harmonics:-

$$V_c = \sum_{n,m} A_n^m \, r^n \, Y_n^m \, (\theta, \phi) \qquad (3\text{-}2)$$

Ignoring any effects of covalent bonding.

The symmetry of the nearest neighbour ions will determine the exact form of the expansion (3-2). A crystal field potential with octahedral cubic symmetry has the form:

$$V_c = A_4^0 \, \bar{r}^4 \left[ Y_4^0 \, (\theta,\phi) + \left(\frac{5}{14}\right)^{\frac{1}{2}} \left\{ Y_4^4 \, (\theta,\phi) + Y_4^{-4} \, (\theta,\phi) \right\} \right] \qquad (3\text{-}3)$$

along the 4-fold rotation axes.

This can be expressed in terms of the cartesian co-ordinates of the electrons of the paramagnetic ions as:

$$V_c = C_4 \, (x^4 + y^4 \, X \, z^4 - \tfrac{3}{5} \, r^4) + D_6 \, (x^6 + y^6 + z^6) \qquad (3\text{-}4)$$

Cubic symmetry is usually found in iron group salts. Other important crystal field potential functions for various crystalline lattice symmetries are given in the review article of Low[3].

The procedure is to set up the secular determinant by evaluating the matrix elements of Vc between the eigen-functions of the ground state Terms. Solution of the secular determinant gives the required eigenstates i.e. the splittings of the ground state Term due to the crystal

field interaction. The effect of the crystal field is to remove some or all of the orbital degeneracy (no forces to couple spin and orbital moments have been included yet). For the iron group ions the crystal field perturbation is frequently sufficient to remove the orbital degeneracy and leave the lowest state as an orbital singlet. This ground state then has spin degeneracy (2S + 1) only. The orbital magnetic moment is said to have been 'quenched' and to first order approximations the magnetic properties of the ion are determined by the electron spins alone.

Spin Hamiltonian

The effect of the rest of the terms in the Hamiltonian (3-1) on the levels produced by the crystal field interactions must be considered next. A useful method for carrying out the perturbation calculations has been given by Pryce[4] and presented in detail in the review articles of Bleaney and Stevens[5] and Bowers and Owen[6]. This method is only applicable when the lowest state is an orbital singlet, which as we have seen is common for the iron group ions. The method consists of carrying out a non-degenerate perturbation treatment where the operators referring to spin variables are treated as non-commuting algebraic quantities. Consequently an expression is obtained which contains components of $\underline{S}$. This is the

so-called spin-Hamiltonian in which the change in energy of the orbital ground state due to the excited orbital states has been taken into account. The spin-Hamiltonian is then made to operate on the spin degenerated ground orbital state and the eigenvalues obtained are the energy levels of the spin states between which the e.s.r. is observed, i.e. the spin-Hamiltonian ($\mathcal{H}_s$) is defined as:-

$$\mathcal{H}_s|m\rangle = E_m|m\rangle$$

where $|m\rangle$ represents the eigenfunction of the $m^{th}$ spin state (using the Dirac notation).
The first order correction to the energy of the ground state orbital singlet is given by:-

$$\langle o|\beta(\underline{L}+2\underline{S}).H+\lambda\underline{L}.\underline{S}|o\rangle \qquad (3\text{-}5)$$

where $|o\rangle$ and $|n\rangle$ represent the orbital wavefunction of the ground and $n^{th}$ excited orbital state respectively.
The correction terms (3-5) reduce to:-

$$2\beta\underline{H}.\underline{S} \qquad (3\text{-}6)$$

using a general theorem of quantum mechanics, the expectation value of $\underline{L}$ i.e. $\langle o|\underline{L}|o\rangle$ in an orbital singlet is zero.

The second order correction is:-

$$-\sum_{n\neq o}\frac{|\langle o|\beta \underline{H}.(\underline{L}+2\underline{S})+\lambda \underline{L}.\underline{S}|^2}{E_n-E_o} \qquad (3\text{-}7)$$

Terms not involving orbital operators vanish, by orthogonality.

i.e. $\langle o|n\rangle$ when $n\neq o$

The non-vanishing elements such as $\langle o|L_x|n\rangle$, $\langle o|L_y|n\rangle$ etc. must be evaluated in each case, but here it is sufficient to notice that the final result will be quadratic in components of $\underline{H}$ and $\underline{S}$, and thus will take the form:-

$$\sum_{i,j} -\beta^2 \Lambda_{ij} H_i H_j - \beta f_{ij} H_i \underline{S}_i + d_{ij} \underline{S}_i \underline{S}_j \qquad (3\text{-}8)$$

where i, j refer to cartesian co-ordinates x, y or z and $f_{ij}$ and $d_{ij}$ are matrix elements.

Pryce[4] has shown that (3-8) can be rewritten:

$$\sum_{i,j} \Lambda_{ij}\left[\beta^2 H_i H_j - 2\beta\lambda H_i \underline{S}_i - \lambda^2 \underline{S}_i \underline{S}_j\right] \qquad (3\text{-}9)$$

where

$$\Lambda_{ij} = \sum_{n\neq o}\frac{\langle o|\underline{L}_i|n\rangle\langle n|\underline{L}_i|o\rangle}{E_n-E_o} \qquad (3\text{-}10)$$

It is usually unnecessary to include any higher perturbation

theory. So that the first and second order terms (3-6) and (3-9) are summed together to give the spin-Hamiltonian:

$$\mathcal{H}_s = \sum_{i,j} \beta H_i (2\delta_{ij} - 2\lambda \Lambda_{ij}) \underline{S}_j - \lambda^2 \Lambda_{ij} \underline{S}_i \underline{S}_j \quad (3\text{-}11)$$

In this expression the term $H_i\ H_j$ has been ignored since it is spin independent and is only an additive constant. It corresponds to a temperature independent paramagnetic susceptibility term. The spin-Hamiltonian can be written in a more convenient form:-

$$\mathcal{H}_s = \beta \underline{H} . g . \underline{S} + \underline{S} . D . \underline{S} \quad (3\text{-}12)$$

where g and D are tensors.

The tensor D describes the splitting of the spin levels in zero magnetic field. The spectroscopic splitting factor g gives the splitting under the influence of an applied magnetic field:-

$$g = 2(1 - \lambda \Lambda_{ij}) \quad (3\text{-}13)$$

This form emphasises the contribution of the higher orbital states via the spin-orbit coupling. For high lying excited orbital states $\Lambda_{ij}$ is small and the g-value approaches the free spin value of 2.

The usefulness of the spin-Hamiltonian lies in the fact that it provides a 'short hand' description of the experimentally observed e.s.r. spectrum in terms of a few parameters such as g and D.

In principle, it is a simple matter to obtain the spin energy levels. A convenient form is taken for the spin-Hamiltonian and the secular determinant is set up by evaluating matrix elements of the spin-Hamiltonian between the spin states. The solution of the secular determinant determines the spin energy levels. In general g and D are anisotropic and the e.s.r. spectrum depends on the orientation of the magnetic field in relation to the axes of crystal symmetry.

If the crystal field perturbation is such that orbital degeneracy remains in the ground state, the derivation of the spin-Hamiltonian described above is invalid. Degenerate perturbation methods must be used, in which small distortions of the basic crystal symmetry are considered. Such distortions will automatically occur via the Jahn-Teller effect. If an ion has a degenerate ground state, paramagnetic and surrounding ions will distort their symmetry in such a way that as much of the degeneracy of the paramagnetic ion as possible is removed. Jahn-Teller distortions along with the spin-orbit interaction, can in

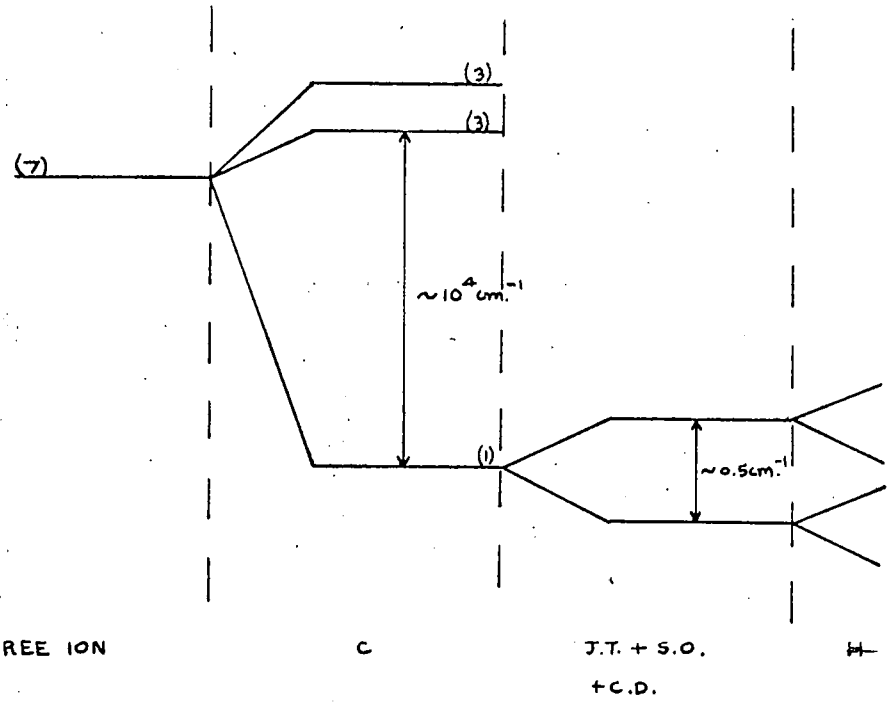


c=cubic field H=magnetic field

J.T.= Jahn-Teller distortion s.o. = spin-orbit coupling

C.D. = crystal distortion(orbital degeneracy shown in parentheses)

FIG. 3-2 Crystal field splittings in the $Cr^{3+}$ ion(not to scale).

principle remove all the degeneracy (orbital and spin) when the number of electrons is even. Then singlet states result, which are well separated from each other (unlike the small zero field splittings encountered when the orbital moment is quenched) and no e.s.r. transitions are to be expected unless the radio frequency is high. Kramer's theorem states when the number of electrons is odd each electronic state must be at least doubly degenerate. A single e.s.r. transition will be observed for the lowest doublet, which may be described by a spin-Hamiltonian as before, in which a fictitious spin $s' = \frac{1}{2}$ is used. Fig. 3-2 shows the splittings due to the various perturbations outlined above for the $Cr^{3+}$ ion.

3-3.2 Rare earths

The 'magnetic' electrons for this group belong to 4f atomic shell and consequently lie well within the core of the atom and do not interact very strongly with the crystal electric field. As a result the spin-orbit interaction is the major perturbation. As is well known in atomic theory the spin-orbit coupling splits the Terms of the atomic configuration into states characterised by the total angular momentum (J). Each state then has degeneracy (2J + 1).

The effect of the crystal field is considered last. Unlike the iron group, the rare earth salts have crystal fields of low symmetry. The ethyl sulphates for example have a crystal field potential of the form [5,6]:-

$$V_c = A_2^o (3z^2-r^2) + A_4^o (35z^4-30r^2z^2 + 3r^4) + A_6^o (213z^6 -315r^2z^4 + 105r^4z^2 - 5r^6) + A_6^6 (x^6-15x^4y^2 + 15x^2y^4-y^6)$$

(3-14)

By evaluating the matrix elements of this perturbation the secular determinant can be set up as before and the eigenvalues of the new states calculated. The symmetry of the field is so low that singlet electronic states result if the number of electrons is even and doublets when the number is odd (Kramer's doublets).

3-3.3 Hyperfine interactions

When the nucleus of the paramagnetic ion possesses a resultant nuclear magnetic moment a so-called hyperfine interaction occurs between the electrons and the nucleus. If the nuclear spin is $\mathbb{I}$, then in an applied magnetic field each electron spin level is split into $2I + 1$ equally spaced ones, due to the quantisation of the

nuclear magnetic moment in the applied magnetic field. To account for this, a term $A.\underline{S}.\underline{I}$ is added to the total Hamiltonian (3-1). It is of smaller magnitude than the other terms and therefore is included in the spin-Hamiltonian. The effect of the interaction is to split each e.s.r. transition into $2I + 1$ lines of equal intensity. Often these hyperfine components are not resolved, being enclosed in the envelope of the inherent e.s.r. line width. Howeverwhen they can be resolved they provide a very useful check on the origin of the e.s.r. spectrum, since the values of the nuclear spins of the paramagnetic ions are usually known.

3-4 Electron Spin Resonance in Semiconductors

The electrical and optical properties of semiconductors are sensitive to small concentrations of impurities and defects in the lattice (see chapter 2). Electron spin resonance is one of the most sensitive and powerful tools for investigating the detailed nature of imperfection sites. Moreover it is often possible to study one imperfection in the presence of a much larger concentration of other imperfections. This is rarely possible with the techniques outlined in section 2-3 and explains, in part, the tremendous interest in the e.s.r. of semiconductors at the present time. The usefulness of the e.s.r. technique

can be greatly enhanced by the simultaneous use of optical excitation. Many of the defects contain electrons which remain paired because of compensation effects, especially in the 2-6 compounds, and no paramagnetism results. Similarly an impurity centre may be in a charge state which renders it diamagnetic. In such cases optical excitation to remove or add an electron to the defect or impurity site can be very useful. Light with photon energy greater than the band gap creates electron hole pairs and either of these charge carriers may be trapped at the imperfection. Light with photon energy less than the band gap may also be effective in adding or removing an electron from an imperfection site. This technique was used during the course of the work reported in this thesis. So far the theory of e.s.r. of paramagnetic ions in ionic solids only has been considered. Clearly, in discussing the e.s.r. in semiconductors, it will be necessary to take into account the partially covalent nature of the bonding that exists between the ions. The discussion will be mainly limited to the 2-6 compounds.

3-4.1 Paramagnetic ions in 2-6 compounds

Many of the 3d iron group and 4f rare earth group ions have been studied in 2-6 compounds. For a review of the work performed up to 1965 see Ref. (7). The form of the e.s.r.

spectra that have been obtained can be adequately explained using the same treatment as for ionic solids, and ignoring any effects of covalency. This is a further indication that the bonding in 2-6 compounds is mainly ionic and is in agreement with the figure of 75% quoted in section (2-1), as the ionic contribution to the bonding in Cds.

However when this treatment is used to estimate the value of the coefficients occurring in the spin-Hamiltonians derived for the iron group ions, e.g. the g-factors, some discrepancies are revealed. In particular it is found that the spin-orbit coupling and hyperfine interaction constants are different from those calculated using the purely ionic model. As a result the basic assumptions of the theory of the static crystal field potential must be reconsidered. The central assumption is that the charged ions surrounding the paramagnetic site can be regarded as point charges. Obviously this is not true in partly covalent solids, since the wave functions of the 3d-electrons of the paramagnetic iron group ions must overlap the wavefunctions of the surrounding ions to some extent. Therefore one cannot speak of the pure d-orbitals of the free paramagnetic ion, but must take into account the wavefunction of the whole complex, e.g. $XY_4$ for a tetrahedral

system where X represents the paramagnetic ion. One possible scheme is to form molecular orbitals from the atomic orbitals of the complex, which correspond to the scheme of symmetry appropiate to the crystal, and to treat the crystal field potential as a perturbation of these new states.

It is however convenient at this stage to consider the splittings of the 3d states in an ionic cubic crystal. A single 3d electron has two units of angular momentum and therefore five orbital states are available to it in the free ion. In a crystal field of tetrahedral cubic symmetry the five states are split into a triplet (described as $(t_2)$ in the conventional group theoretical nomenclature) and a doublet (e), where the doublet has the lower energy. (In the octahedral crystal field usually found in iron group salts the triplet is lower). The spatial parts of the d-wavefunctions vary with direction in the following way:-

( $d\gamma$ ) or e-states $(x^2 - y^2)$, $(3z^2 - r^2)$

( $d\varepsilon$ ) or $t_2$-states xy, $y_z$, zx

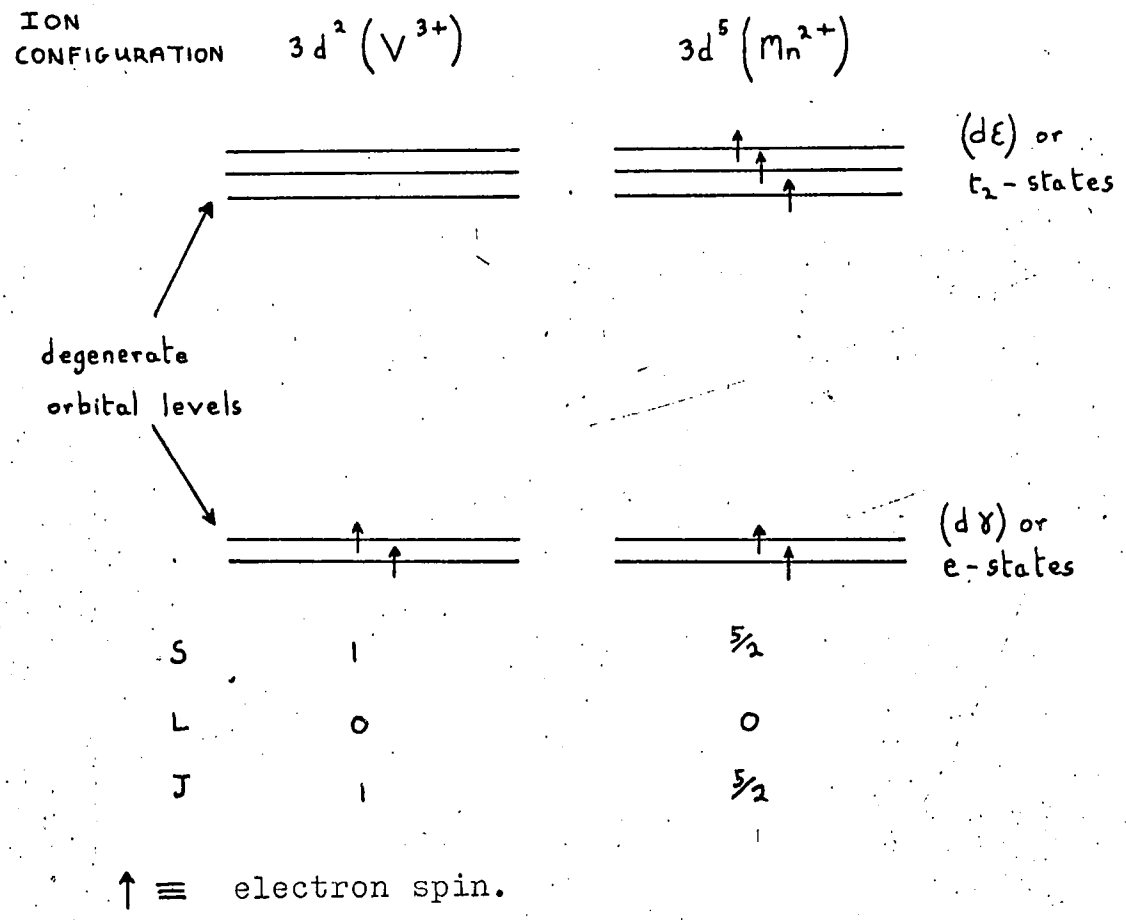


FIG.3-3. Alignment of the electrons spins in the orbital levels for the $3d^2$ and $3d^5$ configurations of the iron group ions in a tetrahedral cubic crystal field.

The splittings between the doublet and triplet are sufficiently small for Hund's rule to be obeyed, then for a configuration $d^n$, the n electron spins arrange themselves among the levels to give maximum spin consistent with the exclusion principle. Thus the configurations $3d^2$, $3d^5$ and $3d^7$ are effective orbital singlets. The configuration $3d^2$ and $3d^5$ are shown schematically in fig. 3-3. The 4s electrons are not required for bonding to the nearest neighbours and are transferred to the 3d shell.

The covalent bonding (molecular) orbitals between the ions can be divided into two kinds $\sigma$- and $\pi$ - orbitals. The $\sigma$-orbitals possess zero angular momentum about the bond axis and are formed when the atomic orbitals which overlap are both directed along the bond axis. The $\pi$-orbitals have unit angular momentum about the bond axis and are formed when the overlapping atomic orbitals are directed perpendicularly to the bond axis.

The consequence of the formation of these molecular orbitals is that the ($d\gamma$) states of the free ion must now be expressed as a linear combination of the ($d\gamma$) orbitals of the central ion plus $\pi$-and$\sigma$-orbitals of the surrounding ions. Similarly for the ($d\varepsilon$) states of the free ion. The appropriate combination must have the

transformation properties under rotations and reflections of the symmetry group of the crystal. The greater the degree of covalent bonding in the solid the larger is the contribution of the $\sigma$-and $\pi$-orbitals to the molecular orbitals.

Owen[8] and Tinkham[9] have discussed the appropiate linear combination for the six-fold co-ordinated iron group salts. In this case the ions surrounding the paramagnetic site are along the x, y and z axes used to define the spatial variations of the d-states of the free ion, which leads to a simplification in the linear combinations required. The modified ($d\varepsilon$) states are composed of the ($d\varepsilon$) states of the free ion plus $\pi$-orbitals from the surrounding ions and the modified ($d\gamma$) states from ($d\gamma$) states of the free ion plus $\sigma$-orbitals from the surrounding ions. Using the modified orbital functions a modified spin-Hamiltonian is derived and in this way the change in the spin-orbit coupling and hyperfine interaction constants due to the covalent contribution can be calculated. This method of analysis leads to the following changes in the magnetic properties of the iron group ions in partially covalent solids:-

(a) The covalent bond reduces the orbital contribution to the g-factor.

(b) There is a reduction in the second order contribution

of the spin-orbit coupling to the g-factor.

(c) The hyperfine structure constant is reduced.

(d) There may be an additional hyperfine interaction between the magnetic electrons and the surrounding nuclei. This can arise because the electron wave-functions of the paramagnetic ion now approach the surrounding nuclei more closely than in the ionic solids. This is referred to as super hyperfine structure in an e.s.r. spectrum.

These conclusions have been shown to apply in the case of the 3d group ions in 2-6 compounds.

There is little reported work on the e.s.r. of rare earth ions in 2-6 compounds. No firm conclusions concerning the environment of the rare earth impurity can as yet be drawn from the limited number of results available. However the results so far obtained have been adequately described in terms of the rare earth ion substituting for the group 2 ion and using the theory of section (3-3.2). The effects of covalency will be less marked for the rare earth ions than for the iron group since the 'magnetic' electrons are in the core of the ion.

In the data so far reported on 2-6 compounds, the spectra of the 3d and 4f ions display the full symmetry of the substitutional site indicating that there is no association

of the impurity ions with defects.

3-4.2 Shallow donor impurities

As we saw in chapter 2, substitutional elements of group 3 of the periodic table which occupy the group 2 ion site or elements of group 7 substituted for group 6 ion site act as shallow donors. There are no shallow acceptor impurity centres in CdS and there is little evidence for interstitial donor sites and so we shall not discuss these cases. There are features which are common to all the resonances observed for these shallow donor impurities in the 2-6 compounds. The e.s.r. in each case consists of a single absorption line with a g-value less than the free electron value of 2 and does not show hyperfine structure even when the donor nucleus has a non-zero angular momentum. Since no hyperfine structure is observed, identification of the centre responsible for the e.s.r. line has usually been made from knowledge of the impurities added during sample preparation.

Lambe and Kikuchi[10] noted that a similarity existed between the donors in 2-6 compounds and the F-centres in alkali halides. By use of an F-centre type wavefunction for the donor, they could account qualitatively for the departure of the g-value from 2. However this model could not explain the absence of any hyperfine structure in the

resonance. The model suggested by Müller and Schneider[11] seems to be more adequate. They noted that in CdS the g-values of the donor electron at a Chlorine and a Galluim substitutional site are almost identical and are in agreement with the g-value for conduction electrons obtained from the analysis of Hopfield and Thomas[12] of the bound and free exciton optical emission spectra in CdS. (The results of this paper were discussed in section (1-2) when dealing with the nature of the band structure in CdS). Hopfield and Thomas point out the g-values of the conduction electrons are essentially determined by the intrinsic band properties of CdS. This suggested to Muller and Schneider that an appropiate wavefunction for the donor electron could be constructed in a manner similar to that for donor electrons in germanium and silicon suggested by Kohn and Luttinger (13,14). Kohn and Luttinger used a Hydrogenic model for the donor electron, which is shown to move in an orbit of large radius (typically 30 Å). Since the electron is weakly bound to the donor impurity its properties are determined mainly by the band structure and dielectric constant of the host lattice. Using this model Kohn and Luttinger obtain solutions for the wavefunction of the donor electron of the form:-

$$\psi(r) = \sum_i \alpha_i \cdot F_i(r) \cdot \psi_i(\underline{K}, r)$$

where $\alpha_i$ are coefficients, $\psi_i(\underline{K}, r)$ are Bloch functions of electrons at the $i^{th}$ minimum of the conduction band and $F_i(r)$ are hydrogen-like modulating functions.

Following this treatment, Roth[15] showed that when the band structure is known the shift of the g-value of the donor electrons from the free electron value because of spin-orbit coupling can be calculated. Ludwig and Woodbury[7] gave the following expressions for the shifts, which are more readily applicable than those found in Roth's original paper:-

$$g_{//} = 2 + I_m \frac{4}{m_e} \sum_{n \neq o} \frac{\langle (+)|P_x|n\rangle\langle n|P_y|(+)\rangle}{E_n - E_o} \qquad (3\text{-}15)$$

$$g_{\perp} = 2 - I_m \frac{2}{m_e} \sum_{n \neq o} \frac{1}{E_n - E_o} \left\{ \langle (+)|P_y|n\rangle\langle n|P_z|(-)\rangle + \langle (-)|P_y|n\rangle\langle n|P_z|(+)\rangle \right\} \qquad (3\text{-}16)$$

for the directions // and $\perp$ to the z-axis of ellipsiod of the constant energy surface of the conduction band in K-space. Where $|(+)\rangle$ and $|(-)\rangle$ are the two spin states of the band considered and $|n\rangle$ is the excited state which is coupled to the ground state by the spin-orbit interaction and is at energy En-Eo above the ground state.

This model can explain the lack of hyperfine structure in the resonance so far observed. If the concentration of donors ($N_D$) is such that the average donor separation is equal to the diameter of the donor electron orbit, then the electron can move from orbit to orbit since they overlap. The electrons are then no longer localised at single donor sites, but become mobile. Resonances of electrons localised at donor sites have been observed in germanium and silicon (for a review of the work, see the review article of Ludwig and Woodbury[7]) and in these cases hyperfine structure due to the donor nuclei was observed. However as the concentration of donors was increased and the electrons became non-localised, the resonance no longer showed hyperfine structure and a single line appeared at a g-value almost identical to that in the localised case. Muller and Schneider[11] have calculated the concentration

of donors in 2-6 compounds at which delocalisation of the donor electrons occurs to be of the order of $10^{17}$ per $cm^3$. They concluded that ~~in~~ all the donor electron resonances so far observed in 2-6 compounds have been for donor concentrations equal to or exceeding this value and that localised donor electron resonances will not be observed until better material is available. In many cases, including CdS, account must be taken of the super hyperfine interactions with the host lattice which may cause line broadening or in certain cases even split the lines.

3-4.3 e.s.r. of defect centres in 2-6 compounds

There is little reported data on the d.s.r. of defect centres in 2-6 compounds. Anion (group 6) vacancies will act as shallow donor centres and Morigaki[16] has reported the e.s.r. of isolated sulphur vacancies in CdS and Kasai and Otomo[17] of Sulphur vacancies in ZnS. These are the only reported resonances of isolated defect centres. However Dielman et al[18] have observed the e.s.r. of what is believed to be a complex donor centre in ZnS. This centre consists of a Sulphur vacancy in nearest neighbour association with a group 1 impurity (Cu., Ag. or Au.) substitutional at a Zinc site. There have also been reports of the e.s.r. of a complementary complex acceptor

centre (the so called 'A' centre) in ZnS[17] and ZnTe[19]. The A centre consists of a Zinc vacancy in association with a donor impurity from either group 3 (Ga., Al., In.) or group 7 (Cl., I.) of the periodic table. It is not possible to outline a general treatment which describes the e.s.r. of defect centres, as was done for the 3d and 4f group ions, since there is no 'free-ion' analogue for a defect centre. The approach usually adopted is to assume that the defect possesses one unpaired electron which has zero angular momentum i.e. assume that the ground state electronic state has $S = \frac{1}{2}$, $L = 0$. This is done because the experimentally observed g-values are only slightly shifted[17,18,19] from the 'spin-only' value of 2. The value of the g-shift is calculated from the assumed model of the centre, by taking account of the spin-orbit coupling between the ground state and first excited state. This requires knowledge of the wavefunction of the electron in the two states by anology with the derivation of the spin-Hamiltonian for ground state orbital singlets in section 3-3.1. Clearly these must be evaluated for each individual model so that a general treatment of the problem would be inappropriate.

The calculations can only provide order of magnitude estimates of the g-shift and so the e.s.r. results can only give an indication of the correctness or otherwise of

the proposed model. Similarly other methods for investigating the centre e.g. luminescence, photoconductivity, etc. cannot provide definite proof that the atomic nature of the defect centre which has been assumed is correct. Thus the criterion for adopting a particular model for a defect centre is its ability to explain all the experimentally observed data more adequately than any other model.

## REFERENCES

(1) J. H. Van Vleck - J. Chem. Phys. 7, 72, 1939.

(2) E. H. Condon and J. H. Shortley - "Theory of Atomic Spectra" C.U.P. London and New York. 1935.

(3) W. Low - "Paramagnetic Resonance in Solids". Solid State Physics, Supplement 2, Section 5. Academic Press. 1960.

(4) M. H. Pryce - Proc. Phys. Soc. A63,25, 1950.

(5) B. Bleaney and K. W. H. Stevens - Rep. Prog. Phys. 16, 108, 1953.

(6) K. D. Bowers and J. Owen - Rep. Prog. Phys. 18, 304, 1955.

(7) G. W. Ludwig and H. H. Woodbury - Solid State Physics 13, 233, 1962.

(8) J. Owen - Disc. Faraday Soc. 19, 127, 1955.

(9) M. Tinkham - Proc. Roy. Soc. A236, 549, 1956.

(10) J. Lambe and C. Kikuchi - J. Phys. Chem. Sols. 9, 492, 1958.

(11) K. A. Muller and J. Schneider - Phys. Letts. 4, 288, 1963.

(12) J. J. Hopfield and D. G. Thomas - Phys. Rev. 122, 35, 1961.

(13) J. M. Luttinger and W. Kohn - Phys. Rev. 97, 869, 1955

(14) W. Kohn and J. M. Luttinger - Phys. Rev. 98, 915, 1955

(15) L. M. Roth - Phys. Rev. 118, 1534, 1960.

(16) K. Morigaki - J. Phys. Soc. Japan 19, 1253, 1964.

(17) P. H. Kasai and Y. Otomo - J. Chem. Phys. 37, 1263, 1962.

(18) J. Dieleman, S. H. DeBruin, C. Z. VanDoorn and J. H. Haanstra - Philips Res. Reports 19, 311, 1964.

(19) R. S. Title, G. Mandel and F. F. Morehead - Phys. Rev. 136, A300, 1964.

# CHAPTER 4

## 3 cm. MICROWAVE SPECTROMETER

### 4-1 Introduction

For economic reasons it was necessary to construct the microwave spectrometer. The object was to design an arrangement with high sensitivity because of the unknown nature of the expected signals. The spectrometer was built around a Newport Instruments magnet of pole face diameter 4 inches, which gave a maximum magnetic field of 6 Kgauss at a pole gap of 2 inches, with a field stability of 1 part in $10^4$ over a volume of about 1 $cm.^3$.

### 4-2 Sensitivity Considerations

The theoretical sensitivity of an electron spin resonance (e.s.r.) spectrometer has been discussed extensively by various authors, including Ingram[1], Feher[2], Misra[3], Goldsborough and Mandel[4], Teaney, Klein and Portis[5] and Low[6].

A determination of the sensitivity can be divided into two main sections:-

(1) The calculation of the maximum possible signal obtainable for a given concentration of paramagnetic centres.

(2) The calculation of the minimum detectable signal in a spectrometer, including a discussion of practical detection systems.

## 4-2.1 Power absorbed in the sample

The susceptibility of a paramagnetic material ($\chi$) is a complex quantity and can be written:-

$$\chi = \chi' - i\chi''$$

where $\chi'$ is the 'in-phase' susceptibility and $\chi''$ the 'out-of-phase' susceptibility.

The magnetisation (M) produced when the material is placed in an r.f. field of amplitude $H_1$, and angular frequency $\omega$ is:-

$$M = H_1 \sin\omega t.\ \chi' - H_1 \cos\omega t.\ \chi'' \qquad (4\text{-}1)$$

The power absorbed in the sample is $H_1.dM$, so that the average power ($P_A$) absorbed per unit volume of sample is:-

$$P_A = \tfrac{1}{2}\omega H_1^2\ \chi'' \qquad (4\text{-}2)$$

i.e. the power absorbed is proportional to the imaginary part of the susceptibility ($\chi''$). The power reflected or transmitted after being incident on the sample also experiences a phase shift which is associated with the real part of the susceptibility ($\chi'$).

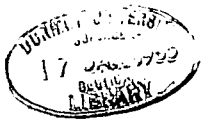

4-2.2 Q-changes associated with the absorption

From equation (4-2) it is evident that a large r.f. magnetic field is required to obtain a large power absorption (with the power levels used in practice $\chi''$ is only slightly dependent on $H_1$). Consequently a resonant cavity is used in nearly all experimental arrangements and was used in our system. The cavity should have a high Q-value and a resonant frequency very close to the operating frequency, (the cavity used in our system had a Q of about 5,000). The Q-value of the cavity changes when power is absorbed in the sample and it is this change in Q which is detected by the spectrometer. The Q of a cavity containing a paramagnetic sample at resonance is given by:-

$$Q = \omega \times \frac{\text{energy stored}}{\text{average power dissipated}} = \frac{\omega \frac{1}{8}\pi \int_{V_c} H_1^2 \cdot dV_c}{P_w + \frac{1}{2}\omega \int_{V_s} H_1^2 \cdot \chi'' \cdot dV_s} \qquad (4\text{-}3)$$

where $P_w$ is the power dissipated in the cavity walls, $V_c$ is the cavity volume and $V_s$ the sample volume.
For the case where the absorption due to the sample resonance is small, equation (4-3) can be expressed to give:-

$$Q = Q_o \left[ 1 - \frac{4\pi \int_{V_s} H_1^2 \cdot \chi'' \cdot dV_s}{\int_{V_c} H_1^2 \cdot dV_c} \cdot Q_o \right] = Q_o \left[ 1 - 4\pi \chi'' \eta Q_o \right]$$

where $Q_o$ is the cavity Q in the absence of cavity losses and $\eta$ is a filling factor which depends on the field distribution in the cavity and sample.

If $\Delta Q$ is the change in cavity Q due to sample absorption then:-

$$\Delta Q = 4\pi \chi'' \eta Q_o^2 \qquad (4\text{-}4)$$

A simple spectrometer arrangement employing a reflection cavity is shown in Fig. 4-1. Throughout this chapter a reflection cavity will be considered since this was the type used in our system. The treatment for a transmission cavity is usually very similar to that for the reflection one. The conclusions are identical so that it is only necessary to consider one type of cavity.

It is now necessary to discuss the coupling between the cavity and waveguide to give maximum sensitivity.

4-2.3 Cavity Coupling

The calculation of optimum coupling is most conveniently dealt with using an equivalent circuit, in which a reflection cavity at the end of the waveguide is represented as a lumped, high Q, L.R.C. network, transformer coupled to the end of a simple transmission line. The circuit is shown in Fig. 4-2.

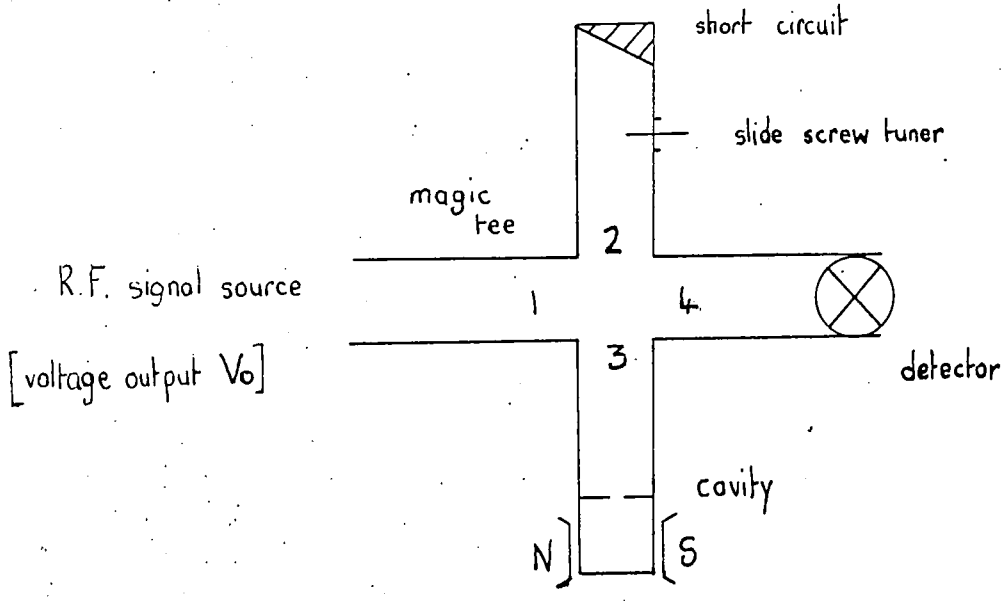


FIG.4-1. A simple arrangement for a reflection cavity system.

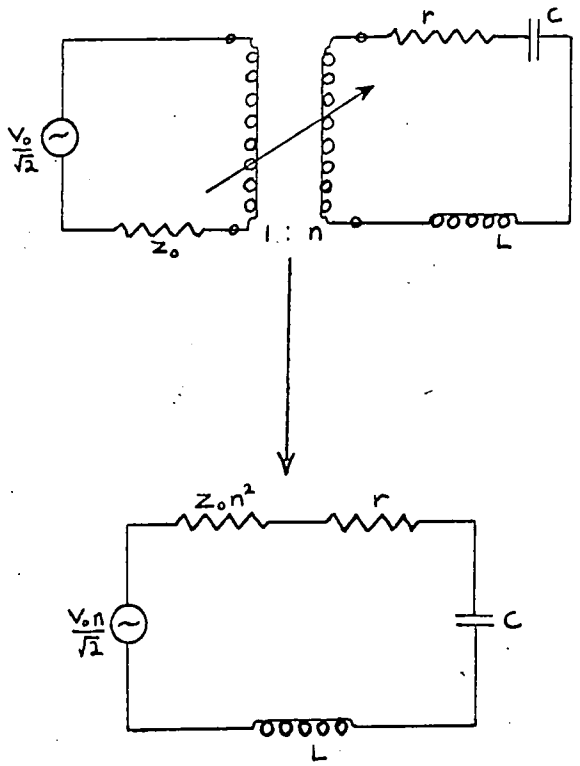


FIG.4-2. Equivalent circuit of a reflection cavity.

NOTE. The variable coupling between the cavity and the waveguide shown by the variable turns ratio transformer is achieved in practice by providing a screw, at less than half a guide wavelength from the cavity iris, which can be moved across the iris.

Feher[1] distinguishes between two cases for optimum coupling depending on whether a power (square law)detector or a voltage (linear) detector is used. Both calculations are simplified by assuming a signal frequency equal to the cavity resonant frequency.

Linear Detector

With a linear detector the change in voltage reflected from the cavity at resonance, when the cavity Q changes by an amount $\Delta Q$, must be optimised.

Let R be the voltage reflection coefficient at the cavity. Then the voltage reflected from the cavity ($V_{refl.}$) is:-

$$V_{refl.} = \frac{Vo}{\sqrt{2}} R$$

By transmission line theory[7], for a line of characteristic impedance $Z_o$ terminated in an impedance $Z_T$

$$R = \frac{Z_T - Z_o}{Z_T + Z_o}$$

with a signal frequency equal to the cavity resonant frequency,

$Z_T = r$ and is real (see fig. 4-2)

$$\therefore \quad |R| = \frac{r - Z_o n^2}{r + Z_o n^2}$$

where the condition $r = Z_o n^2$ corresponds to the condition of the perfect match R = 0.

$Z_o n^2 < r$ corresponds to the case of undercoupling and

$Z_o n^2 > r$ corresponds to overcoupling.

As the coupling changes from undercoupling to overcoupling the sign of R changes.

We are interested in the change of reflected voltage for a change in Q of the cavity.

Writing

$$\Delta V_{refl.} = \frac{\partial V_{refl.}}{\partial r} \cdot \Delta r.$$

Then

$$\Delta V_{refl.} = \pm \sqrt{2}\, V_o\, \Delta r\, \frac{Z_o n^2}{(Z_o n^2 + r)^2} \qquad (4\text{-}6)$$

The positive sign refers to undercoupling and the negative to overcoupling.

Optimum coupling is obtained when

$$\frac{\partial(V_{refl})}{\partial(Z_o n^2)} = 0.$$

This condition corresponds to $Z_o n^2 - r = 0$, i.e. to the situation of perfect match.

For this situation equation (4-6) is:-

$$\Delta V_{refl.} = \pm\sqrt{2}\,\frac{1}{4}\,V_o\,\frac{\Delta r}{r} = \pm\frac{1}{4}\sqrt{2}\,V_o\,\frac{\Delta Q}{Q}$$

Using (4-4) the change in reflected voltage is:-

$$\Delta V_{refl.} = \sqrt{2}\,\pi\,V_o\,\chi''\eta\,Q_o$$

and equation (4-6) can be rewritten

$$\frac{\Delta V_{refl.}}{V_o} = \pm\sqrt{2}\,\pi\,V_o\,\chi''\eta\,Q_o\left(1-|R|^2\right) \qquad (4\text{-}7)$$

A plot of $\frac{\Delta V_{refl.}}{V_o}$ against R is shown in Fig. 4-3. This diagram shows that maximum sensitivity is obtained for operating conditions as close to a perfect match as possible, and this can be demonstrated to be true experimentally. This treatment predicts a discontinuity in the reflected power at the condition of perfect match. It is readily confirmed by experiment that no such discontinuity exists and the plot is con-

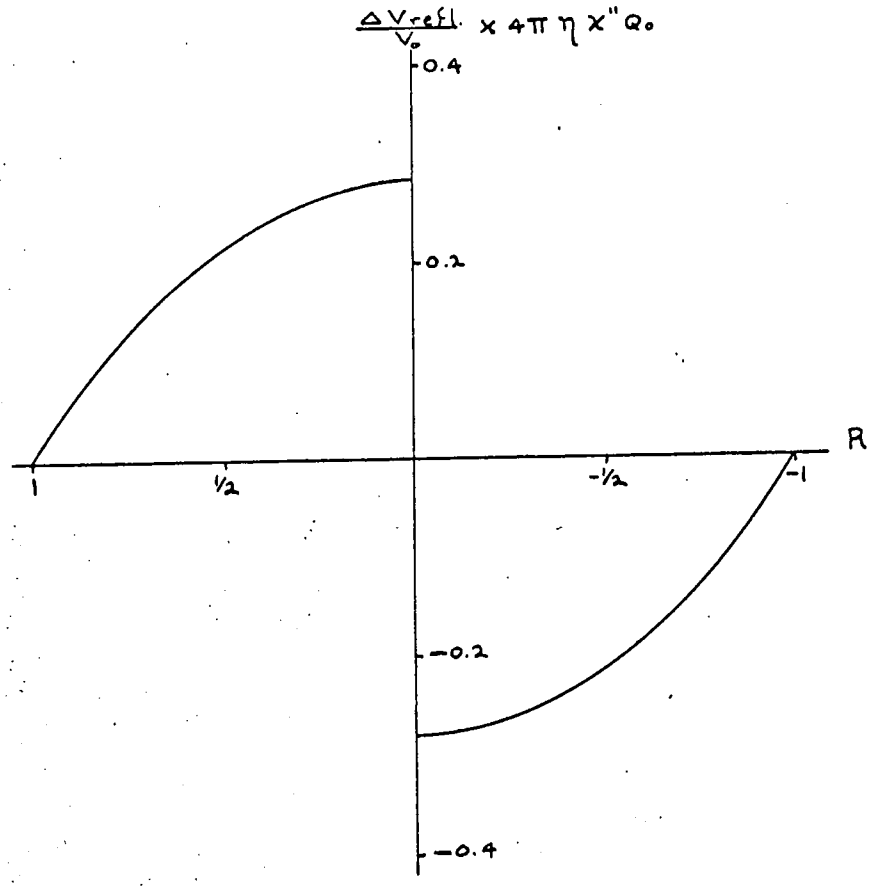


FIG.4-3.A plot $\frac{\Delta V_{refl.}}{V_o}$ versus reflection coefficient (R).

tinuous. Faulkner[8] has shown that the inconsistency is due to an oversimplified approach (see below).

Square law detector

With the square law detector Feher considers optimising the power reflected from the cavity, using the assumption that the change in power reflected from the cavity equals the change in power in the cavity at a constant incident power. This leads to an optimum coupling condition corresponding to R = 0.58. However it can be shown experimentally that the optimum coupling is again very close to the perfect match. Consequently this approach must be incorrect. The method used by Faulkner[8] is to define a complex reflection coefficient (R) where

$$R = R' - jR''$$

Using the same equivalent circuit as that shown in Fig. 4-2 values for R' and R" are obtained in terms of $Q_o$ and $Q_L$ at a frequency $\omega_1$, very close to the resonant frequency $\omega_o$. Where $Q_o = \frac{\omega_o L}{r}$ is the unloaded cavity Q, $Q_L = \frac{\omega_o L}{r+Z_o}$ is the loaded cavity Q, taking into account losses through the coupling hole into the waveguide, and $Z_o' = Z_o n^2$,

Then[9]

$$R' - jR'' = \frac{\left(\frac{r-z_0'}{r+z_0'}\right)\omega_0 + 2jQ_L\Delta\omega}{\omega_0 + 2jQ_L\Delta\omega}$$

where $\omega_0^2 = \frac{1}{LC}$.

$\Delta\omega = \omega_1 - \omega_0$

and $\Delta\omega \ll 1$.

Ignoring quantities of the order of $\frac{1}{Q_0}$ and $\frac{\Delta\omega}{\omega}$ relative to unity.

$$\left.\begin{aligned} R' &= 1 - 2\frac{Q_L}{Q_0} \\ \text{and} \quad R'' &= Q_0\frac{\Delta\omega}{\omega}\left(1 - R'^2\right) \end{aligned}\right\} \qquad (4\text{-}8)$$

$$\left.\begin{aligned} \text{also} \quad -\frac{\partial R'}{\partial X''} &= \frac{\partial R''}{\partial X'} = 2\pi\eta Q_0\left(1 - R'^2\right) \\ \text{and} \quad \frac{\partial R'}{\partial X'} &= \frac{\partial R''}{\partial X''} = 0 \end{aligned}\right\} \qquad (4\text{-}9)$$

Clearly the quantity to be maximised is $\frac{\partial R'}{\partial X''}$. This is a maximum when R' = 0, i.e. the greatest sensitivity is obtained for the condition of perfect match.

The magnitude of the information carrying signal ($V_s$) reflected from the cavity is shown to be:

$$V_s = \pi\eta Q_0\left(1 - R'^2\right)\frac{V_0}{\sqrt{2}} \cdot H_2 \qquad (4\text{-}10)$$

Where $H_2$ is the amplitude of the modulation of an external magnetic field.

This equation is of the same form as that obtained by Feher[4-7], except that equation does not predict a discontinuity at the condition R' = 0.

Goldsborough and Mandel[4], who employed a similar method of calculation to that of Faulkner, also showed that the optimum coupling condition is obtained for the condition of perfect match, when the oscillator frequency is equal to the cavity resonance frequency. Consequently, according to the theory outlined above the coupling between cavity and waveguide should be set as close as possible to a perfect match for maximum sensitivity. With our spectrometer it was readily verified that this was the most sensitive mode of operation.

4-2.4 Frequency choice

It is convenient at this stage to explain more fully the choice of 9.3 Kmc/s as the operating frequency. (This is equivalent to a wavelength of 3 cm).

The minimum detectable number of spins (N min) in a paramagnetic sample is proportional to $\chi'' \frac{\Delta\nu}{\nu}^{(2)}$ where $\Delta\nu$ is the line width of the resonance line in the sample and $\nu$ is the operating frequency. Thus the value of N min is proportional to:-

$$\left(\frac{V_c}{Q_o}\right) \frac{\Delta\nu}{\nu}$$

where $V_c$ is cavity volume.

Assuming that as the frequency is increased the cavity is sealed down to give the same R.F. field configuration, then:

$$V_c \propto \frac{1}{\nu^3}$$

and since

$$Q_o \propto \frac{1}{\nu^{1/2}} \quad \text{Then} \quad N_{min} \propto \frac{1}{\nu^{7/2}}$$

Thus to detect the minimum number of spins, the highest possible operating frequency is required. The upper limit is set by:-

(1) The difficulty of obtaining and handling components in the millimetric range of wavelengths.

(2) The limited power obtained from the available sources at such wavelengths.

3cm. equipment provides a suitable compromise between sensitivity and experimental requirements as well as being readily available commercially. It is in common use for e.s.r. work. In certain special cases, e.g. the study of spin energy level systems with large energy splittings, it is necessary to use higher frequencies.

4-2.5 Minimum detectable signal in practical systems.

The minimum detectable resonant absorption signal can be calculated if the various noise sources in the system are

taken into account. Before discussing noise in the detection system, the other sources of noise in a spectrometer will be considered.

4-2.5(1) Source noise

The microwave power is usually derived from a reflex Klystron. A Varian 2K25 klystron was employed in our system. A klystron exhibits random variations in the amplitude and frequency of its output power. There is little available data on these variations and none for the 2K25.

A.M. noise in the klystron output will have an adverse effect on the signal/noise ratio of detector. But in our spectrometer, noise from this origin was less than that of the detector and can therefore be ignored.

However, with the klystron at maximum power output, the F.M. noise from the klystron provides the dominant contribution to the noise at the detector output. Thus some form of automatic frequency control of high gain was required, to reduce this noise component.

The change in reflected voltage ($\Delta V$) during a resonant absorption is very small, typically $\frac{\Delta V}{V_o} \sim 10^{-6}$ and it is not feasible to maintain the microwave power level constant to this accuracy. Thus a system commonly encountered, which is used in our spectrometer, is to apply a small external magnetic field modulation of angular frequency ($\omega_m$) superimposed on the D.C. magnetic field. In the absence of

resonance the output is zero. If the amplitude of the field modulation ($\Delta H_m$) is small in comparison with the width of the resonance signal, at resonance, the derivative of the line shape is swept out as the D.C. sweep moves across the resonance line. The advantages of this technique are:-

(1) That the requirement of the constancy of the microwave level becomes less stringent.

(2) Amplifiers tuned to frequency $\frac{\omega_m}{2\pi}$ are required, and consequently the band width of the detection system is reduced. However any A.C. components in the F.M. noise of the klystron with frequencies close to that of the modulation frequency ($\omega_m$) will represent noise terms which will pass through the detection system. Thus it is important that the band width of the A.F.C. system is sufficient to cover the modulation frequency range, to remove F.M. noise components at this frequency at the klystron output.

A common feature of the A.F.C. systems is the use of the sample cavity as the stabilising element. Such a system is ideal for the observation of the power absorbed in the sample. This system is conventionally referred to as the absorption mode. In this mode the change in amplitude of the reflected voltage is detected and the phase change

associated with the dispersive component ($\chi'$) of sample susceptibility must be rejected. Locking the klystron frequency to that of the cavity resonant frequency automatically rejects the dispersive part ($\chi'$) since this gives rise essentially to a frequency shift which is compensated by the A.F.C. system. To observe the dispersion mode a form of the Pound stabilisation system[13] must be employed, where the klystron frequency is locked to that of an external cavity tuned to sample cavity.

Both types of A.F.C. systems were available in our spectrometer.

4-2.5(2) Circuit noise

For optimum signal/noise it is necessary to eliminate noise due to microphony and microwave power leakage. Microphonic noise is especially serious in systems employing modulation frequencies less than about 500 c/s. These effects can be minimised by careful construction of the spectrometer.

4-2.5(3) Noise due to cavity vibrations

The magnetic field modulation induces eddy currents in the cavity walls. These currents interact with the D.C. magnetic field to produce mechanical vibrations of the cavity walls, thereby producing noise signals at the detection frequency. There is little that can be done to overcome this problem. The simplest solution is to use a low modulation frequency

$<$ 100 c/s. This however makes the system susceptible to the problems of microphony as outlined in the previous section. In practice, therefore, a compromise has to be effected. In some systems glass cavities with a thin evaporated layer of silver have been successfully employed to decrease the eddy currents without greatly reducing the mechanical strength. However due to the obvious practical difficulties of handling and operating such an expedient was not used in the present spectrometer. Instead brass cavities with a thin plating of gold were used. A modulation frequency of about 70 c/s was chosen so that the problems of modulation pick up could be ignored.

4-2.5(4) Noise in practical detection systems

The detection system consists of a microwave detector feeding into suitable amplication stages. The expression for the noise power ($P_N$) at the output can be written[10]

$$P_N = (GN_K + F_{amp.} + t - 1)\, KT\Delta\nu \qquad (4\text{-}11)$$

where G is the conversion gain of the microwave detector.

$N_K$ is the microwave noise at the detector.

t is the noise figure of the microwave detector.

$F_{amp.}$ is the noise figure of the amplifier.

$\Delta\nu$ is the band width of the detection system.

T is the temperature of the detector.

(NOTE. t is defined as the ratio of the available noise power at output of the crystal to that of a resistor at room temperature).

A comparison of the noise power $P_N$ with the optimum signal voltage from the cavity, equation 4-7, defines the minimum detectable absorption signal in the spectrometer. Let $P_D$ be the power generated in the detector due to the incidence of the signal voltage $\Delta V$. Then:-

$$P_D = \frac{2V_0^2}{Z} \eta^2 \pi^2 \chi''^2 Q_0^2$$

where Z is the equivalent impedance of the detector. For a matched detector Z is equal to Zo the characteristic impedance of the guide:-

Then

$$P_D = 2P_0 \eta^2 \pi^2 \chi''^2 Q_0^2$$

Comparing the signal power with the noise power of the detection system, the minimum detectable value of $\chi''$ ($\chi''$ min) is:-

$$\chi''_{min} = \frac{1}{Q_0 \eta \pi} \left[ \frac{(G N_K + F_{amp.} + t - 1) KT \Delta\nu}{2GP_0} \right] \qquad (4-12)$$

The limit of sensitivity of a spectrometer is determined by the dominating noise factor in equation 4-12. Buckmaster and Dering[12] have carried out an experimental investigation of this expression. They were able to show that a spectrometer can achieve near theoretical sensitivity as predicted by equation (4-12) if the operating conditions are correctly chosen.

The quantities G, $N_k$, $F_{amp}$ and t in equation (4-12) are dependent on the R.F. power and the modulation frequency. The values of G and t for a microwave detector can vary from unit to unit of the same type. Consequently a complete discussion of the quantities in equation (4-12) is long and complicated and is inappropriate in this survey. Instead the conclusions of such a discussion will be presented with emphasis on their importance in spectrometer design.

4-2.5(5) Microwave detectors

There are two main types of detector in common use:-

(1) The crystal diode

(2) The bolometer

Crystal diode detection

A crystal diode behaves as a microwave rectifier producing a D.C. current output from the incident microwave power.

Its characteristics can be divided into two regions:-

1) A square law region, where the rectified current ($I_R$) is proportional to the incident power ($P_{INC}$).(holds for $P_{INC} < 10^{-5}$ watts).

2) A linear region where $I_R$ is proportional to $(P_{INC})^{\frac{1}{2}}$ (Holds for $P_{INC} > 10^{-4}$ watts).

The noise output ($P_c$) for a crystal diode when the incident microwave power is modulated at a frequency f is :- (10,11)

$$P_c = \left( \frac{\alpha I_o^2}{f} + 1 \right) KT\Delta\nu$$

where $\alpha$ is a constant.

For the square law region this becomes:-

$$P_c = \left( \frac{\beta . P_{INC}}{f} + 1 \right) KT\Delta\nu \qquad (4-13)$$

and for the linear region:-

$$P_c = \left( \frac{\gamma P_{INC}}{f} + 1 \right) KT\Delta\nu \qquad (4-13a)$$

$\beta$ and $\gamma$ are constants determined experimentally for each diode.

With a microwave detector the other important factor is the conversion gain G.It can be shown both experimentally and theoretically that :-

In the square law region $G \propto P_{INC}$

and in the linear region $G \sim$ constant

} (4-14)

i.e. the conversion gain is poor at low powers.

It is convenient to define the function $\frac{\chi'' \text{ min-obs.}}{\chi'' \text{ min-th.}}$

which is the ratio of the mimimum detectable value of $\chi''_{min}$ with a practical detection system to that of an ideal system where one is limited only by the thermal noise of the detector.

In this idealised case equation (4-11) can be rewritten:-

$$\chi''_{min-th.} = \frac{1}{Q_0 \eta \pi} \left( \frac{KT\Delta\nu}{2P_0} \right)^{1/2} \qquad (4-17)$$

Then from equations (4-11) and (4-17).

$$\frac{\chi''_{min-obs.}}{\chi''_{min-th.}} = \left[ \frac{(GN_K + F_{amp} + t - 1)}{G} \right]^{1/2} \qquad (4-18)$$

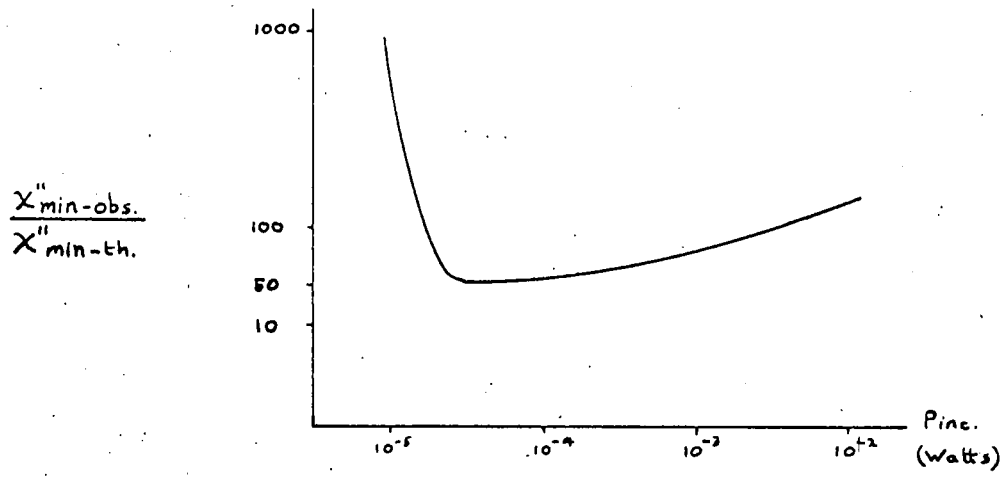


FIG.4-4. A plot of $\frac{\chi''\text{min.-obs.}}{\chi''\text{min.-th.}}$ versus $P_{inc.}$ for a simple crystal diode detection scheme.

Buckmaster and Dering[12] have shown that in a well designed spectrometer, using good klystrons and amplifiers that are commercially available, the microwave noise figure ($N_k$) is negligable and the noise figure ($F_{amp}$) of the amplifier is very close to unity.

With these assumptions and using equations (4-13),(4-13a) and (4-14) equation (4-16) can be rewritten as :-

$$\left.\begin{aligned} \frac{\chi''_{min\text{-}obs.}}{\chi''_{min\text{-}th.}} &= \left(\frac{1 + \frac{B P_{inc}}{F}}{G}\right)^{1/2} \\ \text{for the square law region and as} \qquad & \\ \frac{\chi''_{min\text{-}obs.}}{\chi''_{min\text{-}th}} &= \left(\frac{1 + \frac{\gamma P_{inc.}}{F}}{G}\right)^{1/2} \end{aligned}\right\} \qquad (4\text{-}19)$$

for the linear region.

A plot of the functions in equation (4-19) against incident power is shown in Fig. 4-4, using values obtained with a typical crystal [2].

At low powers the crystal diode has poor conversion gain, while at high powers there is excess crystal noise.

With the simple reflection cavity system shown in Fig.4-1 it is clearly difficult to obtain the optimum power level at the detector in all cases,since this depends on the power incident on the cavity and the degree of balance

obtained by arm 2.The situation can be improved by the technique of microwave 'bucking',i.e. some power is taken from arm 1 using a directional coupler and is added to that falling on the detector in arm 3.The amount of 'bucking' can be varied to ensure that the detector is working in its optimum range for any level of power incident on the cavity.This greatly enhances the usefulness of the spectrometer.

Since our object was to construct a spectrometer of very high sensitivity the homodyne scheme was rejected in favour of the more complex super heterodyne one.A superhetrodyne system gives a significant increase (~10 times) in sensitivity over that of a homodyne arrangement.

It is evident from equations(4-13) and (4-13a) that crystal detection noise falls off with increasing modulation frequency.However practical considerations,such as power requirements for obtaining a given modulation depth and the effect of the high frequency modulation on the line width of the resonance line,set an upper limit onto the frequency of modulation at about 100Kc/s.However crystal noise output ($P_c$) only becomes negligible at frequencies of the order of tens of megacycles.The conventional method of obtaining such high modulation frequencies at the crystal is to beat the reflected signal from the cavity with a signal from a local

oscillator klystron which is displaced in frequency from the signal klystron by a few tens of megacycles.The I.F. beat frequency is detected by the crystal and is amplified by a standard I.F. amplifier.The power level at the detector is made sufficiently high to maintain a high conversion gain by the local oscillator power.The noise figure (t) of the detector is then very low and the noise figure of the I.F. amplifier ($F_{amp}$) becomes important.In order to eliminate the noise from the local oscillator signal a balanced mixer is employed.The limit of sensitivity of such a system has been found by Buckmaster and Dering[12] and Teaney,Klein and Portis[5] to be set by the noise figure of the I.F. amplifier and the balanced mixer.When the good mixers and amplifiers which are commercially available are employed the value of equation (4-18) becomes:-

$$\frac{\chi''_{min-obs.}}{\chi''_{min.-th.}} \sim 4 \text{ to } 5$$

This is a significant increase in sensitivity compared with that obtainable with a homodyne system and justifies our decision to build a superheterodyne spectrometer, using crystal diode microwave detection.(NOTE-In our spectrometer the value of equation (4-20) will be higher since klystron F.M. noise becomes a dominating factor at high klystron powers.

Bolometer detection

A bolometer comprises a small resistive element which is capable of dissipating microwave power, and utilising the heat developed to effect a change in its resistance. There are two common types. One has an appropriately mounted short length of wire usually platinum and the other a small bead of semiconducting material. Theoretically their noise temperature should be close to unity, but in practice it is very much higher. They can be made into sensitive microwave detectors but in practice they have many disadvantages. The more important of these are their low response times and poor conversion at low powers. Thus they must be used at high powers where microwave noise ($N_K$) becomes the limiting factor. The situation can be improved by using a balanced mixer but it is difficult to obtain matched bolometers. Consequently it is difficult to build a spectrometer employing bolometer detection with as high a sensitivity as a crystal superheterodyne system. As a result a bolometer detection scheme was rejected in favour of the crystal diode detection scheme outlined above.

4-3 Conclusions

The sensitivity conditions of section (4-2) led to a decision to build a 3cm superheterodyne spectrometer employing balanced mixer crystal diode detection. The I.F.

frequency was chosen to be 30 mc/s because of the availability of amplifiers tuned to this frequency. A reflection cavity was used as this was simpler to design and operate. The magnetic field modulation frequency was chosen to be 70 c/s. An A.F.C. for the signal klystron using the sample cavity as the stabilising element was built and had sufficient band width to cover the field modulation frequency. The practical details of the spectrometer are given in the next section.

4-4 Practical details

A block diagram of the spectrometer is shown in Fig. (4-5). The signal and local oscillator klystrons, the 30 mc/s I.F. amplifiers and their respective power supplies were obtained from an ex-U.S.A.F. radar set. The microwave circuitry was obtained commercially. The spectrometer was also designed to measure spin-lattice relaxation times by the pulse saturation technique. The large pulse of microwave power required to produce the resonance transition saturation was provided by a travelling wave tube type TWX-8 which could be inserted into the microwave circuit between the signal klystron and the microwave bridge. A diode switch was placed in front of the microwave detector to protect it during the large power pulse. This facility was not used during the course of the work reported here.

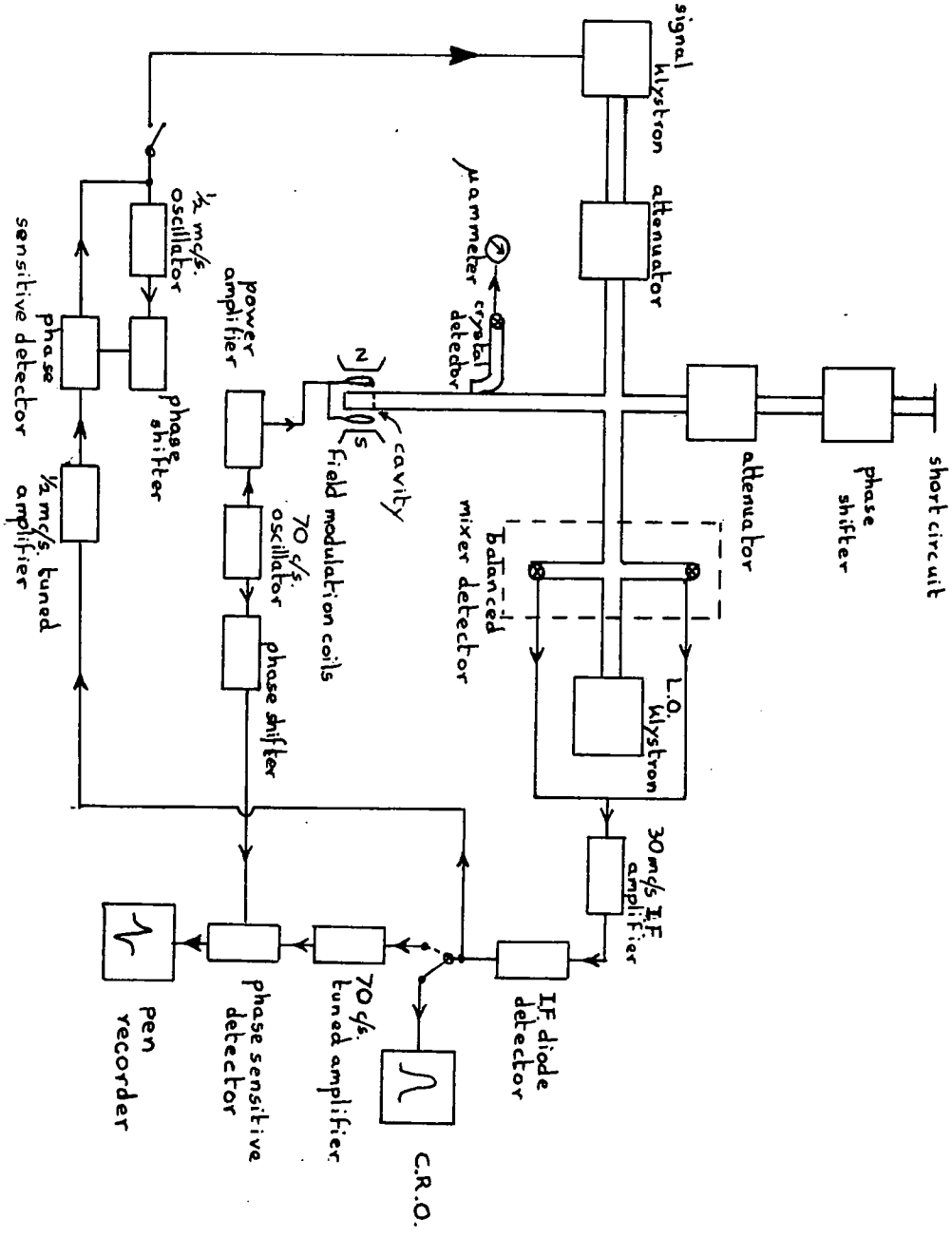


FIG.4-5. Block diagram of the 3cm. microwave spectrometer.

Circuit diagrams of the low frequency (70c/s) power oscillator, low frequency (70c/s) tuned amplifier and phase sensitive detector are given in Figs. (4-6) and (4-7).

A double concentric glass dewar cryostat enabled measurements to be made in the temperature ranges 1.5 - 4.2°K and 55 - 77°K with the use of pumped liquid Helium and pumped liquid Nitrogen respectively.

The microwave cavity was gold plated brass wall rectangular type, operating in the $H_{102}$ mode. It has a Q-factor of a few thousand at room temperature. The cavity could be split to facilitate sample mounting. The samples were usually mounted on the narrow face of the cavity where the R.F. magnetic field is greatest and vertical so that the D.C. magnetic field, which rotated in the horizontal plane, is always perpendicular to the R.F. field. A brass sealing can, which surrounded the cavity and screwed into the waveguide was to prevent liquid Helium or Nitrogen from leaking into the cavity. The presence of liquid coolant in the cavity causes noise on the microwave power reflected from the cavity because of bubbling and so this step was taken to prevent it entering the cavity. For optical illumination of the sample while immersed in the coolant a second cavity was constructed with a slit cut across the narrow face as indicated in Fig. (4-8). A

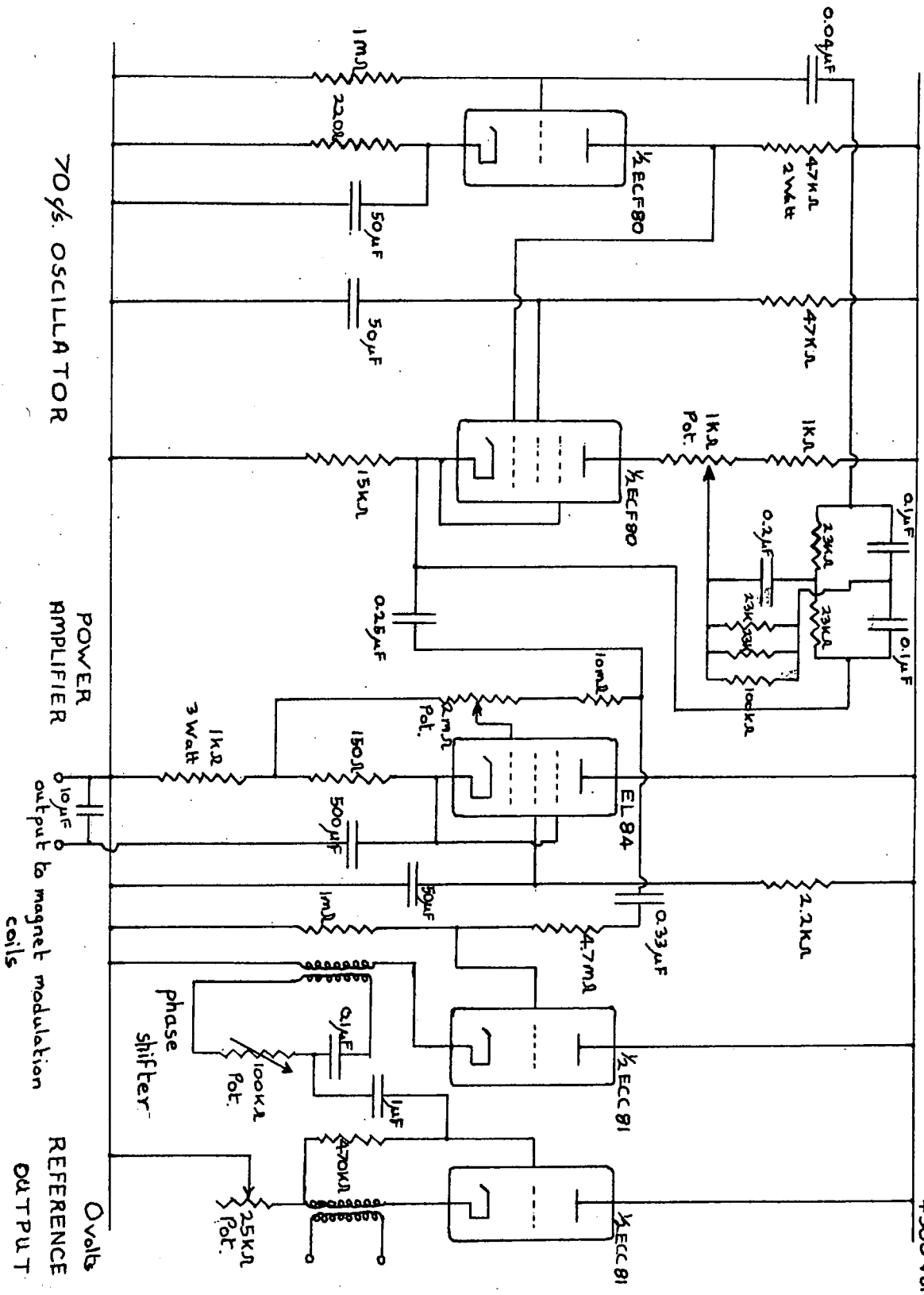


Fig.4-6. Circuit diagram of the 70 c/s. oscillator, power amplifier and phase shifter.

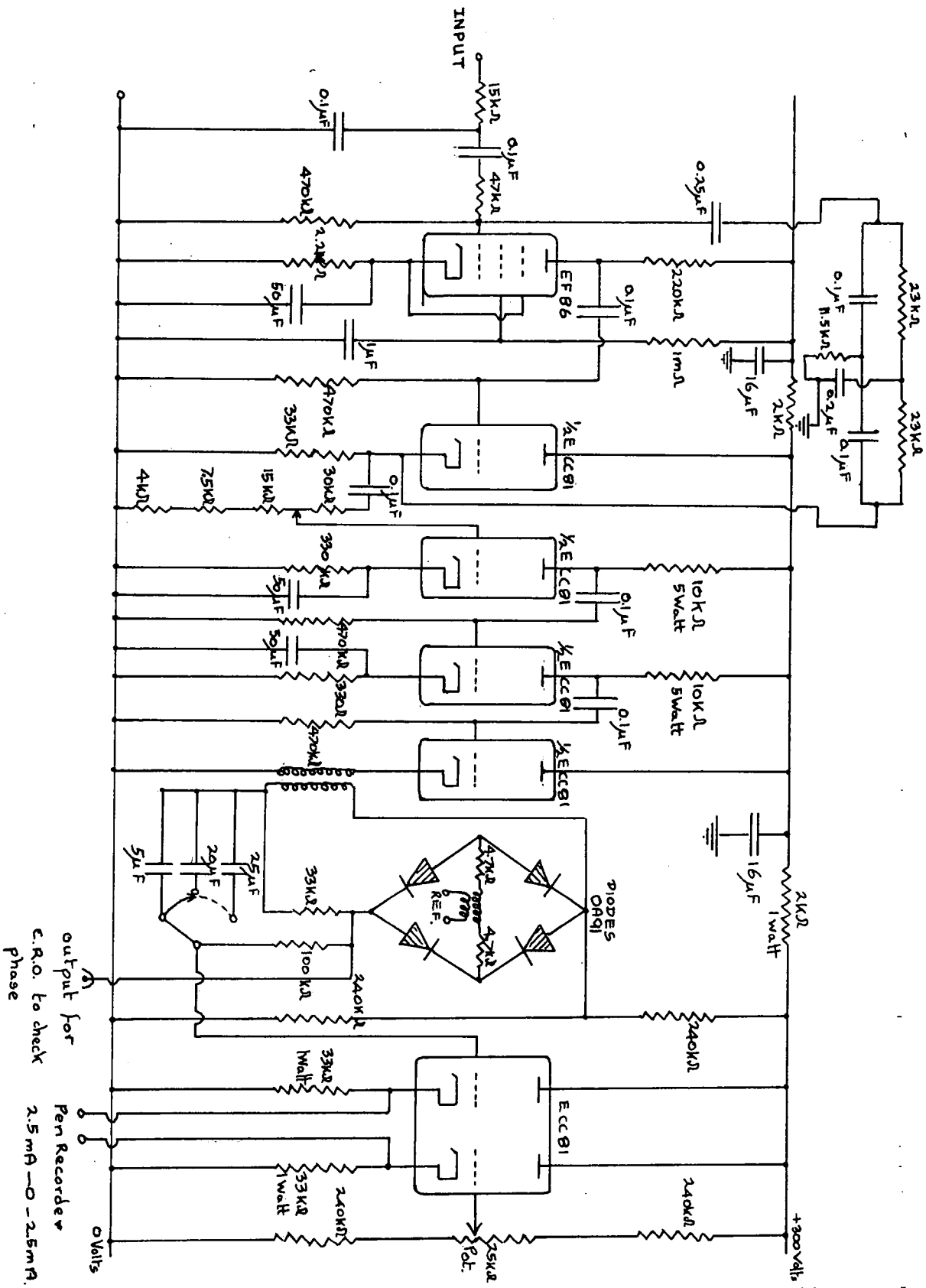


FIG. 4-7 Circuit diagram of the 70 c/s. tuned amplifier and phase sensitive detector.

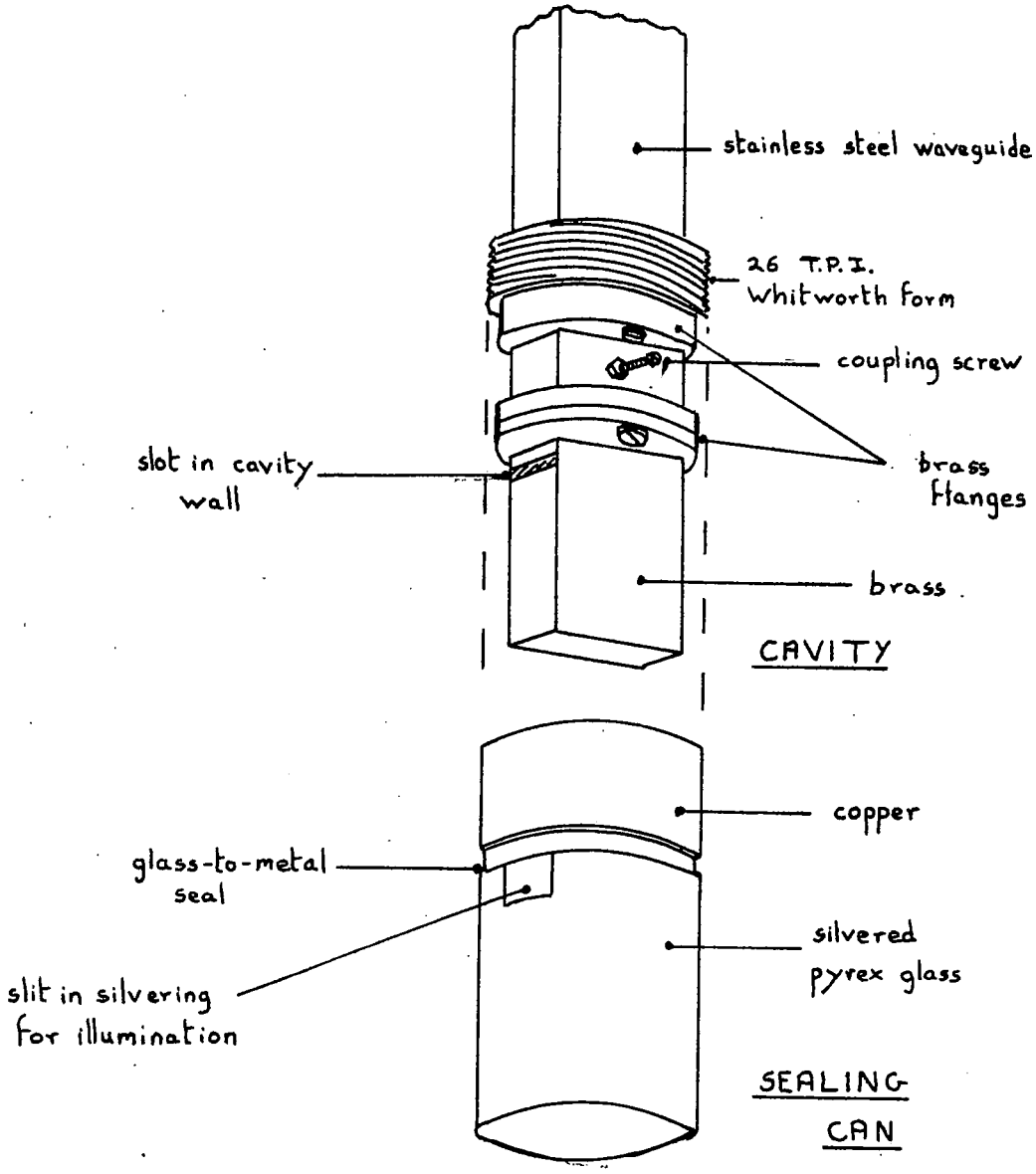


FIG.4-8 .Optical cavity and sealing can for sample illumination.

composite glass and metal sealing can was employed (see Fig. 4-8). The glass bottom section of the can was silver plated except for a slit corresponding to the one in the cavity. This step was found necessary because microwave power which leaks from the joint and the slit in the cavity is reflected back into the cavity from the silvering. Before the can was silvered this power was reflected from the glass dewar walls and because it had to pass through the ~~bubbling~~ bubbling coolant was a source of noise on the signal microwave power. Silvering of the sealing can greatly reduced the noise due to this cause.

A second method of optical illumination was tried. A flexible fibre optic light guide was passed down the side of the waveguide feeding the cavity and directly into the cavity. However any slight movement of this light guide caused a change in the power level reflected from the cavity and so was a source of spurious signals and noise at the detector and no reliable results were obtained with this system. A future modification of this scheme would be to use a rigid light pipe. A system employing a light pipe is preferable, since the sample can be kept in complete darkness if required. A situation which is difficult to achieve with the system employing a slit in the cavity wall.

## REFERENCES

(1) D. J. E. Ingram - "Spectroscopy at Radio and Microwave frequencies". Butterworth's Scientific Publications. London 1955, and D. J. E. Ingram - "Free radicals as studied by E.S.R.". Butterworth's Scientific Publications. London 1955.

(2) G. Feher - Bell Systems Tech. J. 36, 449, 1957.

(3) M. Misra - Rev. Sci. Inst. 29, 590, 1958.

(4) Goldsborough and Mandel - Rev. Sci. Inst. 31,1044, 1960.

(5) Teaney, Klein, and A. M. Portis - Rev. Sci. Inst. 32, 721, 1961.

(6) W. Low - "Paramagnetic Resonance in Solids" Solid State Physics Supplement 2, Academic Press. 1960.

(7) "The Services' Textbook of Radio" Vol. 5. Transmission and propagation, p.60. H.M.S.O. London 1958.

(8) M. Faulkner - Laboratory Practice , 1065, 1964.

(9) B. I. Bleaney and B. Bleaney - "Electricity and Magnetism" Clarendon Press Oxford, p.223.

(10) Torrey and Whitmer - "Crystal Rectifiers" Rad. Lab. Series Vol. 15. M$^{c}$Graw Hill 1947.

(11) R. V. Pound - "Microwave Mixers" Rad. Lab. Series Vol. 16. M$^{c}$Graw Hill 1948.

(12) Buckmaster and Dering - Can. J. Phys. 43, 1088, 1965.

(13) R. V. Pound - Rev. Sci. Inst. 17, 490, 1946.

# CHAPTER 5

# SAMPLE PREPARATION

## 5-1 ORIGIN OF THE SAMPLES

Most of the samples investigated in this work were grown in our own laboratories and were very kindly made available by Dr. L. Clark and Mr. D. S. Orr. The samples were taken from large undoped single crystal boules of CdS, unless otherwise stated. Clark and Orr have used two distinct methods of growing the single crystal boules:-

(1) Sublimation of a CdS charge in an argon atmosphere and

(2) Sublimation in vacuo.

A number of samples prepared at other laboratories were also investigated during the course of the e.s.r. work.

### 5-1.1 Growth of Single Crystal Boules by Sublimation in argon.

This method was a modification of that of Piper and Polich[1] and is described fully in the paper by Clark and Woods[2]. Two crystals grown by this technique were used in the e.s.r. work and will be designated LR25 and LR26. Both samples were of an irregular shape with approximate dimensions of 0.5 cm x 0.5 cm x 0.2 cm. The crystals were transparent with a brownish yellow coloration. They both had a high resistivity at room temperature ($>10^6$ ohm-cm). Chromium impurity ions were detected in LR26 by the e.s.r. technique.

TABLE 1

| Sample | Growth temp. | Sulphur vap. press. | Cooling time from growth temp. |
|---|---|---|---|
| R9 | 1125°C | 20 mm.hg. | approx.4hrs. |
| R11 | 1100°C | $2.10^{-1}$ " " | " 4 " |
| R12 | 1100°C | $10^{-4}$ " " | " 4 " |
| R13 | 1100°C | $10^{-4}$ " " | " 4 " |
| R14 | 1100°C | $2.10^{-1}$ " " | " 6 " |
| R23 | 1050°C | $10^{-4}$ " " | " 10 " |
| R27 | 1075°C | $10^{-4}$ " " | " 12 " |
| R29 | 1075°C | $10^{-4}$ " " | " 30 " |
| R35 | 1075°C | $10^{-4}$ " " | " 24 " |
| R39 | 1150°C | $10^{-4}$ " " | " 30 " |

5-1.2 Growth by Vacuum Sublimation

As indicated by Clark and Woods[2] non-stoichiometry in the starting charge dominates the growth mechanism of CdS in sealed evacuated tubes, making control of the growth difficult. To overcome this problem a vacuum growth technique has been evolved in this laboratory where the vapour pressure of one of the components (usually sulphur) can be controlled independently of the growth temperature. The growth tube is pulled vertically through the furnace to minimise radial temperature gradients. At the present time the vapour pressure of the sulphur over CdS has been controlled over the range $10^{-4}$ mm to 100 mm and the effect on the growth and the properties (including e.s.r.) studied. Many of the results of this programme will be discussed in chapter 7.

Table 1 gives a list of the vacuum sublimed samples used during the course of the e.s.r. work together with some of the growth details. The samples were all of an irregular shape with a volume of about 0.1 $cm^3$ and were all transparent with a bright yellow or yellowish brown coloration. Back reflection x-ray studies demonstrate that many of the samples were good single crystals. However a few were clearly polycrystalline and using optical microscopy cracks and

voids could be observed in the bulk of the material. X-ray studies showed that even in these samples the different grains were aligned in approximately the same direction and as far as the e.s.r. spectra were concerned it was sensible to refer to directions parallel and perpendicular to the crystallographic c-axis. No impurities were detected in these samples by the e.s.r. technique except in sample R12 in which an e.s.r. spectrum due to cobalt was found (see section 6-1.3).

5-1.3 Other samples

A number of undoped single crystals of CdS were obtained from the G.P.O. research laboratories, Dollis Hill, London. These samples were grown from an ultra high purity grade powder and thought to be purer than our own samples. However the e.s.r. technique showed that one sample contained cobalt as an impurity and another manganese. No analysis of the impurity content was available nor were details of the growth technique and the subsequent handling. The two samples investigated, - G.P.O. 17 A 35 and G.P.O. x93 - were transparent with a brownish-yellow coloration. An Eagle-Picher ultra high purity grade single crystal (EPx96) was also available.

## 5-2 Heat treatment after growth

A number of samples were subjected to heat treatment after growth to ascertain the effect on the e.s.r. spectra. The samples treated in this way were fired in an atmosphere of either cadmium or sulphur vapour, the vapour pressure of which was greater than the equilibrium vapour pressure of that component over CdS at the firing temperature.

### 5-2.1 Sulphur treatment

The specimen was placed in a quartz tube of wall thickness not less than 2 mm with sufficient 6N pure sulphur to maintain the saturated vapour pressure at the required treatment temperature. The tube was evacuated and sealed off at a pressure of about $10^{-5}$ Torr. In every case the treatment temperature was maintained at 700°C for 20 hours. At 700°C the vapour pressure of sulphur is approximately 30-40 atmospheres. The tube was placed in a stainless steel 'bomb' inside the furnace, in case the tube fractured. The samples were cooled from 700°C by quenching the treatment tube in water. The surface layer of each sample was removed by a 30 sec etch in cold concentrated hydrochloric acid.

### 5-2.2 Cadmium treatment

Here the procedure was similar to the above, except that 6N cadmium metal was placed in the evacuated tube. The sample at one end of the tube was heated to 600°C while the

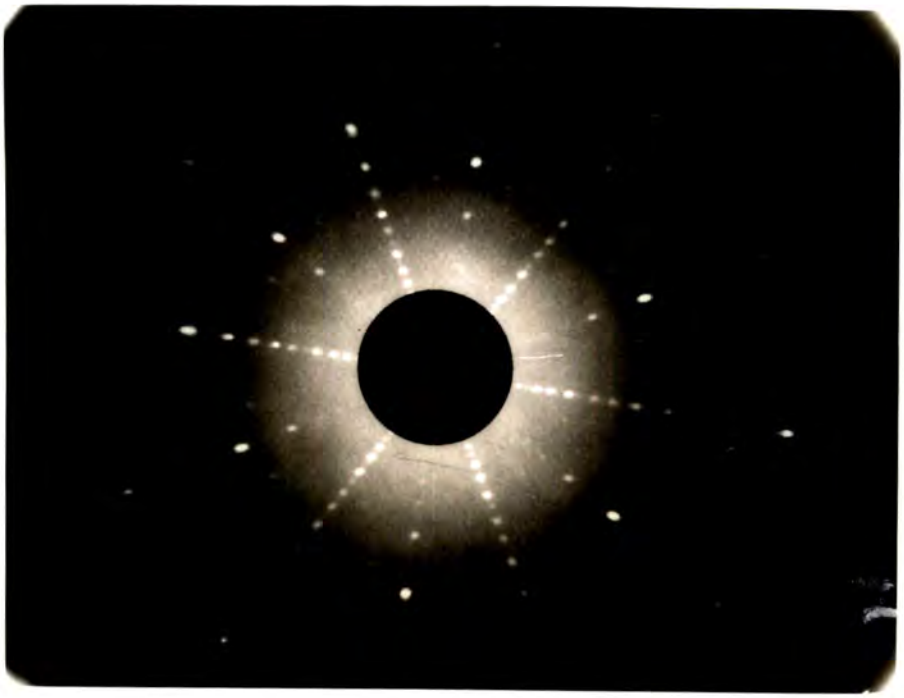

FIG.5-1 Back reflection x-ray photograph of a single crystal of CdS with the incident x-ray beam parallel to the c-axis.

other end of the tube was maintained at 200°C. In this way the CdS was heated at 600°C in a cadmium vapour pressure of approximately $10^{-3}$ Torr. for approximately twelve hours. The tube was quenched from 600°C into water. The surface layer of the sample was again etched away using concentrated hydrochloric acid.

5-3 X-ray Analysis

Sample orientation was carried out by the back reflection Laue X-ray technique. This method was also useful in assessing the degree of polycrystallinity of the samples. On each sample the directions of the crystallographic c-axis and one of the a-axes were identified. Many crystals could be cleaved along the basal (0001) plane and the $(11\bar{2}0)$ plane. When this did not occur a face which was aligned parallel to the (0001) plane to better than 1° was ground on the sample using carborundum grinding paste and the direction of an a-axis identified, using the back reflection technique. Fig. (5-1) shows the back reflection photograph of a CdS crystal with the incident X-ray beam parallel to the c-axis. The irregular shape of the crystals prevented rectangular or cubic shaped samples being prepared.

The method of analysis of the X-ray photographs is

illustrated in Figs. (5-2) and (5-3). Fig. (5-2) shows the standard (0001) projection of a number of the high order planes of CdS. (For CdS the ratio of the length of the unit cell in the c-direction to that in the a-direction (c/a) is 1.62). The directions of the a-axes are indicated in Fig. (5-2). Fig. (5-3) shows the stereographic projection of the poles of the planes responsible for the spots on the back reflection photograph in Fig. (5-1). Comparison of Figs. (5-2) and (5-3) shows that the X-ray photograph of Fig. (5-1) is for the (0001) direction and demonstrates clearly how the directions of the a-axes in a crystal can be obtained from the X-ray photograph. Fig. (5-2) and Fig. (5-3) were drawn with the aid of a Wulf net and a Greninger chart.

5-4 Etch pit studies

An estimate of the dislocation density has been made on some of the samples by etch pit studies. The samples were oriented by X-ray analysis as outlined above and a surface which was parallel to the c-plane to within $1^{o}$, was ground on each sample using carborundum grinding paste of grit size 400. This surface was then polished using two micron alumina powder until it showed no irregularities under x300 magnification, except for scratch marks due to foreign particles in the polishing powder which could not be

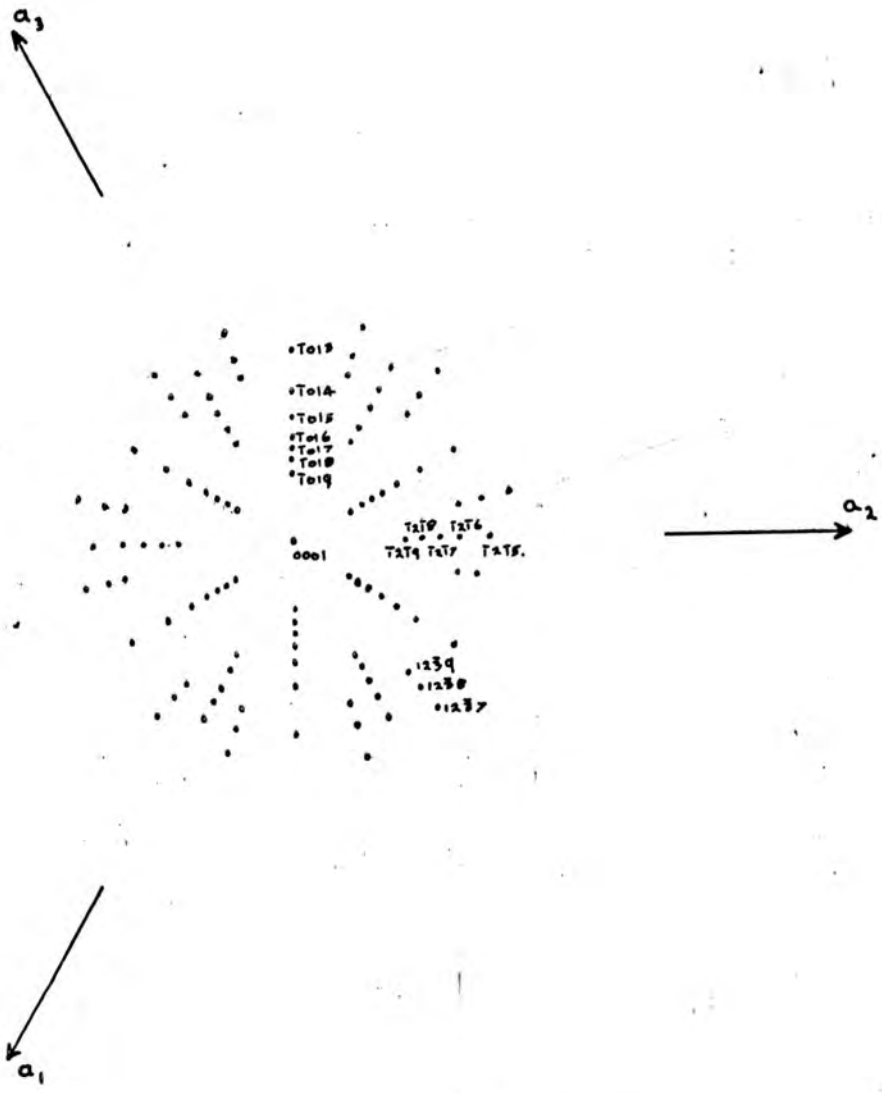


FIG.5-2. Standard (0001) projection of CdS showing many of the high index planes.

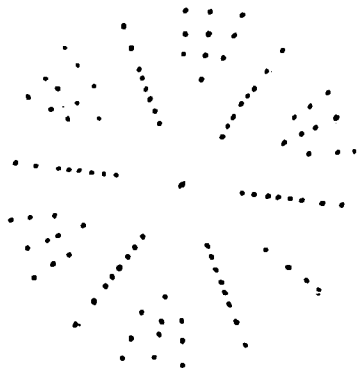

FIG.5-3. Stereographic projection of the poles of the planes responsible for the spots on the x-ray photograph shown in fig.5-1.

removed. It is well known that mechanical polishing of this type damages the periodic structure at the surface so that a chemical polish is essential before etch pits can be successfully produced. A wide variety of polishing solutions were tried, the most successful of which were:-

(a) 89% orthophosphoric acid heated at 220°C and used for one minute. The samples were washed in isopropyl alcohol to remove the products of the polishing solution.

(b) A 1:1 solution of oxalic acid and potassium iodide crystals in distilled water heated at 100°C and used for one minute. Samples were washed in water after polishing.

However neither of these solutions was completely successful and for certain crystals no polishing action at all was obtained. This behavior is not understood at the present time and a more thorough study of the polishing process is required.

A range of etching solutions was investigated to determine the most suitable. The solutions tried included:- hydrochloric, sulphuric, acetic, chromic and phosphoric acids of varying concentrations and at different temperatures; mixtures of hydrochloric and nitric acids and a solution of potassium bichromate in nitric acid.

The most successful solutions which produced well defined etch pits, after polishing, were:-

(a) Chromic acid at 80°C for about five minutes. The samples had to be thoroughly washed in water to remove the acid, before exposing to the air or a film of cadmium chromate formed over the surface of the sample and destroyed the pits.

(b) 89% orthophosphoric acid at 280°C for approximately one minute followed by washing in iso-propyl alcohol.

The performance of these solutions was critically dependent on the success of the polishing technique outlined above. Distinguishable etch pits were obtained on approximately 50% of the samples investigated. Both etching solutions gave reproducible etch pits densities on each sample. The densities were of the order of $10^4$ - $10^5$ $cm^{-2}$ on all samples. Fig. (5-4) shows photographs of the etch pits obtained on two typical samples on the c-plane (0001). It was found that conical etch pits only could be produced whereas the hexagonal pits which are normally found on the (000$\bar{1}$) basal plane of the crystals [3,4] could not be obtained. This was thought to be a function of the polishing procedure. It was noted by Woods[3] that dissolution proceeds much more quickly on the basal plane on which hexagonal pits are formed than the other faces so that the chemical polish

(a)

(b)

FIG. 5-4 Conical etch pits on the c-plane (0001) of undoped CdS crystals. Magnification (a) x200 (b) x300.

may proceed too quickly on this surface and not produce a polishing effect. However a further investigation of this point is required.

The high density of etch pits observed indicates a high density of dislocations in the samples. This suggests that they are quite highly strained during growth. This proposition is supported by the fact that many of the crystals cracked on being removed from the growth tube, and is also supported by the e.s.r. measurements reported in chapter 7. Clearly a wide variety of undoped CdS samples were available for the e.s.r. work. The majority of these were single crystal material as determined from the X-ray studies which also served to orientate the samples. Some estimate of the dislocation density is available which suggests that the samples are somewhat strained during growth.

5-5 Doped samples

A number of small single crystals of CdS doped with the group 3 metal ions B; Al; Ga; In; and Tl; and the group 7 ion Cl. were available. All of these samples were grown by sublimation of CdS powder in a stream of argon gas and are referred to as 'flow' crystals. The required dopant was introduced by placing it in metallic form in a silica boat in the furnace in front of the CdS powder charge,

except for the chlorine doping where the argon gas was bubbled through dilute hydrochloric acid before entering the growth tube. The samples used in this work were approximately cylindrical in shape, about 1 cm. long and 1 mm diameter. Some of the rods had a hexagonal cross section. These samples are rather small for the e.s.r. work and work has begun to grow large doped single crystals of CdS using the vacuum sublimation growth technique discussed in section 5-1.2. The dopant is included in the powder charge. It is hoped that these crystals will be available for the e.s.r. work in the near future.

# CHAPTER 5

## REFERENCES

(1) W. W. Piper and S. J. Polich - J.A.P. 32, 1278, 1961.

(2) L. Clark and J. Woods - B.J.A.P. 17, 319, 1966.

(3) J. Woods - B.J.A.P. 11, 296, 1960.

(4) D. C. Reynolds and L. C. Greene - J.A.P. 29, 559, 1958.

# CHAPTER 6

## DISCUSSION OF THE E.S.R. OF IMPURITY IONS DETECTED IN THE CdS SAMPLES.

Although the purpose of this work was to establish the atomic structure of native lattice defects in CdS, a certain amount of experimental work was carried out on the e.s.r. of impurity ions. In some cases the samples were intentionally doped to ascertain the effects on the e.s.r. lines tentatively assigned to defects. Samples doped with group 3 metal ions (B. Al. Ga. In. and Tl.) and group 7 (Cl.) ions were available for this purpose. In the undoped samples resonance lines due to impurity ions could not be detected in the majority of samples. However in a number of samples resonance lines attributed to chromium, manganese or cobalt were observed at 4.2$^{o}$K. Only one impurity was detected in any one sample. An analysis of the impurity content of the undoped samples by mass spectrometry showed that in general the 3d transition metal ions were present in concentrations of a few p.p.m. by weight. Thus the e.s.r. signals due to these were below the level of detection in the majority of samples, as was observed. Why some of the samples should occasionally have a larger concentration of the above-mentioned impurities is not understood at present. The

analysis of the impurity content showed that the concentrations of other paramagnetic groups, e.g. 4d, 4f etc. were far too small to be detected with our equipment. The discussion of the e.s.r. of the 3d transition metal ions observed will be presented in section (6-1) and that for the group 3 and 7 ions in section (6-2).

## 6-1.3d transition metal ions

### 6-1.1 Chromium

Resonance due to chromium was observed at 4.2°K in sample LR26. The e.s.r. of chromium is interpreted in terms of chromium ions substituting at $Cd^{2+}$ sites in $Cr^{2+}$ charge states. The spectrum consisted of six narrow lines with anisotropic g-values. When the magnetic field was rotated in the (0001), the $(11\bar{2}0)$ and the $(10\bar{1}0)$ planes the positions of the e.s.r. lines changed with the field orientation as shown in Figs. (6-1), (6-2) and (6-3) respectively.

Fig. (6-1) shows that the spectrum repeats with a 60° period when the magnetic field is in the basal plane. Three lines should have appeared, A, B and C on Fig. (6-1), each being a superposition of two components. However the line B was not observed because the sample was unfortunately aligned

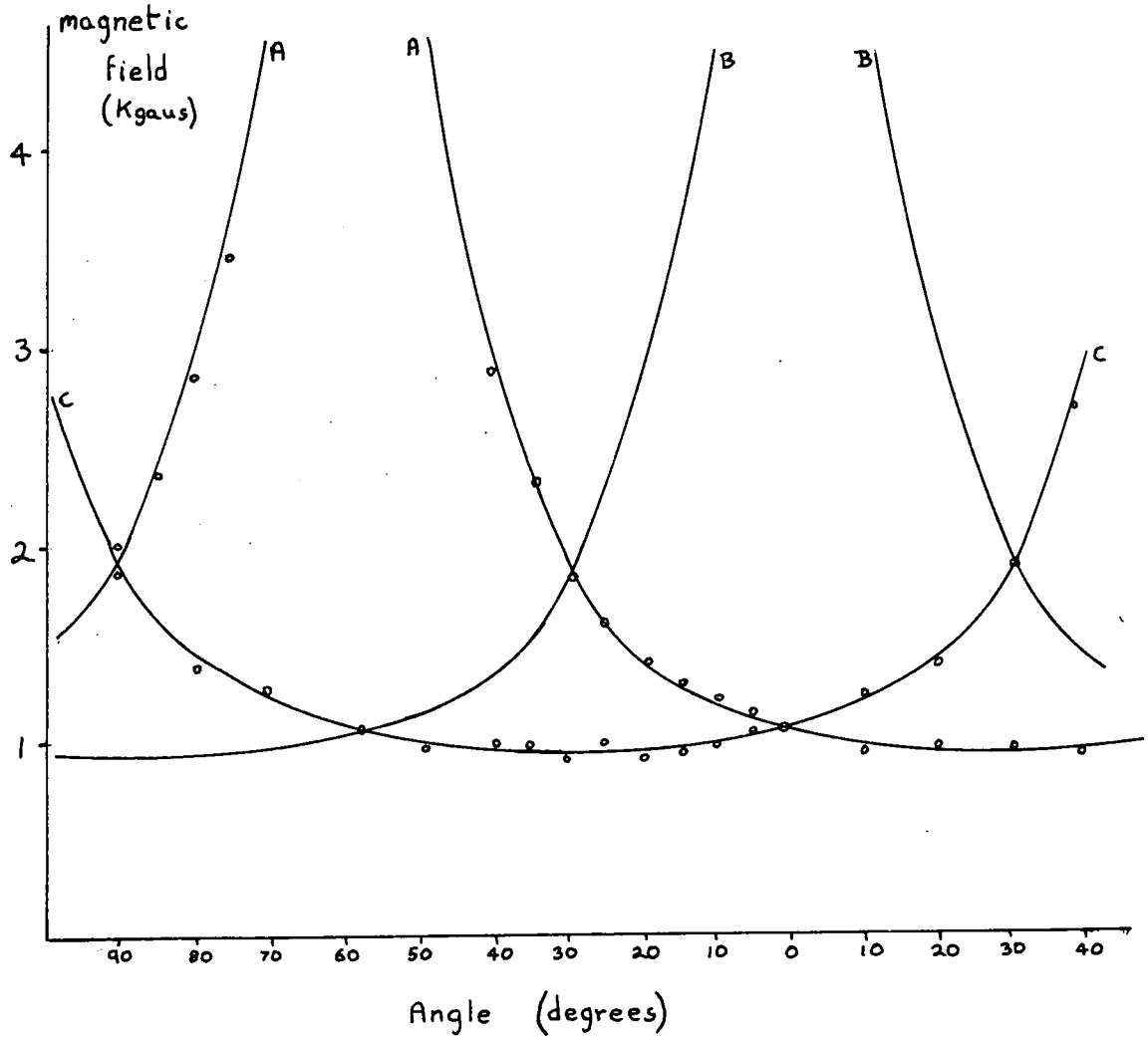


FIG.6-1. Positions of resonance lines for the magnetic field in the (0001) plane at 4.2°K and 9630 Mc/s. The angle is measured from the $[11\bar{2}0]$ direction. The solid lines represent the theoretical resonance fields.

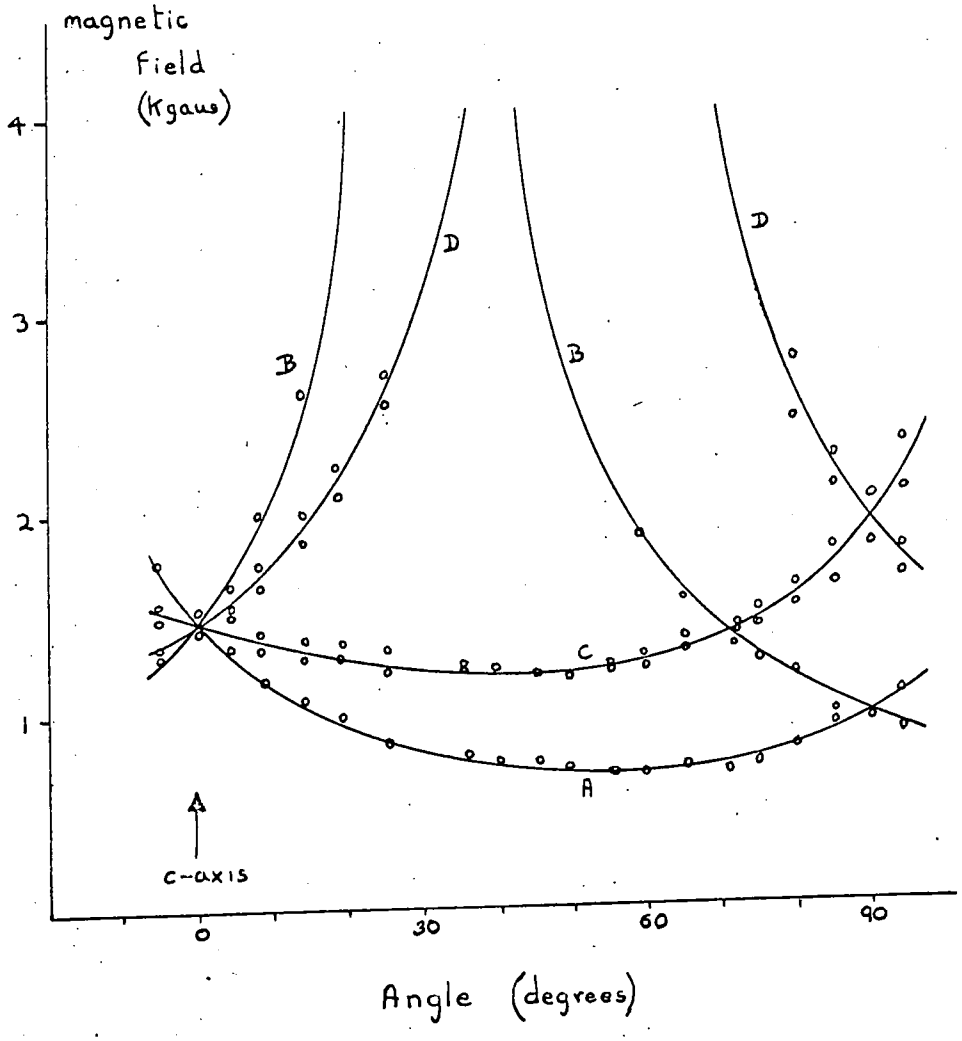


FIG.6-2. Positions of resonance lines for the magnetic field in the $(11\bar{2}0)$ plane at 4.2°K and 9482 Mc/s.The solid lines represent the theoretical resonance fields.

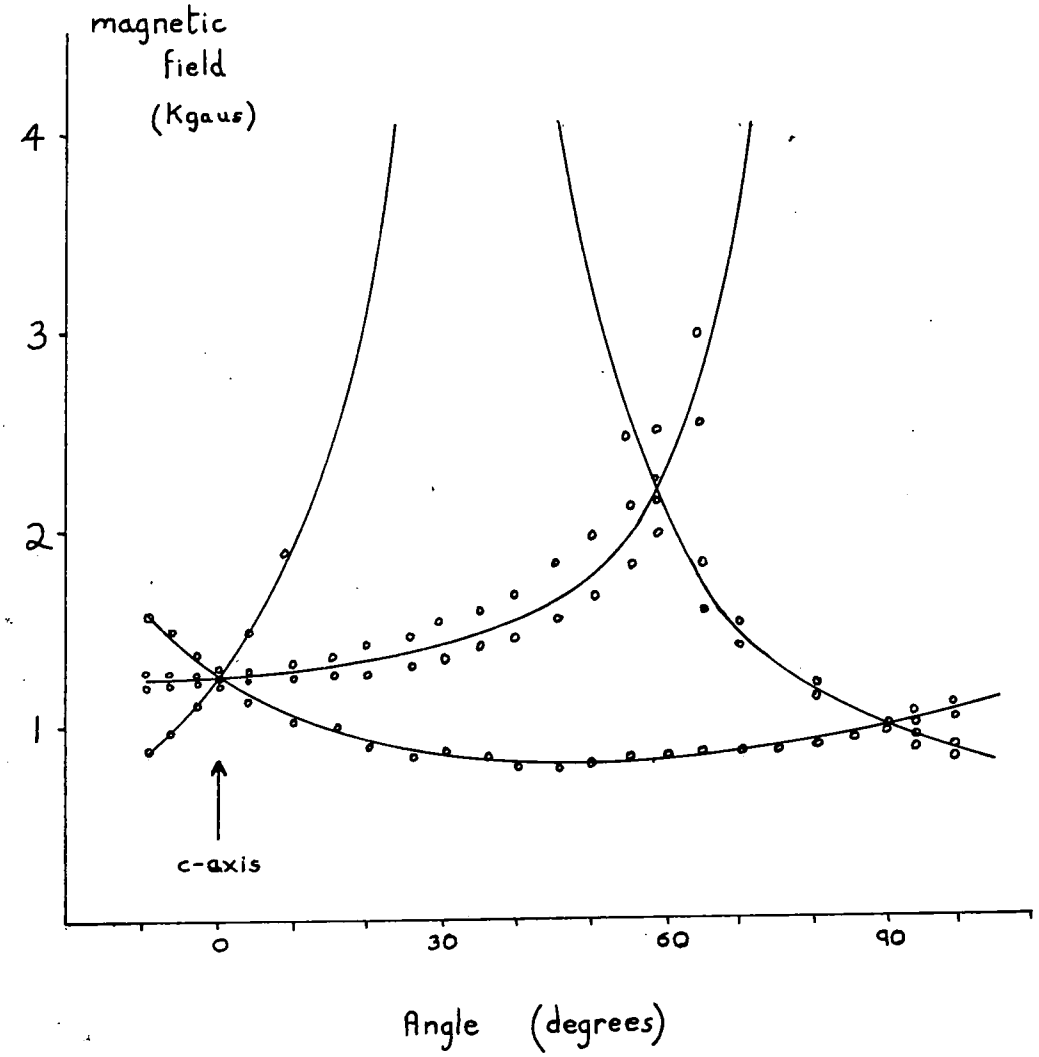


FIG.6-3. Positions of resonance lines for the magnetic field in the $(10\bar{1}0)$ plane at 4.2°K and 9480 Mc/s. The solid lines represent the theoretical resonance fields.

in the cavity in such a way that the R.F. magnetic field was perpendicular to the z-axis of the centre responsible for this line, and in this orientation the transition probability for the e.s.r. transition is zero. At some orientations of the magnetic field the lines A and C were resolved into closely spaced doublets. This effect was due to slight mis-alignment of the sample.

With the magnetic field in the $(11\bar{2}0)$ plane four lines were observed, A, B, C and D. (see Fig. (6-2)). C and D were a superposition of two lines which became closely spaced doublets at some field orientations. In the $(10\bar{1}0)$ plane three lines were observed, each being a superposition of two components.

The solid lines representing the theoretical resonance fields were calculated using the values for the spin Hamiltonian parameters given by Morigaki[1] and Estle et al[2] who have previously reported the e.s.r. of $Cr^{2+}$ in CdS. The agreement between the theoretical and observed resonance fields is very close and clearly identifies the spectrum as due to $Cr^{2+}$. The superhyperfine structure associated with the interaction with surrounding cadmium nuclei reported by the above authors could not be observed because the spectrometer sensitivity was insufficient.

6-1.2 Manganese

Manganese is expected to substitute for a $Cd^{2+}$ ion and to be in the $Mn^{2+}$ configuration. The ground state of the free ion is an orbital singlet with fivefold spin degeneracy. When the ion is placed in a crystal field small zero field splitting of five spin states occurs so that an e.s.r. spectrum is obtained which consists of five closely spaced resonance lines. Each of these lines is split into six hyperfine components by interaction with the $Mn^{55}$ nucleus which has a nuclear spin of $^5/_2$. Consequently $Mn^{2+}$ is recognised by a characteristic spectrum of thirty closely spaced e.s.r. lines. Since the ground state is an orbital singlet, there is only a small interaction between the spin states and the lattice and the spin-lattice relaxation time is sufficiently long to allow the spectrum to be observed at room temperature. The spectrum shown in Fig. (6-4(a)) was obtained from a sample of CdS deliberately doped with manganese. The assignment of the transitions was based on the intensity ratios. Back reflection X-ray studies of the sample showed that it was polycrystalline which probably explains why the $M_{5/2-3/2}$, $M_{3/2-1/2}$, $M_{-1/2--3/2}$, $M_{-3/2--5/2}$ transitions of the $m = \frac{3}{2}$ and $\frac{5}{2}$ hyperfine components were not resolved. Fig. (6-4(b)) shows the spectrum that was obtained for the same sample at the same orientation at $4.2^{o}K$. It can be seen that the lines are sharper and more clearly resolved

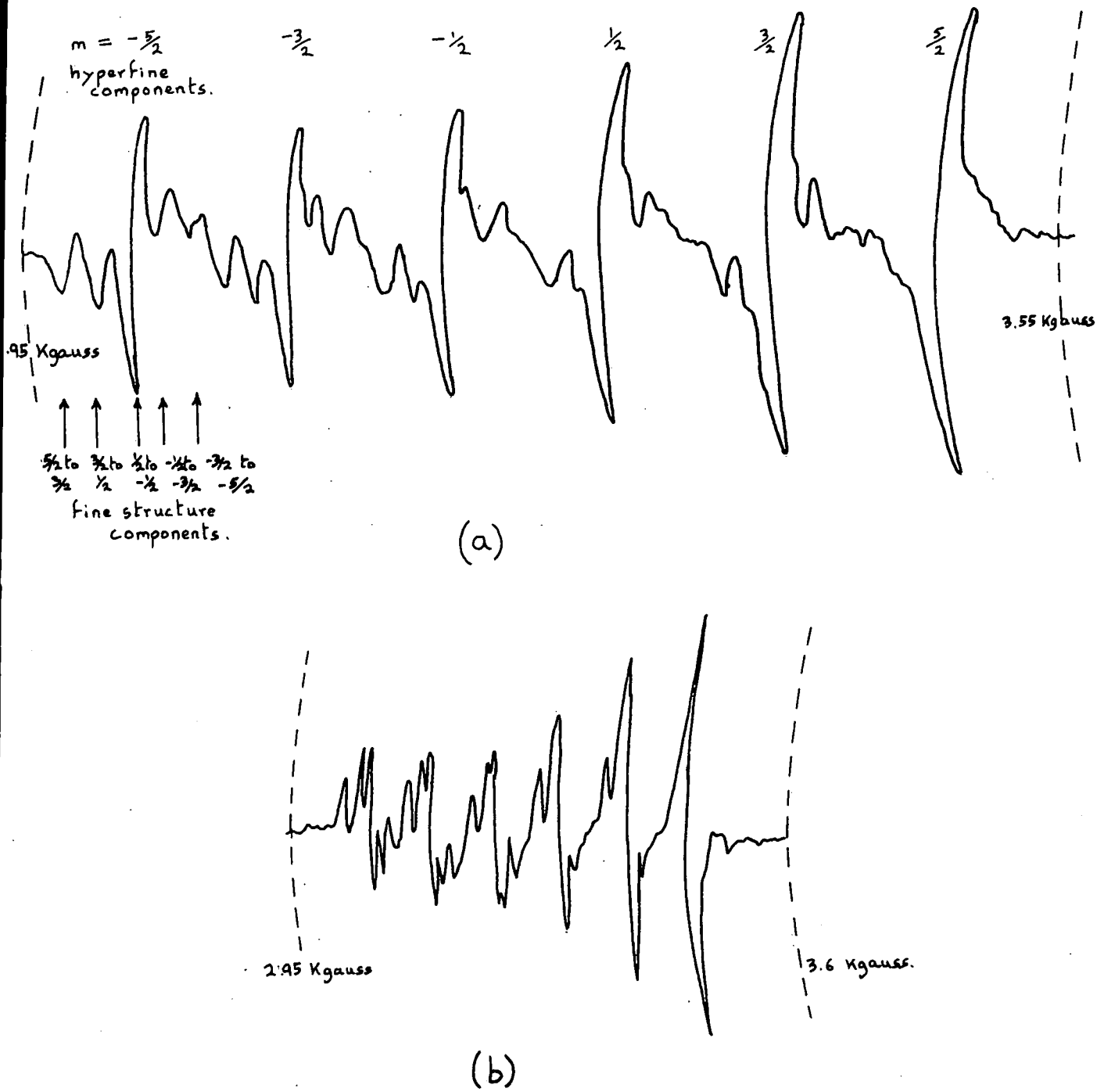


FIG.6-4.e.s.r. spectrum of $Mn^{2+}$. in CdS at x-band frequencies at (a) 300°K and (b) 4.2°K.

at this temperature. The e.s.r. of $Mn^{2+}$ in single crystals of CdS has been reported by Dorain[3], Lambe and Kikuchi[4] and Deigen et al.[5]. All these workers described the characteristic $Mn^{2+}$ spectrum illustrated in Fig. (6-4). The measurements at 4.2°K demonstrated that the $Mn^{2+}$ spectrum began to show saturation effects at incident r.f. power levels of a few milliwatts. This is to be expected since the spin-lattice relaxation time is known to be long at 4.2°K and is in agreement with the observations of Deigen et al.[5] The intensity of the $Mn^{2+}$ spectrum increased linearly with power incident on the cavity up to a power level of about 1 mwatt. Above this power level up to the maximum output of the klystron, 25 mwatts, the intensity remained constant. At the maximum power level the lines in the spectrum did not appear to be broadened. These remarks will be important when we come to discuss the resonance of the defect centres in chapter 7.

6-1.3 Cobalt

A resonance attributed to cobalt was detected at 4.2°K in samples G.P.O.x93 and R12. Cobalt is expected to substitute at the cadmium site and to be in a $Co^{2+}$ charge state. One line due to $Co^{2+}$ impurity was observed. The position of the line as a function of the magnetic field orientation

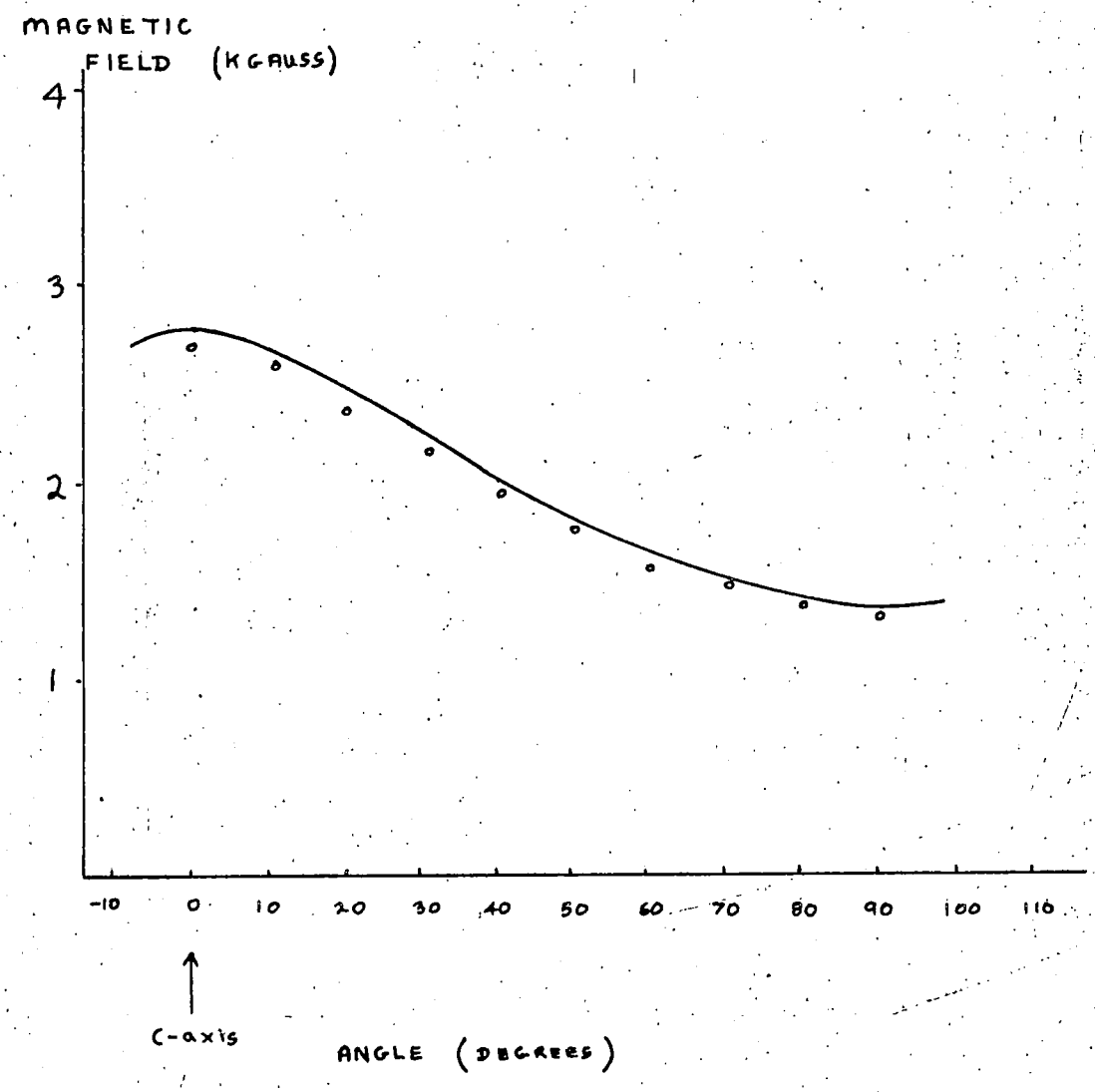


FIG.6-5. Positions of the resonance line of $Co^{2+}$ for the magnetic field in the (1010) plane at 4.2°K at x-band frequencies. The solid line represents the theoretical resonance fields using the parameters given by Morigaki[6].

in the $(10\bar{1}0)$ plane is shown in Fig. (6-5). The solid line representing the theoretical resonance fields was calculated using the spin Hamiltonian quoted by Morigaki[6] with the values of the parameter measured by him, namely

$$g_{//} = g_{\perp} = 2.275 \pm 0.001$$

where $g_{//}$ refers to the g-tensor parallel to the c-axis. There is some disagreement between the calculated fields and those observed. This was later found to be due to sample misalignment. The measured g-value was:-

$$g_{//} = g_{\perp} = 2.38 \pm 0.02$$

This corresponds to a misorientation of the sample away from the c-axis of approximately $3^{o}$. Re-examination of the sample alignment by back reflection X-ray studies confirmed this result.

The hyperfine structure which might be expected to result from the interaction with the $Co^{59}$ nucleus which has nuclear spin $\frac{7}{2}$ was not observed, because the intensity of the observed line was too small. However the line shape closely resembles that obtained by Morigaki[6] as can be seen from Fig. (6-6(a) and (b)).

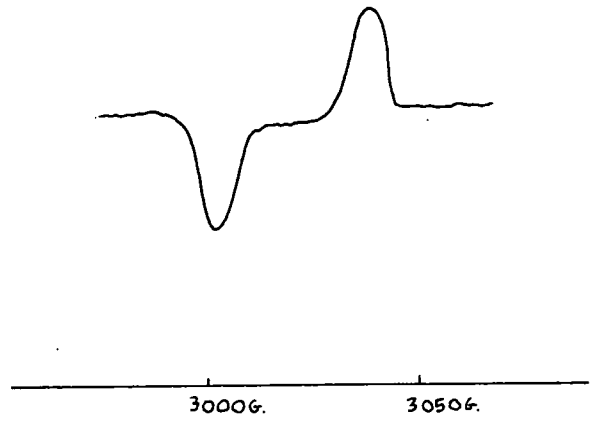


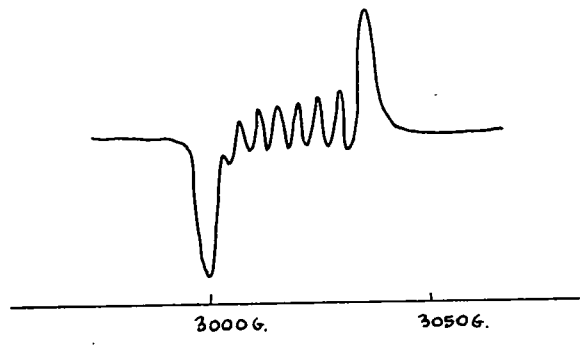


FIG.6-6. Line shape for the $Co^{2+}$ line parallel to the c-axis at x-band frequencies.

(a) observed in this work.

(b) observed by Morigaki[6].

Clearly the e.s.r. data is in agreement with assignment of the centre as $Co^{2+}$.

6-2 Group 3 and Group 7 impurities

Group 3 and group 7 impurities introduce donor levels into CdS. The e.s.r. of Cl.[7], Br.,I[8] and Ga.[9] have previously been reported. During the course of the work to be described here the e.s.r. due to Cl., Ga., In.,Tl., Al. and B. has been observed. Identification of the centre responsible for the e.s.r. signal was made from knowledge of the donor impurity added during growth.

6-2.1 CdS:Cl

Chlorine will substitute for a sulphur ion and it is well known that it provides a shallow donor level approximately 0.03eV below the conduction band. The e.s.r. was only observable at 4.2°K. At room temperature and down to 77°K the samples were very lossy as the large degradation of the resonance cavity Q indicated. As the samples were cooled from 77°K to 4.2°K the cavity Q suddenly sharpened up at some intermediate temperature, indicating an increase in sample resistivity as the free electrons froze out into the donor levels.

At 4.2°K a single e.s.r. line of half width 15 gauss was observed with an almost isotropic g-value. No hyperfine structure was observed.

The measured g-values were:-

$$g_{//} = 1.80 \pm 0.02$$
$$g_{\perp} = 1.79 \pm 0.02$$

These values are in close agreement with those found by Lambe and Kikuchi[7].

$$g_{//} = 1.792 \pm 0.002$$
$$g_{\perp} = 1.785 \pm 0.002$$

As indicated in section (3-4.2) the e.s.r. of shallow donors impurities in CdS can be understood using the model of Müller and Schneider[10]. In this model the trapped electron moves in a diffuse orbit of large radius and its properties are essentially determined by the intrinsic band properties of CdS. Slagsvold and Schwerdtfeger[11] have used equations (3-15) and (3-16) of section (3-4.2) to calculate the g-shift for the e.s.r. of iodine in CdS assuming the band picture of chapter 1. The predicted sign of the shift was not observed in practice. They concluded that more information concerning the detailed nature of the states forming the valence and conduction bands was required (see section 1-2) but that the model for the donor centre was correct. Con-

sequently at this stage it is inappropriate to attempt to calculate the g-shift for the e.s.r. for any of the shallow donor centres.

6-2.2 CdS:Ga

The gallium ion substitutes at a cadmium site and also behaves as a shallow donor centre. As with the CdS:Cl the samples were lossy from 300°K down to 77°K and trapping of the donor electrons was observed as the samples were cooled from 77°K to 4.2°K. The e.s.r. signals were observed at 4.2°K.

No e.s.r. absorption due to Ga. could be detected in samples 'as grown', but absorption was detected after the samples had been heated at 700°C for twenty hours in 30 atmospheres of sulphur vapour. This treatment was expected to create a large concentration of cadmium vacancies and cause diffusion of Ga. into these sites.

A single e.s.r. line was observed with a half width of 10 gauss with an almost isotropic g-value practically equal to that of the CdS:Cl. Again no hyperfine structure could be detected.

The measured g-values were:-

$$g_{//} = 1.80 \pm 0.02$$

$$g_{\perp} = 1.79 \pm 0.02$$

The values are in close agreement with those given by Dieleman[9].

$$g_{//} = 1.796 \pm 0.002$$
$$g_{\perp} = 1.782 \pm 0.002$$

These results support the model of Müller and Schneider[10] which predicts a delocalised electron orbital which does not depend on the donor site, since the Ga. ion is at a different site from that of the Cl. ion but still gives essentially the same g-value.

6-2.3 CdS:In

Indium is the element directly below gallium in group 3b of the periodic table and also substitutes at the $Cd^{2+}$ site. It is expected to be a shallow donor centre but there is no reported value for the donor depth. The resistivity changes on cooling to 4.2°K were similar to those for CdS:Cl and CdS:Ga. and indicate that In. behaves as a shallow donor centre, as also do the g-values of the observed e.s.r. signals.

As with the CdS:Ga e.s.r. absorption was only observed in samples which had been heat treated in sulphur vapour. However it was observed that the signals could be seen only immediately after heat treatment. They quickly decayed if the sample was left at room temperature for a

few days and could not be made to re-appear even if the sample was heated again in sulphur vapour. This behaviour was not understood. The e.s.r. consisted of a narrowly spaced doublet which coalesced into a single line when the magnetic field was perpendicular to the c-axis. Unfortunately the g-values were not measured accurately the first time the sample was investigated and as indicated above the e.s.r. could not be reproduced. However the g-values were approximately identical to those of CdS:Ga. and CdS:Cl. This supports the model that the In. forms a shallow donor centre in CdS. The doubling of the line can be explained if one postulates that the centre forms a deeper level below the conduction band than CdS:Ga. and CdS:Cl. so that the bound electron is more localised at the donor site. Then the In. may be substituted at two inequivalent sites which are equivalent in the c-plane. This may be due to the two inequivalent $Cd^{2+}$ sites in the wurtzite CdS lattice. However the donor depth for In. is still of the same order as for Ga. and Cl. and so the bound electron is still probably sufficiently delocalised for the two inequivalent sites not to affect the wavefunction of the bound electron. There is insufficient information at the present time to confirm this proposed explanation. It will be necessary to investigate the angular variation of the spectrum in different crystallographic planes to determine the nature

of the indium site. This was not carried out because the samples were too small to allow accurate orientation studies to be made. There is no previously reported data on the resonance spectrum of In. in CdS.

6-2.4 CdS:Tl

Thallium is the final element in the group 3b series. There is no reported data on the nature of this substitutional impurity in CdS, but from the above information on CdS:Ga. and CdS:In. it is expected to be a donor. The change in resistivity on cooling to 4.2°K agrees with this assignment. The change from low to high resistivity occurred just above 77°K which suggests that thallium provides a deeper level than the donor impurities described above.

The e.s.r. was detected at 77°K and 4.2°K in the samples as grown, and was enhanced by heat treatment in sulphur vapour. However as with the CdS:In. following heat treatment the lines quickly decayed and could not be reproduced by subsequent heat treatment. As with the CdS:In. the e.s.r. spectrum consisted of a doublet which coalesced into a singlet for the magnetic field in the c-plane. The splitting of the doublet was much greater than for CdS:In. and the g-values were significantly shifted towards the spin only value of 2.

The measured g-values were:-

$$g_{\perp} = 1.96 \pm 0.02$$

$$g_{//} \begin{cases} = 1.89 \pm 0.02 \\ = 1.88 \pm 0.02 \end{cases}$$

The spectrum was highly saturated at 4.2°K and was only observable with power levels of approximately a few micro watts incident on the cavity. It was easily detectable at 77°K at maximum incident power (25 milliwatts). No hyperfine structure was observed.

If the splitting of the line is considered to be due to the existence of two inequivalent sites because of the reduction of the radius of the electron orbital then the splitting could be greater with Tl than with In. because Tl. is the deeper donor. This view is also supported by the tendency of (a) the g-value to shift towards the free electron value and (b) the spin-lattice relaxation time to increase. These features are indicative of the bound electron being in a state which is tending to an s-state, which would be expected since the outermost unoccupied atomic orbital of the impurity is in each case an ns orbital, where n = 3, 4 and 5 for Ga. In. and Tl. respectively.

6-2.5 CdS:Al and CdS:B

These two ions belong to group 3a of the periodic table. Crystals doped with either Al. or B. were too small for

e.s.r. signals to be observed in individual rods. To increase the signal level five or six rods were aligned in the same direction inside a glass tube, which was placed in the microwave cavity. Clearly the observations obtained must be treated with some caution, but they support the conclusions of the previous section.

The increase of resistivity on cooling indicates that Al. and B. both act as donor centres in CdS with levels below the conduction band at approximately the same depth as those of thallium.

The e.s.r. signals were observed in samples as grown and were enhanced after heat treatment in sulphur vapour. After the sulphur treatment the e.s.r. spectrum decayed with time and could not be reproduced. The signals were highly saturated at 4.2°K and were detected without saturation at 77°K. The spectra consisted of two lines with a splitting comparable to that of CdS:Tl with a g-value between that of shallow donor signals ($g = 1.8$) and the free electron value ($g = 2.0$). The lines were rather broader than CdS:Tl but this was probably due to slight misorientation between the rods composing the sample. Clearly these observations are very similar to those for CdS:Tl and lend support to the model outlined earlier.

## 6-2.6 Conclusions

Before any definite conclusions can be drawn from the above observations many more measurements are required on larger single crystals. In particular the angular variations of the spectra in different crystallographic planes must be investigated. In addition measurements of the donor depths of the impurity centres would be useful. However some useful conclusions can be drawn from the present data. From the resistivity observations it appears that all the six impurities act as shallow donor centres. There seems to be an increase in the depth of the donor level below the conduction band following the sequence:-

$$\text{Cl.} \sim \text{Ga.} < \text{In.} < \text{Tl.} \sim \text{Al.} \sim \text{B.}$$

The Cl. and Ga. impurities are known to give rise to donor levels 0.03eV below the conduction band. The deeper levels of Tl., Al. and B. are estimated to be $\sim$0.1eV below the conduction band, since with these donors the free electrons freeze out at temperatures $\sim$2 or 3 times higher than for CdS:Cl. and CdS:Ga. The radius of the trapped electron orbit will be correspondingly reduced and the electron is more localised at the impurity site. The radius of the

electron trapped at Cl. site in CdS is ~30 Å therefore the radius for these deeper donors is expected to be ~10 Å i.e. approximately four lattice spacings. The e.s.r. data suggests that the impurity occupies two inequivalent substitutional sites because of the splitting of the e.s.r. line into a doublet for the deeper donor centres. It is impossible at this stage to indicate the nature of these sites and this must await further measurements.

The outermost unoccupied atomic orbital of the impurity ion is in each case an s orbital. Thus the more localised electron orbital of the deeper donors will tend to have an s-character. As pointed out above, this assumption is supported by the fact that the spin-lattice relaxation time is much longer for the deeper donors and the g-value is shifted towards the free electron value of 2. Recently Title[12] has reported a similar effect for S. Se. and Te. donor impurities in GaP. The donor ionisation energies for these impurities in GaP. are ~0.1eV, whereas the hydrogenic model for shallow donors (as used by Müller and Schneider[10] for CdS.) predicts a value of 0.046eV. This is a similar situation to that for CdS, discussed above. Kohn and Luttinger[13] have outlined a treatment for correcting the calculation of the g-shift for deep donor states. Formally,

this is done by dividing the wavefunction of the trapped electron into two parts, an outer region where the effective mass formalism used for the shallow states is still valid and an inner region where, since the dielectric constant is no longer a good concept, a new wavefunction is required. A recalculation of the g-tensor with the corrected wavefunctions has not been carried out. However Title[12] indicated that since the electrons of a deep donor impurity are in a smaller orbit they are less influenced by the lattice, a g-value between that calculated from the uncorrected effective mass theory and the 2.0023 expected for a tightly bound s-like state would be predicted. This is observed in CdS for the deep donor states associated with Al., B. and Tl. However this does not explain the doubling of the e.s.r. lines for CdS:Tl, CdS:Al and CdS:B which remains unexplained at present.

# CHAPTER 6

## REFERENCES

(1) K. Morigaki - J. Phys. Soc. Jap. 19, 187, 1964.

(2) T. L. Estle, G. K. Walters and M. DeWitt - Proc. First Int. Conf. Paramagnetic Resonance, Edited by W. Low (Academic Press, New York, 1963) Vol. 1 p. 144.

(3) P. B. Dorain - Phys. Rev. 112, 1058, 1958.

(4) J. Lambe and C. Kikuchi - Phys. Rev. 119, 1256, 1960.

(5) M. F. Deigen, V. M. Maevskii, V. Ya. Zevin and N. I. Vitrikhovskii - Soviet Physics - Solid State 9, 2193, 1965.

(6) K. Morigaki - J. Phys. Soc. Japan 19, 2064, 1964.

(7) J. Lambe and C. Kikuchi - J. Phys. Chem. Sols. 9, 492, 1958.

(8) B. J. Slagsvold and C. F. Schwerdtfeger - Can. J. Phys. 43, 2092, 1965.

(9) J. Dielman - Proc. 11$^{th}$ Colloque Ampere, Eindhoven 1962, North-Holland Publ. Co. Ltd. p. 409, 1963.

(10) K. A. Müller and J. Schneider - Phys. Letts. 4, 288, 1963.

(11) B. J. Slagsvold and C. F. Schwerdfeger - Can. J. Phys. 45, 127, 1967.

(12) R. S. Title - Phys. Rev. 154, 668, 1967.

(13) W. Kohn and J. M. Luttinger - Phys. Rev. 98, 915, 1955.

# CHAPTER 7

## MEASUREMENTS AND DISCUSSION OF E.S.R. LINES OBSERVED WHICH ARE NOT ATTRIBUTED TO ISOLATED IMPURITY IONS

The e.s.r. results obtained during the course of this work which were attributed to isolated impurity ions have been discussed in chapter 6. In addition to these spectra, further e.s.r. lines of unknown origin were observed at $4.2^{\circ}K$. The work that has been carried out suggests that some of these lines are due to defect centres in the lattice but their origin is still uncertain. The results discussed in this chapter were obtained from the large undoped single crystals of CdS that were available (see chapter 5), unless otherwise stated. The lines which occurred in the e.s.r. spectra of these samples and which were identified as due to impurity ions have already been discussed in chapter 6 will not be included.

### 7-1 Form of the spectra

As can be seen from chapter 5 a wide variety of samples of undoped CdS were available. However the e.s.r. spectra obtained from these samples can be classified into four types. The general shape of these spectra is shown in Figs. (7-1) to (7-4). (In these figures the derivative of the imaginary part of the susceptibility against field

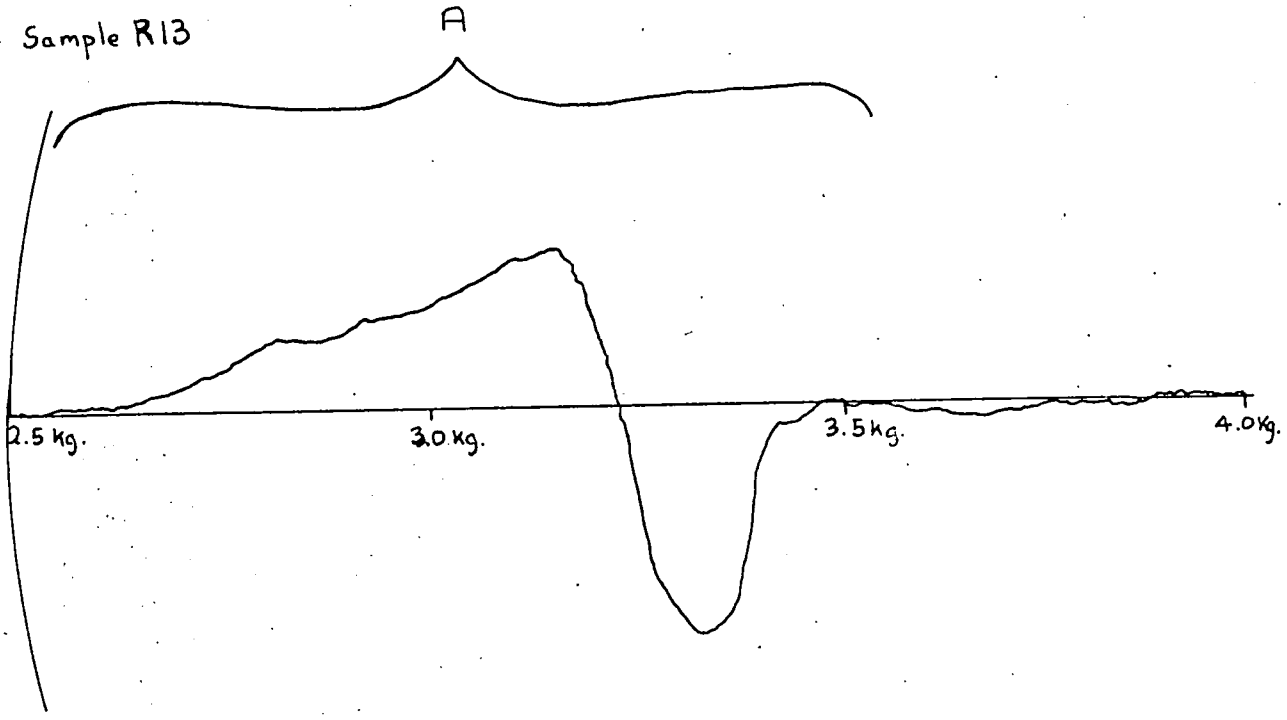


FIG.7-1. e.s.r. spectrum 1 obtained in undoped CdS at 4.2°K at x-band frequencies. Magnetic field along the c-axis.

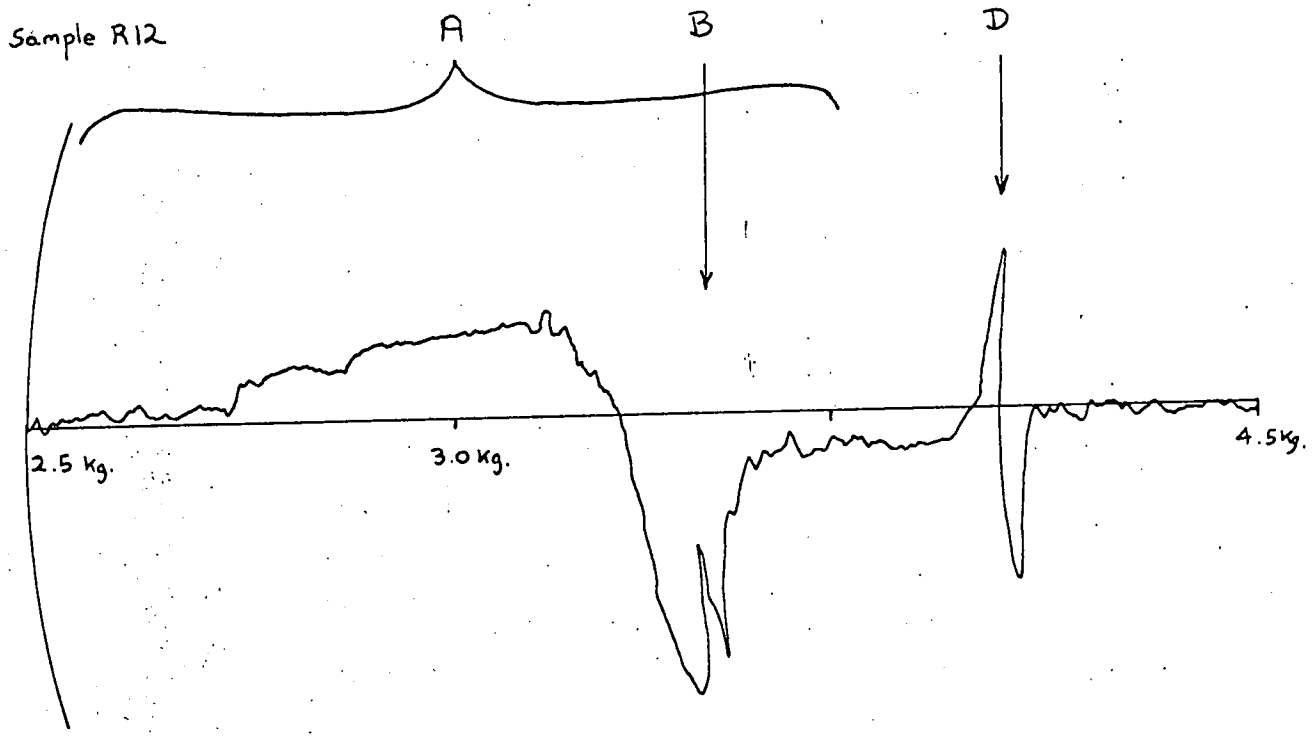


FIG.7-2. e.s.r. spectrum 2 obtained in undoped CdS at 4.2°K at x-band frequencies. Magnetic field along the c-axis.

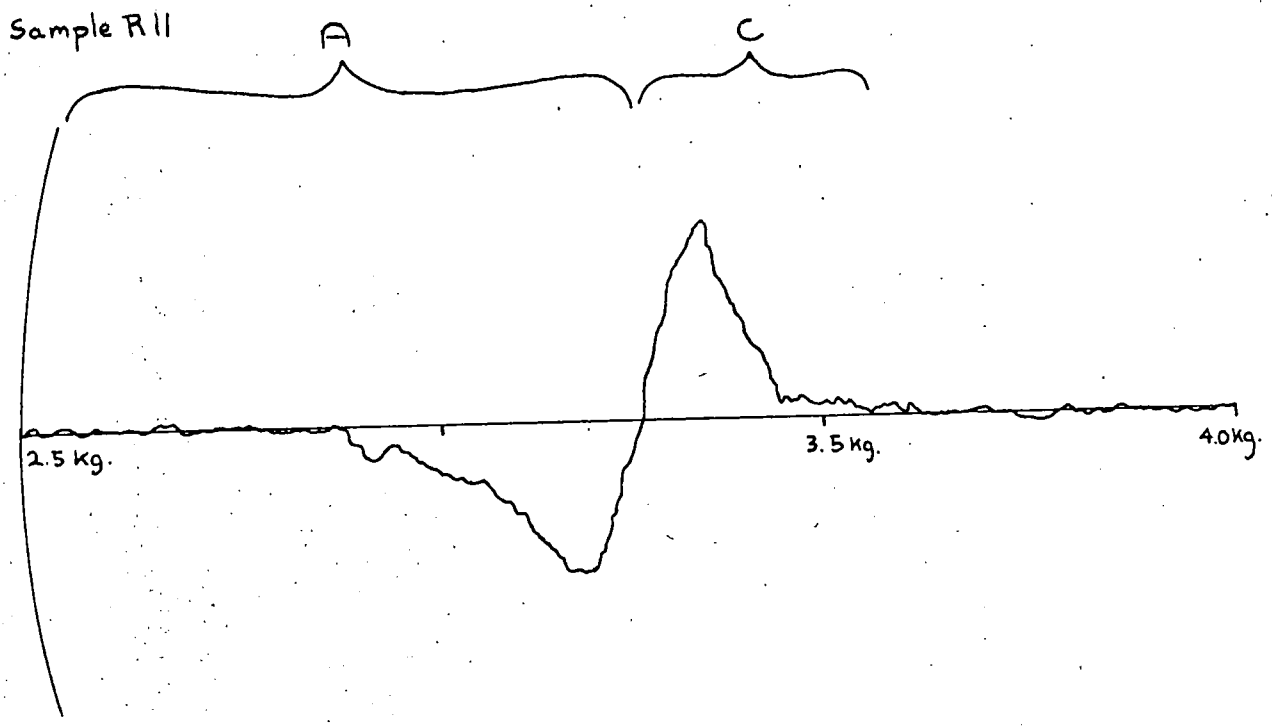


FIG.7-3. e.s.r. spectrum 3 obtained in undoped CdS at 4.2°K at x-band frequencies. Magnetic field along the c-axis.

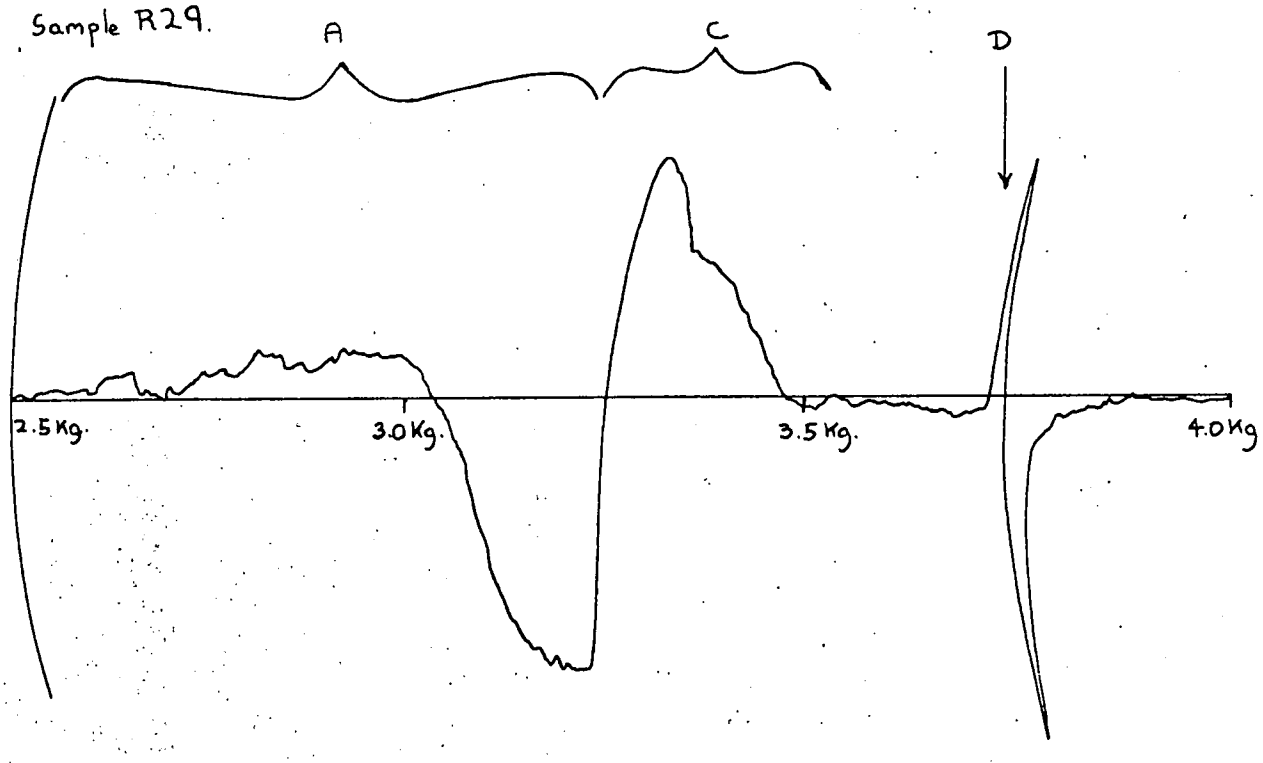


FIG.7-4. e.s.r. spectrum 4 obtained in undoped CdS at 4.2°K at x-band frequencies. Magnetic field along the c-axis.

$\frac{\partial \chi''}{\partial H}$ vs. $H$ is shown). The relative intensities and detailed structure of the spectra varied from sample to sample, but this will be discussed later. It can be seen that altogether four absorption lines, lettered A, B, C and D for identification, have been observed. Of these lines, only line D can be related to reported data, the other lines have not previously been reported.

The line A has been observed in all the samples investigated. It is characterised by an extremely large line width. The line width (which for this work is defined as the width between the peaks of the derivative curve, i.e. the width at maximum slope) was typically 130 gauss. It was difficult to measure g-values accurately because of the width and the asymmetry. Also it appears to have slightly different g-values in different samples. The values obtained for R14 and G.P.O. x 93 emphasise this point.

$$\text{R14} \qquad \begin{cases} g_{//} = 2.12 \pm 0.02 \\ g_{\perp} = 2.10 \pm 0.02 \end{cases}$$

$$\text{G.P.O. x 93} \qquad \begin{cases} g_{//} = 2.08 \pm 0.02 \\ g_{\perp} = 2.07 \pm 0.02 \end{cases}$$

$g_{//}$ is the g-value // to c-axis. $g_{\perp}$ is $\perp$ to c-axis.

The line appears to be axially symmetric about the c-axis. The difference in g-values will be explained later, when a model for the centre responsible for the line is presented. The line D was observed in most samples and has an almost isotropic g-value which is very close to that obtained for the shallow donor centres discussed in chapter 6.

$$g_{//} = 1.80 \pm 0.02$$
$$g_{\perp} = 1.79 \pm 0.02$$

The line B was always observed as a small shoulder on the broad line A and was seen in about half of the samples investigated. It's intensity was dependent on whether the sample was cooled in the dark or under illumination. It has an almost isotropic g-value:-

$$g_{//} = 2.00 \pm 0.02$$
$$g_{\perp} = 1.98 \pm 0.02$$

The line C was a very broad and asymmetric absorption peak. Because of the asymmetry it was not possible to measure a g-value, but the line always appeared at the same values of magnetic field and was isotropic with field orientation. It was observed only in a few of the samples.

## 7-2 Correlation of the spectra with other properties

Having discussed the general nature of the e.s.r. spectra it is useful to compare the occurrence of the spectra with other properties of samples.

There was no correlation between the growth conditions and the e.s.r. spectra. This was not unexpected since none of the other properties e.g. resistivity, luminescence, could be consistently related to the growth conditions.

### (a) Resistivity

A better correlation was obtained with the sample resistivity. The resistivities were not measured accurately, but were estimated from the damping caused by the sample of the cavity Q. Therefore the values quoted are only correct to within an order of magnitude. Table 1 gives the comparison between the resistivities and the type of spectrum observed. Clearly there is a good deal of correlation, especially between the resistivity and occurrence of line D.

The resistivity will be closely related to the density of the shallow donor levels. The e.s.r. line D, which from its g-value, has been interpreted above as due to shallow donor centres. Thus, if this interpretation is correct, there should be a correlation between the intensity of line D and the resistivity.

TABLE 1

| Sample | Resistivity | | e.s.r. spectrum | |
|---|---|---|---|---|
| | at 300°K | at 4.2°K | under band gap illum. | unillum-inated. |
| LR26 | $>10^6\Omega$.cm. | $>10^6\Omega$.cm. | 2 | 1 |
| R13 | | | 1 | 1 |
| R14 | | | 1 | 1 |
| R27 | | | 2 | 2 } Line D not detected |
| G.P.O.X93 | | | 2 | 2 } Line D not detected |
| LR25 | $\sim10^6\Omega$.cm. | $\sim10^6\Omega$.cm. | 4 | 2 |
| R11 | $\sim10^3\Omega$.cm. | $\sim10^4\Omega$.cm. | 3 | 3 |
| R9 | | | 3 | 3 |
| R29 | $\sim10\Omega$.cm. | $\sim10^4\Omega$.cm. | 4 | 4 |
| G.P.O.17A35 | | | 4 | 4 |
| R12 | $\sim10\Omega$.cm. | $>10^6\Omega$.cm. | 2 | 2 |
| R23 | | | 2 | 2 ← Line D not detected |
| R35 | | | 2 | 2 |
| R39 | | | 2 | 2 |
| Eagle Picher | | | 2 | 2 ← Line D not detected |
| U.H.P. grade | | | | |

In the group of samples LR26, R13 and R14 in table 1 which have a high resistivity at 300°K and 4.2°K, the e.s.r. line D is either not observed or is of low intensity. The other two samples in this group, R27 and G.P.O. x 93, do not show the line D with the sample in the dark, but under band gap illumination a large line is observed. These observations indications indicate that a large concentration of ionised shallow donor centres are present at 4.2°K in these two samples and that the high resistivity is caused by compensation of the donors by acceptors. The group of samples R12, R35 and R39 have a very low resistivity at 300°K which becomes high at 4.2°K. It is observed that the resistivity changes sharply at a temperature below 77°K, as the samples are cooled to 4.2°K. This suggests that there is a high density of donor levels which are ionised at 300°K but which are filled at 4.2°K. (The same behaviour was observed in the samples doped with impurities Cl. and Ga. which produce shallow donors. See section 6-2). In the undoped samples R12, R35 and R39 the line D is of large intensity. The other two samples in this group, R27 and the Eagle-Picher U.H.P: grade crystal, show the line D under band gap illumination only. This possibly indicates the presence of another set of shallow donors with levels

which are at a slightly greater energy separation from the conduction band. These donors are not paramagnetic. In support of this model it was found that the change from low to high resistivity on cooling occurred at a temperature above 77°K, whereas in the other samples this occurred below 77°K.

Clearly the e.s.r. line D is associated with shallow donor centres. The observations from the e.s.r. measurements clarify the conclusions that can be drawn from the resistivity data and should prove very useful in interpreting Hall effect measurements to be made at 4.2°K.

The other groups of samples in table 1 cannot be dealt with as easily as those above, and it is apparent that recombination centres and other defects are important in determining the electron population in the conduction band. For the same reason it is not possible to obtain any correlation between the occurrence of the other three e.s.r. lines and the resistivity measurements.

(b) Edge emission

The edge luminescence spectra of the samples used in the e.s.r. work (and others) have been measured at 4.2°K in this department. I am very grateful to Dr. L. Clark for allowing me to discuss his results before publication.

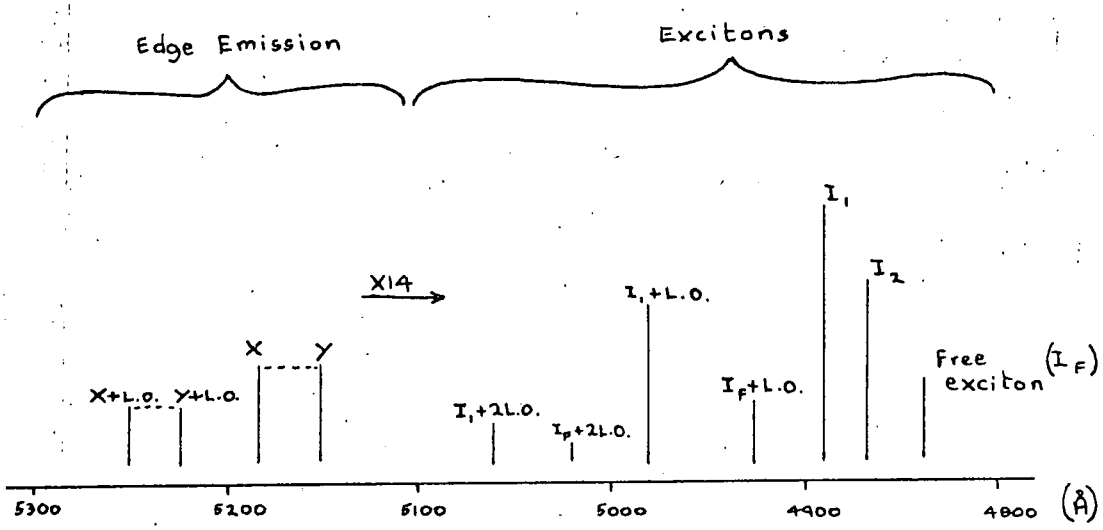


FIG.7-5. Luminescent emission from R12 at 4.2° K. The position of the lines indicate the position of the maxima of the emission peaks.The height of the lines indicate the intensity.

(L.O. ≡ longitudinal optical phonon.)

The luminescence was excited by a 500 watt high pressure mercury lamp and recorded using an 'optica' CF4NI grating spectrophotometer. An outline of the nature of the edge emission has been discussed in section (2-3.4). It consists of 2 series X and Y of phonon assisted bands. The series X is thought to be due to the recombination of an electron bound at a shallow donor and a hole bound to an acceptor which is about 0.17eV above the valence band. The Y series is due to recombination of a conduction electron and a hole bound at the same acceptor levels. Often at 4.2°K there are a number of emission lines situated at higher energies which are attributed to exciton recombination. Fig. (7-5) shows the position of the emission peaks at 4.2°K for a typical sample R12. In all the samples the dominant exciton lines were those denoted as $I_1$, $I_2$ or the free exciton.

Small peaks corresponding to other bound excitons were observed in some samples but these did not occur in a consistent way and therefore will be ignored. It is generally agreed that the line $I_1$ is associated with recombination of an exciton bound to a neutral acceptor and that $I_2$, which may be a superposition of several components, is due to excitons bound to neutral donors.(1)

Following from this identification of the exciton lines, the intensity and occurrence of $I_2$ can be correlated with the intensity of line D in the e.s.r. spectra. This provides further evidence that line D is due to shallow donor centres. It is not possible however to correlate the e.s.r. lines A and B with any features of the luminescence. It is concluded therefore that the centres responsible for these resonance lines are not involved in the luminescent transitions. This view is supported by the results obtained from the G.P.O. x 93 sample and the Eagle-Picher U.H.P. crystal, which did not show the normal green edge emission at 4.2°K. Instead a broad structureless emission band centred at about 7000 Å was obtained. In both these samples, however, the e.s.r. lines A and B were observed and were of comparable intensity with those observed in samples with good green emission. Also, in samples which emitted strongly in the green, the lines A and B were unaffected by the U.V. irradiation necessary to excite the edge emission.

The crystals in which the resonance line C was found (R9, R11, R29 and G.P.O. 17A35) showed unusual resistivity and luminescence features. They all had a low resistivity $\sim 10^4$ ohm.cm. at 4.2°K which is not yet understood. The luminescence spectra of these crystals showed only one

dominant exciton, which was at the position of $I_2$, and the intensity of the edge emission was much lower than that for R12. R12 was chosen as typical of 'normal' crystals and spectral emission distribution is shown in Fig. (7-5).

The intensity of the other excitons was very low. In samples R9 and R11 the edge emission consisted of a single series which was significantly shifted from the position of the X and Y series of Fig. (7-5). In these two samples the line D was not observed in the e.s.r. spectrum despite the fact that there was an exciton at the position of $I_2$. However recently Clark and Woods[2] have discussed the possibility that this exciton is $I_5$ which lies very close to $I_2$. $I_5$ is an exciton bound to an acceptor. This might explain the non-appearance of line D and why a different edge emission series is observed. These rather unusual features of the e.s.r. luminescence and resistivity are not understood at the present time and will be discussed again in section (7-6) when the nature of the centre responsible for the resonance line C is discussed. It can be seen that a comparison of the e.s.r. data with the resistivity and edge luminescence of a crystal enables some conclusions to be drawn concerning the nature of the centres responsible

for the levels in the forbidden gap of CdS. At the outset of the work reported in this thesis it was hoped that the e.s.r. technique would provide information which would allow the nature of these centres to be determined unambiguously. It has become apparent during the course of this investigation that this is not possible from the e.s.r. measurements alone and that these measurements are most useful when considered in relation to the other data obtained on the same samples. Consequently it is planned to measure the I.R. luminescence and thermally stimulated current spectra of the samples used in this work which it is hoped will complement the e.s.r. data.

Having discussed the general form of the e.s.r. spectra and related certain features to some of the other properties of the samples we are now in a position to discuss the individual lines, and try to determine the nature of the centres responsible for them.

7-3 Resonance line D

The results discussed above demonstrate that the resonance line D is due to electrons trapped at shallow donor centres. The e.s.r. of this type of centre has been treated in some detail in section (6-2) in the discussion of the resonance of group 3 and group 7 donor impurities in CdS. The

nature of the centre responsible for the resonance line cannot positively be identified from the position of the line since, as shown in section (6-2), all donor centres with levels less than about 0.05eV below the conduction band lead to a line with the same g-value. Consequently to see if the same centre is responsible for the resonance or whether there are different ones in different samples, it would be necessary to compare the e.s.r. spectrum with estimates of the trap depth of the shallowest trap, obtained, for example, from thermally stimulated current measurements.

The shape of the resonance line varied in different samples. This might indicate that different centres were present in different samples. However no definite conclusions can be drawn since the influence on the line shape of such factors as neighbouring donor and acceptor sites, lattice defects, dislocations, grain boundaries and elastic strain is not known. It is unlikely that the donor centres are due to impurity ions because different samples grown from the same starting material showed variations in the intensity of the donor resonance. However the growth technique may have introduced different degress of donor-acceptor compensation in the various samples thus causing a variation in the

'effective' concentration of donor impurities. This seems unlikely because in most of the high resistivity samples there was no evidence of acceptor compensation of the donor levels. Consequently the shallow donor levels are probably due to intrinsic lattice defects. The simplest defect that can be considered is the Sulphur vacancy. (Recently Woodbury et al[3] have indicated that interstitial cadmium and sulphur atoms are probably neutral and do not form trapping levels in the forbidden gap of CdS.) The ionic contribution to the bonding in CdS was quoted in section (2-1) as 75%. This value is consistent with an effective charge of +e on the cadmium ion and -e on the sulphur ion. Consequently a sulphur vacancy would be expected to have an effective charge of +e and it can be treated in the same way as a group 7 substitutional ion, at a sulphur site. Thus the theory of Müller and Schneider[4] for an electron trapped at such a site is appropriate as was discussed in sections (3-4.2) and (6-2). In this model the trapped electron is assumed to move in a delocalised orbital of large radius. The theory predicts that an isotropic e.s.r. line $g \simeq 1.80$ will result. This is consistent with the observed data. Morigaki[5] has reported the observation in CdS at $1.5^{o}K$

of a resonance line with $g_{//} = 1.783 \pm 0.003$ and $g_{\perp} = 1.764 \pm 0.003$ which he attributed to sulphur vacancies. However he discussed a model where the trapped electron was localised at the vacancy site. He used this model to estimate the value of the g-shift for the centre using the method presented by Kasai and Otomo[6], which is outlined below.

The sulphur vacancy is surrounded by four cadmium ions, $Cd_A$, $Cd_B$, $Cd_C$ and $Cd_D$. If $Sp^3$ hybridisation of the valence electron orbitals of the cadmium ions is assumed then let $\phi_o\ (Cd_A)$ represent the orbital of $Cd_A$ directed towards the vacancy and $\phi_1\ (Cd_A)$, $\phi_2\ (Cd_A)$ and $\phi_3\ (Cd_A)$ the three orbitals directed away from the vacancy. The ground state wavefunction of a single localised electron at the vacancy can be approximated to:-

$$\phi_o = \tfrac{1}{2}\left[\phi_o(Cd_A) + \phi_o(Cd_B) + \phi_o(Cd_C) + \phi_o(Cd_D)\right] \qquad (7\text{-}1)$$

Equation (3-13) shows that the deviation of the g-tensor from the free electron value, caused by spin-orbit coupling of the form $\lambda \underline{L}.\underline{S}$ is to a first approximation given by:-

$$\Delta g_i = -2\lambda \sum_{n \neq o} \frac{\langle o|L_i|n\rangle\langle n|L_i|o\rangle}{E_n - E_o} \qquad (7\text{-}2)$$

In this approximate molecular orbital model, the most significant excited states are those in which the electron is transferred into one of the twelve orbitals of the surrounding cadmium ions not directed towards the vacancy. The $sp^3$ hybridised orbitals can be written in the form[7]

$$\phi_o(Cd_A) = \tfrac{1}{2}\,\psi_{5s}(Cd_A) + \tfrac{\sqrt{3}}{2}\,\psi_{5p}(Cd_A) \qquad (7\text{-}3)$$

Where $\psi_{5s}$ and $\psi_{5p}$ are the 5s and 5p atomic orbitals of the cadmium ion.

Clearly from the symmetry of the vacancy centre the g-tensor is isotropic and the g-shift is given by $\Delta g$. Combining equations (7-1), (7-2) and (7-3) the shift of the g-tensor is given by:-

$$\Delta g = -\frac{\lambda}{\Delta E} \qquad (7\text{-}4)$$

Where $\Delta E$ is the energy separation of the ground state and the excited states.

The small anisotropy of the observed g-tensor is assumed to be due to small distortion along the c-axis of the wurtzite lattice. The value of $\lambda$ is estimated to be 0.067eV from the atomic levels of the free cadmium ion[8]. The experimental value of $\Delta g$ can be explained by assuming $\Delta E$

is 0.29eV. This should be of the order of the ionisation energy of the donor levels. However this is hardly a shallow level and so this model for the sulphur vacancy is inconsistent with the experimental evidence for the centre responsible for line D. Thus if the line D is associated with sulphur vacancies, the trapped electron is expected to be in a delocalised orbital of large radius and not localised at the vacancy site.

Clearly at the present time the centre responsible for the line D cannot be established from the e.s.r. data. As shown in section (3-4.2) if the density of shallow donors is greater than about $10^{17}/cm^3$ the electron orbitals overlap and the electrons are not localised at one donor site and so no hyperfine structure due to interactions with the donor nucleus can be observed. Thus if the e.s.r. of donors of lower concentration than this can be observed and hyperfine structure can be observed, this would suggest that the donors are impurity atoms. It may also be possible to observe superhyperfine structure due to the interaction between the trapped electron and the surrounding cadmium ions to establish the form of the electron orbit. This may enable one to determine unambiguously the nature of the donor site.

The experimentally observed effects of the heat treatment on the magnitude of resonance signal favour the sulphur vacancy model since the intensity of line D decreases when the sample is heated at 700°C in 30-40 atmospheres pressure of sulphur vapour and increases when heated at 600°C in $10^{-3}$ Torr pressure of cadmium vapour. This is to be compared with the results of section (6-2), where it was noted that heat treatment in a sulphur atmosphere increased the intensity of the e.s.r. lines due to group 3 impurities and did not affect those due to group 7 impurities.

In conclusion, it can be seen that measurements of the occurrence and intensity of the e.s.r. line D provides information about the concentration of shallow donor centres in a sample and can determine whether there is appreciable compensation by acceptors or not. This data may prove useful in the interpretation of resistivity and Hall effect measurements. However at the present time no unambiguous identification of the centre can be presented.

7-4.1 Resonance line A

This line, which has been observed in every sample investigated, has not previously been reported in the literature. In every specimen it was observed as a broad asymmetric line as can be seen from Figs. (7-1) to (7-4).

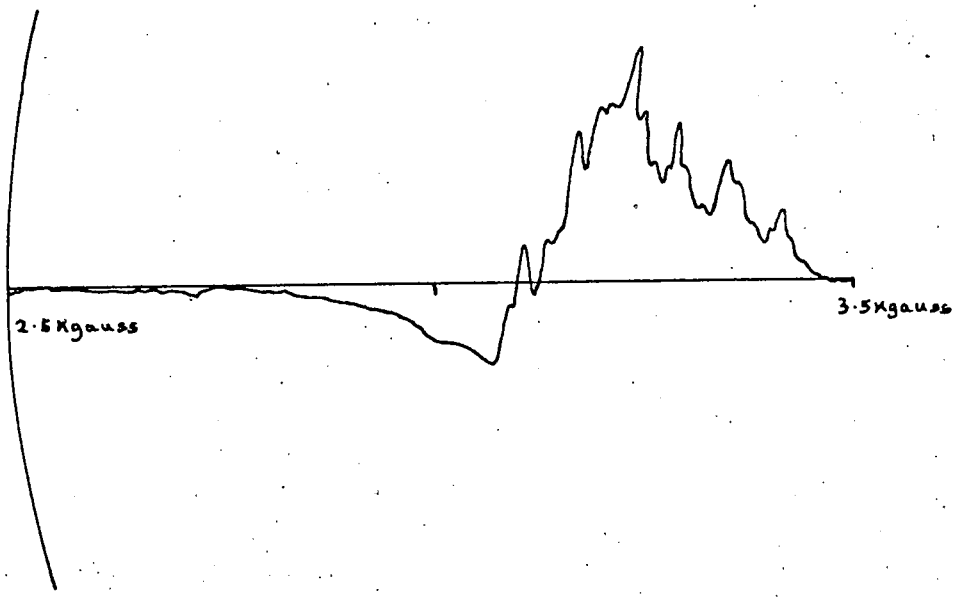


FIG. 7-6. e.s.r. spectrum obtained in CdS sample containing a significant concentration of $Mn^{2+}$ impurity at 4.2°K and 9.35 Kmc/s. The magnetic field was oriented along the c-axis.

The intensity did not vary greatly from sample to sample. The maximum variation was about an order of magnitude except for a sample which was heavily doped with silicon, where the intensity was an order of magnitude greater than the largest intensity observed in the undoped samples. The variation of the intensity does not seem to be related to any of the other properties of the samples which have been studied in this laboratory nor to the expected total impurity content. For example in the Eagle-Picher U.H.P. grade crystal the intensity of the line was of the same order as for many of the samples grown in our own laboratories, the impurity content of which is expected to be about 10-100 times greater.

In most samples the line showed no structure, however some was observed in a few samples. This was rather vague and did not occur in any consistent manner. A further difficulty in interpreting the structure arises because the line A overlaps the region in which the $Mn^{2+}$ spectrum occurs (see section 6-1.2). In a sample grown at the A.E.I. Ltd. central research laboratories, Rugby (kindly supplied by Dr. P. D. Fochs), the spectrum shown in Fig. (7-6) was obtained. The sample contained a sufficient concentration of manganese impurity for the characteristic

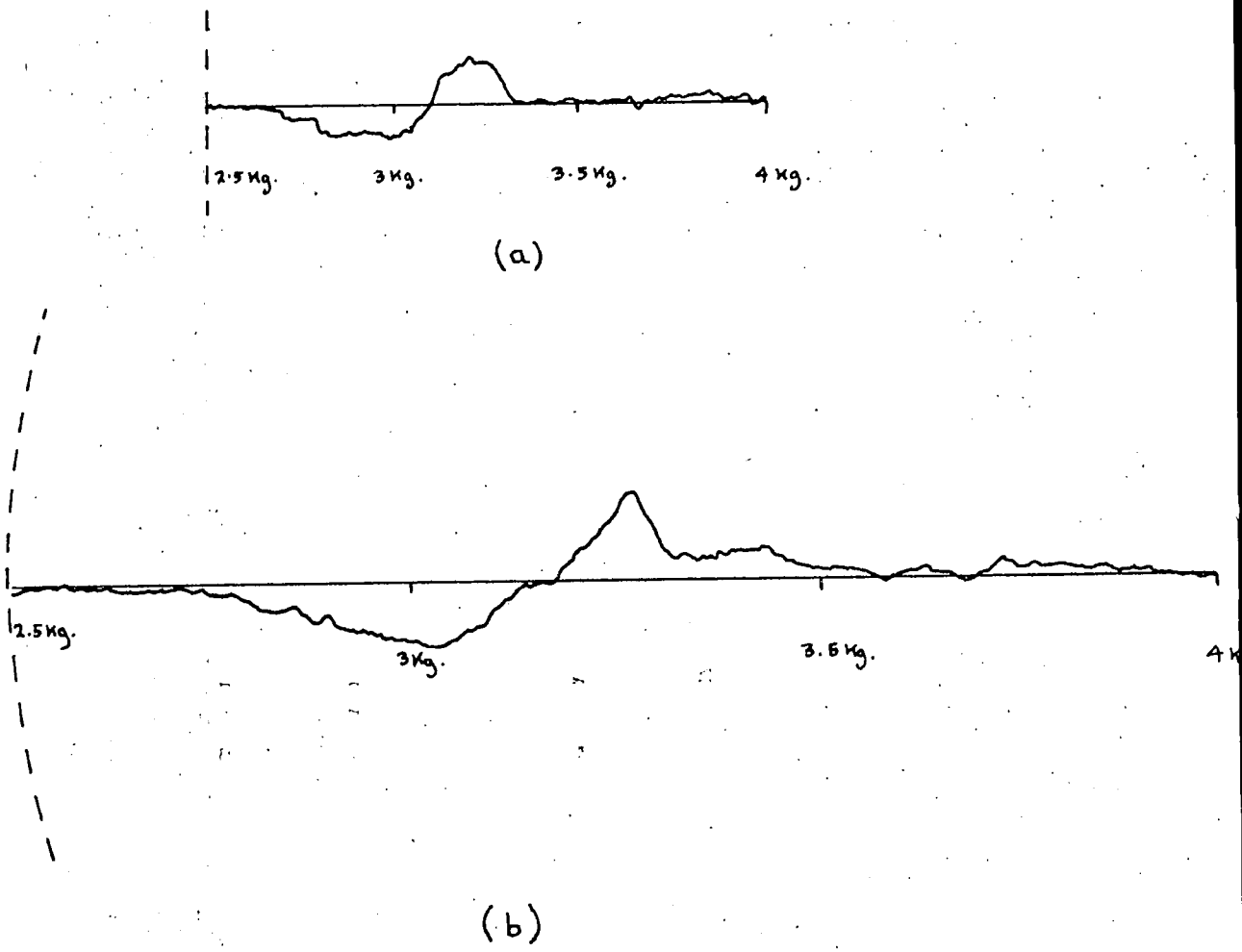


FIG. 7-7. e.s.r. spectrum for L.R.26 at 4.2°K. Magnetic field along the c-axis.

(a) Using the 'Varian' spectrometer.

(b) Using our own spectrometer.

C

spectrum of the $Mn^{2+}$ ion to be resolved above the background of the broad line A.

Clearly the structure that was observed in some of the undoped samples may have been associated with $Mn^{2+}$ impurity.

An attempt to clarify this point was made by carrying out e.s.r. measurements on samples LR25 and LR26 using a 'Varian' x-band spectrometer belonging to A.E.I. Ltd., Central Research Laboratories, Rugby, and which was far more sensitive than our own spectrometer. Using operating conditions comparable with those employed in our own spectrometer to observe the line A the spectrum shown in Fig. (7-7(a)) was obtained from the Varian spectrometer with sample LR26 at $4.2^{o}K$. The spectrum obtained from this sample using our own equipment is shown in Fig. (7-7(b)). Clearly the two spectra are essentially the same. When the same field range was investigated using the Varian spectrometer, but with a greatly reduced microwave power and field modulation, and utilising of the maximum sensitivity of the instrument, the characteristic $Mn.^{2+}$ spectrum was clearly identified. The measurements reported in section (6-2.1) showed that the $Mn.^{2+}$ spectrum could still be resolved using the operating conditions employed to obtain the

spectra shown in Fig. (7-7) if there was sufficient concentration of manganese impurity. Thus the measurements made with the Varian spectrometer demonstrate clearly that in the magnetic field region 2.5 to 3.5 Kgauss there is a broad e.s.r. line whose origin is not obvious and in addition there is the characteristic structured spectrum due to $Mn.^{2+}$. For a sufficient concentration of manganese impurity the $Mn.^{2+}$ spectrum can be resolved above the background of line A. We are now in a position to discuss some of the experimentally observed features of the broad line A, and will ignore the effects of the $Mn.^{2+}$ spectrum since this was not observed in the undoped samples employed in this work.

Because the intensity of line A cannot be related to the expected total impurity content in the undoped samples, it is reasonable to assume that the centre responsible for this line is composed partly or wholly of intrinsic defects. The work that has been carried out on samples subjected to heat treatment in cadmium or sulphur vapours support this model. (For experimental details of the heat treatment procedure see chapter 5). The effect of the heat treatment in sulphur vapour was to increase the intensity of line A. No quantitative measurements have been carried out at this stage.

In addition, a distinct narrowing of the line was observed. In certain cases a narrow line, which we shall designate A' was observed on top of the broad line A and this suggests that the narrowing of line A is due to the appearance of this new component A'. Fig. (7-8(a) and (b)) shows the spectrum of line A for R39 before and after the heat treatment. The new component A' can easily be resolved. The centre responsible for this line is apparently unstable since the intensity was noticeably reduced after the sample had been left at room temperature in the dark for several days. The cadmium vapour treatment was complementary to that of the sulphur and produced a reduction in the intensity of line A. No new e.s.r. components were observed. Once again no quantitative measurements have been made. These observations suggest that the centre (s) responsible for line A are associated with cadmium vacancies. As indicated in section (2-3.1) cadmium vacancies are expected to behave as hole traps. The fact that the g-shift for the line is positive suggests that trapped holes are involved, since the spin-orbit coupling constant ( $\lambda$ ) is negative for holes. It also appears that what has been described as line A is in fact composed of at least two components A and A'. More careful measurements after heat treatment in varying sulphur vapour pressures may reveal more

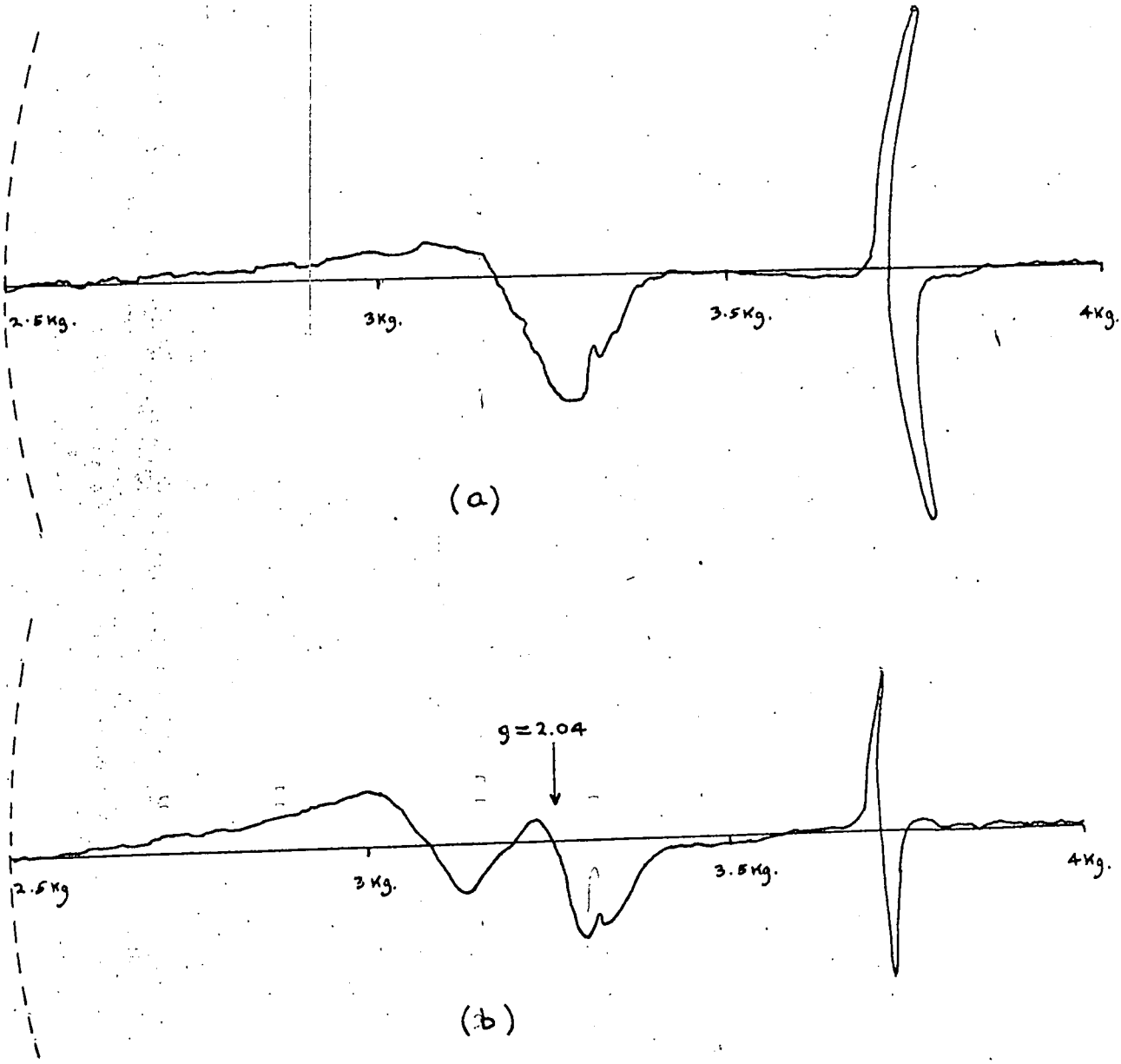


FIG. 7-8. e.s.r. spectrum for sample R39 at 4.2°K. Magnetic field along the c-axis.

(a) Sample as grown.

(b) Immediately after heat treatment at 700°C in 30 atmospheres of sulphur vapour.

components. However the presence of at least two components would explain the variation in line shape and width in different samples and also the variation of the apparent g-value of the line noted in section (7-1).

The effect of illuminating the samples with visible I.R. and U.V. irradiation was studied. Irradiation with light of energy greater than the band gap did not noticeably affect the line, even when the sample was emitting green edge emission. Obviously the centres responsible for line A are not associated with those responsible for the edge emission as was also noted in section (7-2). However irradiation with light in the wavelength range 0.6 - 0.9 microns brought about a reduction in the intensity of line A. The I.R. luminescence work reported in section (2-3.4) indicated that there is a level about 0.7eV above the valence band which is composed in part of cadmium vacancies. Recently Cowell and Woods[9] have suggested that the I.R. luminescence centres are identical with photoconductivity sensitising centres. If the e.s.r. line A is assumed to be due to these same centres then the effects of irradiation on line A can be understood. If these centres are acceptor-like, which is to be expected from their position in the forbidden gap, then they will be filled with electrons in the dark because they will act as compensating centres for

the donor levels. Consequently the band gap light which produces free hole-electron pairs would be expected to change the population of the centres responsible for line A, since they would trap the free holes. The fact that intensity of line A does not change suggests that the band gap light is absorbed close to the surface and therefore so few of the centres are affected that their effect cannot be observed. However the irradiation with red light will change the population of the centres, since it is not absorbed at the surface, by exciting electrons into the conduction band. If these electrons are not retrapped at the centres but are trapped elsewhere then the intensity of line A will be reduced, as was observed in a number of samples.

The most direct evidence to support this compensated acceptor model for the centre (s) responsible for line A was obtained from samples R23 and G.P.O. x 93. As discussed in section (7-2) these crystals have a high resistivity due to compensation since the donor line D is only observed when the sample is illuminated. When these samples were illuminated with red light in the range 0.6 to 0.9 microns, the donor line D appeared and the intensity of line A was reduced. There was a linear relationship between the

increase in the area under line D and the decrease for line A for varying intensities of illumination. The illumination was provided by a tungsten lamp with an intensity of 1000 foot candles at the sample which was passed through chance glass filters OR2 and ON1 and a copper sulphate cell to separate the required band of illumination. The position of the acceptor centre was estimated to be about 1.7eV below the conduction band, in agreement with I.R. luminescence data. This estimate was obtained using a narrow pass band interference filter centred at 7700 Å in conjunction with the same tungsten lamp. This illumination produced almost the same change in the intensity of line A as the broad band illumination. Consequently this wavelength must be close to the peak absorption wavelength for the electron transfer process. Once the donor line D had been produced it decayed very slowly, taking several hours to decay to half intensity, while the sample was maintained at 4.2°K in the dark. This decay probably represents slow thermal release of electrons to the conduction band. However irradiation with I.R. illumination of greater than 1 micron quickly reduced the intensity of line D and restored that of line A to its original value. This process can be compared with

the I.R. quenching of photocurrent in CdS. The effect of I.R. illumination is to create free holes in the valence band by transferring electrons to the paramagnetic centres which are ~0.7eV above the valence band. The free holes recombine with the donor electrons very rapidly. Thus the intensity of the resonance line A is restored to its original value and there is a rapid decay in the intensity of the donor resonance. These observations of changes in the e.s.r. spectrum when the samples are irradiated with red and then I.R. illumination suggest that in these two samples R23 and G.P.O. x93 there are two dominant centres, which give rise to a set of deep acceptor levels that compensate a set of shallow donor levels.

There is clear evidence of electron transfer between these two sets of levels. The position and behaviour of the acceptor levels suggests that they are identical with the I.R. luminescence and photoconductivity sensitising centres in CdS, but no measurements have been carried out on the I.R. luminescence and photoconductivity of these samples.

NOTE - In specimens R9, R11, R29 and G.P.O. 17A35 which show the resonance line C, the illumination with red light led to changes in the intensity of line A which corresponded to changes in line C. This is believed to be a different process from that discussed above and will be treated

in section (7-6) with the model for line C.

We are now in a position to discuss in a more quantitative manner the nature of the centre responsible for the e.s.r. line A, taking into account that it probably contains several components which give rise to compensated acceptor levels in the forbidden gap. The observations on heat treated samples suggest that the centres are composed partly or wholly of cadmium vacancies. Two models will be discussed:-

(a) An association of a cadmium vacancy and a donor impurity and higher associations of this type.

(b) A system of isolated, pairs, triads and higher clusters of cadmium vacancies, with the possibility of the inclusion of sulphur vacancies, i.e. a model consisting of intrinsic lattice defects.

The measurements made so far on CdS in this laboratory favour the second model, but the measurements are insufficient to allow a definite decision to be made. Further measurements are planned to try to provide information which will allow the model for the centre to be determined unambiguously. This may show that in fact the centre is a complex with a composition somewhere between the two extreme models (a) and (b) given above.

(a) Cadmium vacancy - donor impurity associate model

The reasons for considering this model are based on the fact that associations of oppositely charged centres are expected. Since no definite evidence has been found to suggest that centres containing equal numbers of sulphur and cadmium vacancies are important in CdS, it is reasonable to consider an association between cadmium vacancies and positively charged donor impurities. This view is supported to some extent by the work of Woodbury[10] on the diffusion of Cd in CdS where he concluded that the concentration of cadmium vacancies in CdS was determined by the donor impurity concentration. Also an e.s.r. spectrum of this type of vacancy - donor centre has been observed in ZnS[6], ZnSe[11] and ZnTe[12]. In each case the g-value was greater than the free electron value, in agreement with the observations of line A, and varied slightly with different dopings. The fact that the g-shift is positive suggests that a trapped hole is involved, and is trapped at the cadmium vacancy. The symmetry of the site as indicated by the e.s.r. measurements [6, 11, 12] is in agreement with that expected. The model for the complex, which is described as the A-centre, in cubic ZnS is shown in Fig. (7-9(a) and (b)) for group 3 and group

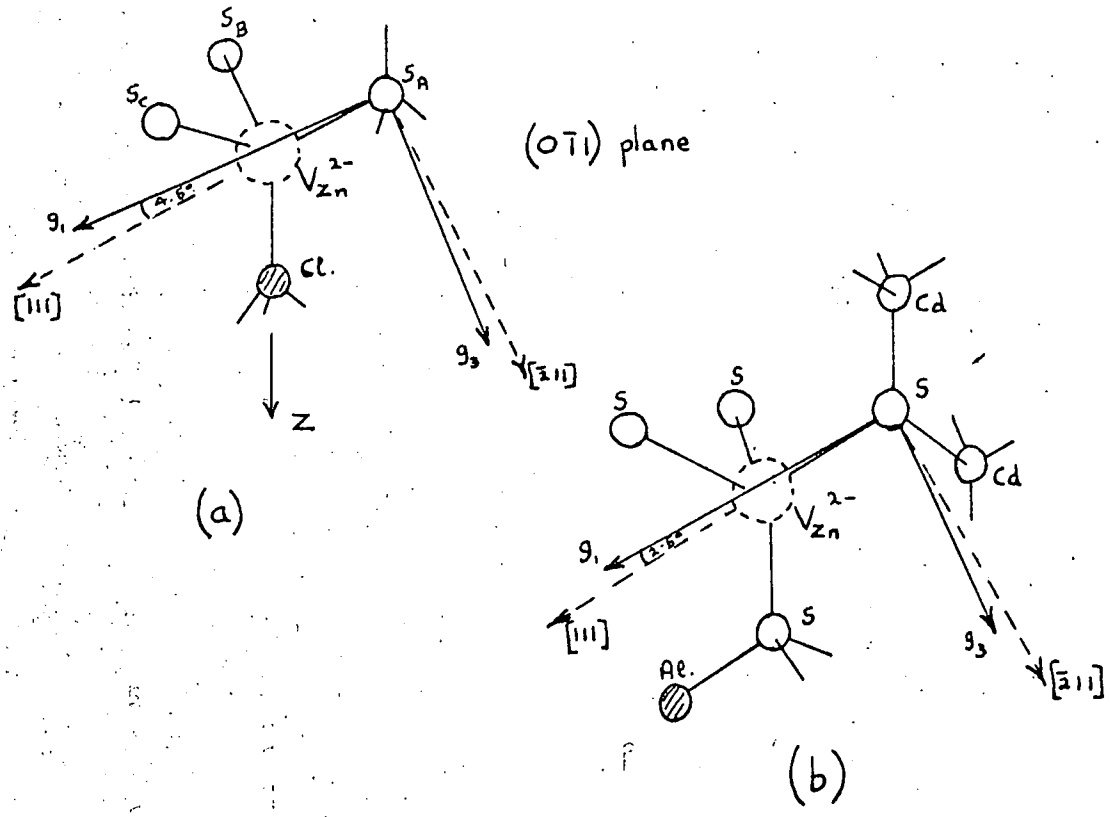


FIG.7-9. Model of the A-centre in ZnS. The two types of centre are indicated, where the zinc ion vacancy is in association with (a) a group 7 impurity and (b) a group 3 donor. The orthorhombic axes $g_1$ and $g_3$ are shown. $g_2$ is along the [0$\bar{1}$1] direction.

7 donor impurities respectively.

Consider first the A-centre of Fig. (7-9(a)). Because of the effective positive charge of the donor centre there is an electrostatic repulsion of a trapped hole away from it. At 4.2°K the hole can be pictured as being localised in one of the three sulphur bonds directed towards the vacancy and the resulting symmetry will be orthorhombic as is observed in ZnS[6]. At higher temperatures (77°K) the hole is able to 'hop' among the three equivalent sulphur bonds and the symmetry will become axial about the [111] axis. This is observed to occur[6]. In the hexagonal wurtzite lattice two types of A-centre are possible depending on the orientation of the zinc ion vacancy and the impurity relative to the crystallographic c-axis. The e.s.r. lines due to the two types of A-centre in hexagonal ZnS have been observed at 77°K[6]. The $g_{\parallel}$ axis of the g-tensor is rotated away from the [111] axis by a small amount because of the electrostatic repulsion of the ionised donor impurity.

The model of the A-centre in the cubic lattice in which a group 3 impurity is involved is shown in Fig. (7-9(b)). A hole trapped at this centre will be repelled to the sulphur ion most distant from the impurity because of the effective charge of the ionised group 3 impurity.

No 'hopping' between sulphur bonds is expected and the symmetry of the resonance line will then be orthorhombic. For the hexagonal modification there are three types of centre, with a corresponding increase in the complexity of the spectrum. However this spectrum has not yet been reported in a hexagonal 2-6 material.

With this knowledge of the position of the trapped hole let us consider a wavefunction for the hole from which the g-tensor can be calculated. Kasai and Otomo[6] have discussed the g-shift for the centre shown in Fig. (7-9(a)) in terms of a linear combination of atomic orbitals of the heighbouring sulphur ions. They included the effect of hole 'hopping' between the sulphur orbitals. This calculation is very similar to the one discussed in the treatment of the g-shift for the sulphur vacancy in section (7-3) and many of the expressions can be taken over directly. Since the hole is repelled from the donor impurity, the ground state wavefunction ( $\Phi_0$) for the hole can be approximated to:-

$$\Phi_0 = \frac{1}{\sqrt{3}}\left[\phi_0(s_a) + \phi_0(s_b) + \phi_0(s_c)\right] \qquad (7\text{-}5)$$

where once again we assume that $\phi_0(s_a)$ etc. represents the

orbital of sulphur ion $S_A$ etc. directed towards the vacancy and is an $sp^3$ hybridised orbital of the form:-

$$\phi_o(S_A) = \tfrac{1}{2}\psi_{3s}(S_A) + \tfrac{\sqrt{3}}{2}\psi_{3p}(S_A) \qquad (7\text{-}6)$$

We note that this centre in cubic ZnS has axial symmetry at 77°K. The symmetry axis is the parallel to the line joining the group 7 impurity and the vacancy and is denoted as the Z-axis in Fig. (7-9(a)). Following the treatment of section (7-3), the g-shift can be calculated from equation (7-3), using the wavefunctions defined by equation (7-5) and equation (7-6), giving:-

$$\left.\begin{aligned} \Delta g_{//_z} &= -\tfrac{4}{3}\cdot\frac{\lambda}{\Delta E} \\ \Delta g_{\perp_z} &= -\tfrac{5}{6}\cdot\frac{\lambda}{\Delta E} \end{aligned}\right\} \qquad (7\text{-}7)$$

Let us now consider whether this type of centre can be responsible for the experimentally observed e.s.r. data for line A. It seems impossible to explain the broad component of line A by this model since in ZnS the A centre lines were all narrow (~10 gauss half width) and with the variety of impurities studied, i.e. Cl; Ga; Br; I and Al; the peaks of the lines lay within a magnetic field range ~30 gauss at x-band frequencies. There is no obvious reason why this situation should be radically

different in CdS. If one considers an association of several vacancies and impurity centres then it may be possible to explain the broad line. However the fact that the intensity of the line is not related to the impurity content of the samples does not support this model. However a proper analysis of the individual impurity content of the samples is necessary before any definite conclusions can be reached. The observations made on single crystals of CdS doped with Al., B., Ga., In. and Tl. do not support the model cadmium vacancy - impurity donor complex. (The e.s.r. of the isolated donor impurities has already been discussed in section (6-2)). Unfortunately these samples were too small to make any quantitive observations and so no definite conclusions were reached. However it was observed that in these samples the shape of line A was not appreciably different from that of the large undoped single crystals and that the intensity, taking into account the relative volume of the doped and undoped samples, was not significantly larger. In addition, the fact that the centre responsible for line A is a compensated acceptor level cannot be understood. The maximum effective charge of the cadmium vacancy is -2e if a complete ionic model for CdS is assumed. Thus the effective charge

of the associated complex cannot be greater than $\lambda$-e and so it can only trap one hole from the valence band. The neutral centre therefore is paramagnetic and electron compensation by donor levels renders it diamagnetic. In ZnS the e.s.r. associated with the A-centre was only observed after illumination with light of photon energy greater than the band gap[6]. This is contrary to the observations for line A.

It is worth considering whether the narrow component of line A, A', which was observed in samples which had received heat treatment in a sulphur atmosphere, may be due to this type centre. As indicated in Fig. (7-8(b)) the line A' has a g-value of $2.04 \pm 0.02$ with the magnetic field along the c-axis. It was found impossible to follow the angular variation of this line round to the perpendicular position because of the complication presented by the broad component A. However to within an accuracy of about 3% the line A' appears to be isotropic. The calculated g-shifts from equation (7-7) are $\Delta g_{//} = 0.05$, $\Delta g_{\perp} = 0.03$. The value of $\lambda$ evaluated from the atomic energy levels for free sulphur was 0.025eV[8]. ($\lambda$ has a negative sign because this is a trapped hole centre). The value of $\Delta E$ was estimated from the height of the acceptor level above the valence band, which has been shown to be approximately

0.7eV. The concentration of the individual donor impurities will presumably be comparable with the density of the associated pairs. Hence an e.s.r. line would be expected which comprises a super-position of the lines due to all the different complexes, which contain the group 3 and group 7 donor impurities which are present in the samples, and which is isotropic with a g-value of about 2.04. However there was no correlation between the intensity of the resonance with the expected impurity content of the samples, moreover in the doped samples there was no noticeable increase in the intensity of this line even though many of the samples were heated in sulphur vapour to make the e.s.r. spectrum of the isolated impurity observable (see section 6-2). Once again, therefore, it is unlikely that the e.s.r. line A' is due to a centre which contains donor impurity ions, but more quantitiative measurements on large doped single crystals are necessary before any definite conclusions can be drawn.

The present evidence suggests that the centre(s) responsible for the e.s.r. line A and the components in this region do not contain donor impurity ions, or if they do the impurity ions do not make a significant contribution to e.s.r properties of the centre.

(b) Clusters of Cadmium Vacancies

Since the possibility that impurities are important components of the centres responsible for line A has been eliminated and it is known that cadmium vacancies are important, it remains to consider the e.s.r. signals expected from a cluster of an association of cadmium vacancies. There is a certain amount of experimental evidence to suggest that cadmium vacancy clusters exist in CdS. For example, Boer and Kennedy[13] interpreted their work on thermally stimulated currents and photoconductivity in samples of CdS heat treated in ultra high vacuum in terms of dissociation of defect associates containing cadmium vacancies with the consequent production of paired and single cadmium vacancies. Similarly Cowell and Woods[9] interpreted their results on thermally stimulated currents and I.R. luminescence in terms of complex centres which were composed partly or wholly of cadmium vacancies.

Complex associations of lattice defects are known to exist in the alkali halide group of materials and a great deal of experimental and theoretical work has been carried out on these materials. For a comprehensive review of this topic see the review article of Compton and Rabin[14].

In KCl., e.s.r. spectra have been reported which have been attributed to the association of two F-centres[15] and three F-centres[16] at nearest neighbour sites. Thus it is not unreasonable to expect to observe the e.s.r. spectrum of an association of cadmium vacancies. A rigorous treatment of the spin Hamiltonian of such a defect containing more than one 'force centre' is beyond the scope of this thesis. Some attempts have been made to predict the values of the parameters which occur in the spin Hamiltonian of associated defect centres in alkali halide materials[17] but there have been no attempts at such calculations for other materials. Consequently an approximate treatment will be presented where it will be assumed that each cadmium vacancy contains one trapped hole, which is localised at that vacancy (some support for this assumption will be given later), and the effects of exchange interactions between neighbouring vacancies in a cluster will be taken into account.

7-4.2 Exchange interactions

The close proximity of two paramagnetic ions allows a so called exchange interaction to take place between the electrons in the ions. This interaction arises because electrons are indistinguishable from one another and as a result two electrons may change places without any

change in the apparent configuration. The effects of exchange interaction are demonstrated when proper allowance for the possibility of quantum jumps of this nature is made. All of the experimental and theoretical work so far reported has been concerned with systems of pairs and triads of paramagnetic transition and rare earth metal ions.

The usual treatment of exchange follows that originated by Dirac[18]. He showed that for a system of electrons where the electrons are confined to different specified orthogonal orbitals of which a typical pair have wavefunctions $\psi_i(r)$ and $\psi_j(r)$, the exchange interaction coupling the spins can be written:-

$$V_{ex.} = -\sum_{ij} J_{ij}\, \underline{S}_i \cdot \underline{S}_j \qquad (7\text{-}8)$$

where $J_{ij}$ is the 'exchange integral' and depends on the overlap of the orbital wavefunctions and $\underline{S}_i$ and $\underline{S}_j$ refer to electron spins in the orbitals.

This form is correct when spin-orbit coupling interactions are neglected and can be used unchanged in considering the exchange interaction between paramagnetic ions in a crystal in this approximation. Although in many aspects of

paramagnetism it is not permissible to neglect spin-orbit interactions, no detailed treatment of the effects on the exchange of its inclusion seems to be available. The custom, therefore, is to use an equation of the form of (7-8) in dealing with exchange between paramagnetic ions. This interaction is then said to be an 'isotropic exchange interaction', because it depends only on the relative orientations of the spins. However the value of J will probably depend not only on the separation but also on the positions of the ions, because in a crystal field potential the charge densities are generally not spherically symmetrical. This leads to the so-called 'anisotropic exchange' and this term is used to account for those parts of the exchange interaction which have a form different from equation (7-8). If the line joining the two ions is an axis of symmetry of the two ions and their surroundings, the anisotropic exchange can be written in a form similar to that of the dipole-dipole interaction between the ions[19]:-

$$\mathcal{H}_{an} = \sum_{ij} f_{ij} \left[ \underline{S}_i . \underline{S}_j - 3 r_{ij}^{-2} (\underline{S}_i . r_{ij})(\underline{S}_j . r_{ij}) \right]$$

7-4.3 Position of e.s.r. lines due to exchange coupling

The spin Hamiltonian for pairs and triads of exchange coupled paramagnetic ions will be discussed next. The form of the spin energy levels and expected e.s.r. spectra will be indicated. It is usually found that exchange is only important between nearest neighbour ions.

Pair spectra

The spin Hamiltonian for a pair of exchange coupled paramagnetic ions of spin $\underline{S}_1$ and $\underline{S}_2$ respectively has been discussed by several authors, including Owen[20], Bleaney and Bowers[21] and Slichter[23]. With no exchange let the Hamiltonian for the isolated ion of spin $\underline{S}_1$ be of a typical form:-

$$\mathcal{H}_1 = g\beta \underline{H}.\underline{S}_1 + D_c\left[(S_{1z})^2 - \tfrac{1}{3}S_1(S_1+1)\right] + E_c\left[(S_{1x})^2 - (S_{1y})^2\right] + A\,\underline{I}_1.\underline{S}_1 \qquad (7\text{-}9)$$

There is a similar Hamiltonian $\mathcal{H}_2$ for the ion with spin $\underline{S}_2$. The first term represents the Zeeman energy, the term in A is the hyperfine structure interaction and those in $D_C$ and $E_C$ the usual second order crystal field terms with axial and rhombic symmetry respectively.

An exchange interaction is now introduced so that the Hamiltonian for the pair system is:-

$$\mathcal{H} = \mathcal{H}_1 + \mathcal{H}_2 + J\,\underline{S}_1\cdot\underline{S}_2 + D_e\left[3S_{1z}\cdot S_{2z} - \underline{S}_1\cdot\underline{S}_2\right] + E_e\left[S_{1x}\cdot S_{2x} - S_{1y}\cdot S_{2y}\right] \qquad (7\text{-}10)$$

The term in J represents the isotropic part of the exchange. Higher order terms, e.g. $J_2(\underline{S}_1\cdot\underline{S}_2)^2$ have been assumed to be negligible. Similarly it is assumed that the anisotropic part of the interaction is of low order and is described by the terms in $D_e$ and $E_e$, which have axial and rhombic symmetry respectively. It has also been assumed that the axes of the interaction x, y and z are the same as those of the crystal field.

Equation (7-10) can be rewritten:-

$$\mathcal{H} = g\beta H\cdot\underline{S} + \frac{J}{2}\left[\underline{S}(\underline{S}+1) - \underline{S}_1(\underline{S}_1+1) - \underline{S}_2(\underline{S}_2+1)\right] + \frac{A}{2}\underline{S}\left(\underline{I}_1+\underline{I}_2\right)$$

$$+3\left(\alpha_s D_e + \beta_s D_c\right)\left[S_z^2 - \tfrac{1}{3}\underline{S}(\underline{S}+1)\right] + \left(\alpha_s E_e + \beta_s E_c\right)\left[S_x^2 - S_y^2\right] \qquad (7\text{-}11)$$

Where $\underline{S} = \underline{S}_1 + \underline{S}_2$, and it is assumed from now on that $\underline{S}_1 = \underline{S}_2$ which will be the case for like ions. S is referred to as the total spin and can have values:

$$S = S_1 + S_2,\ S_1 + S_2 - 1,\ \text{----------}0$$

$\alpha_s$ and $\beta_s$ are constants which Judd[20] has calculated

$$\left.\begin{aligned} \alpha_S &= \tfrac{1}{2}\left[\frac{S(S+1) - 4S_1(S_1+1)}{(2S-1)(2S+3)}\right] \\ \beta_S &= \frac{3S(S+1) - 3 - 4S_1(S_1+1)}{(2S-1)(2S+3)} \end{aligned}\right\} \qquad (7\text{-}12)$$

In the approximation that $g\beta\underline{H} \gg J \gg A$, $\underline{S}_1 = \underline{S}_2 = \frac{1}{2}$ (which will be the approximation used in the description of the cadmium vacancy centres) and ignoring the anisotropic terms, the term in J gives states with well defined total spin values S = 0 and 1. The lowest state if J is positive (antiferromagnetic exchange) is S = 0 with an energy $\frac{-3J}{4}$ below the spin state of the isolated ion. The S = 1 state lies at an energy $\frac{J}{4}$ above that of the isolated ion. In this case, which is the one most commonly observed, the system is diamagnetic at temperature T where $KT \ll J$. The triplet e.s.r. spectrum will be observed at higher temperatures $KT \gtrsim J$. If $\underline{S}_1 = \underline{S}_2 > \frac{1}{2}$ then the lowest state is still S = 0, the next is S = 1 which is J higher in energy, then S = 2, which is 3J higher etc. The order of the levels is reversed if J is negative (ferromagnetic exchange).

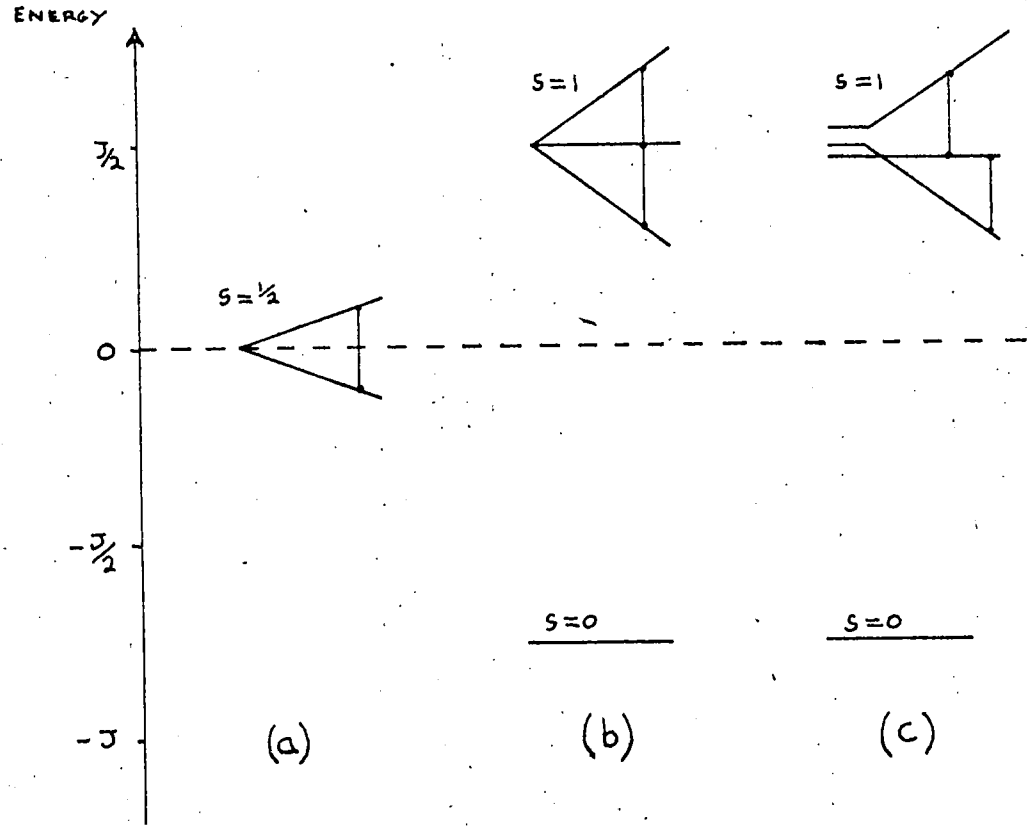


FIG.7-10. Energy level scheme for exchange coupled paramagnetic ions.

(a) Single ions ($S=\frac{1}{2}$).

(b) Pairs with isotropic exchange.

(c) Pairs with anisotropic exchange.

The effect of the small anisotropic terms in equation (7-11) is to give small zero field splittings of the (2S + 1) substates belonging to each total spin state. These splittings are calculated by considering each state of total spin separately. A typical energy level scheme for pairs of paramagnetic ions assuming isotropic and anisotropic exchange coupling is shown in Fig. (7-10) for $\underline{S}_1 = \underline{S}_2 = \frac{1}{2}$. The e.s.r. lines of a pair system with isotropic exchange will fall exactly on top of those due to the isolated ions. The effect of the anisotropic contribution is to allow the pair lines to be observed if the zero field splittings are greater than the line width of the isolated ion lines. In their work on three exchange coupled (triads) irridium ions ($Ir^{4+}$) in $(NH_4)_2$ Ir, $PtCl_6$ mixed crystals. Harris and Owen[22] concluded that it was necessary to include exchange between next neighbouring $Ir^{4+}$ ions as well as between nearest neighbours. This interaction was found to be an order of magnitude smaller than that between nearest neighbours. They found no evidence for exchange between more distant neighbours.

In the approximation that $J \gg A$ the hyperfine structure term is of the form $\frac{A}{2}\,\underline{S}.(\underline{I}_1 + \underline{I}_2)$. Thus 2(2I) + 1 hyperfine lines at half the normal spacing are expected. If they

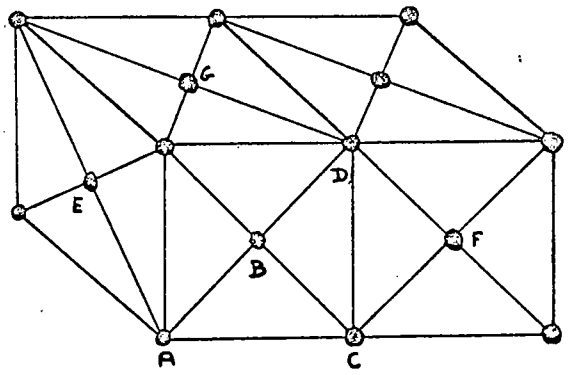


FIG.7-11. F.C.C. lattice indicating the different types of triad of $Ir^{4+}$ ions.

● $\equiv Ir^{4+}$ ion.

can be resolved the hyperfine lines serve to identify the spectrum from an exchange coupled pair of ions unambiguously.

Triad spectra

There is little reported work on the magnetic properties of three exchange coupled ions. The most thorough report has been by Harris and Owen[22] on $Ir^{4+}$ ions. Their treatment will be outlined since it will be useful in discussing the e.s.r. spectrum observed in CdS and reported in this thesis.

The $Ir^{4+}$ ions, in the mixed crystals of $(NH_4)_2Ir,PtCl_6$ which were used by Harris and Owen, form a face centred cubic structure while the other ions comprising the salt are arranged in the space between the $Ir^{4+}$ ions. The structure is indicated in Fig. (7-11). The work of Harris and Owen[22] on the pair spectra of $Ir^{4+}$ in this salt had established that there is a large exchange interaction between nearest neighbours (nn.) $Ir^{4+}$ ions characterised by an isotropic term with $J_1 \sim 5$ $cm^{-1}$ and anisotropic terms which allow the n.n. pair spectra to be observed. There is also an exchange between next nearest neighbour (n.n.n.) ions characterised by an isotropic term with $J_2 \ll J_1$ and no anisotropic terms.

To describe the spin Hamiltonian for the triads, let $\mathcal{H}_{12}$

TABLE 2 Types of triad and their Hamiltonians.

| Name | Structure | Hamiltonian |
|---|---|---|
| line triad | A B D | $\mathcal{H}_{12} + \mathcal{H}_{23}$ |
| right angle triad | A B C | $\mathcal{H}_{12} + \mathcal{H}_{23} + J_2 \underline{S}_1 \cdot \underline{S}_3$ |
| skew triad | A B G | $\mathcal{H}_{12} + \mathcal{H}_{23}$ |
| n.n.pair plus n.n.n. (135°, 90°) | A B F<br>E A C | $\mathcal{H}_{12} + J_2 \underline{S}_2 \cdot \underline{S}_3$ |
| equilateral triad | A B E | $\mathcal{H}_{12} + \mathcal{H}_{23} + \mathcal{H}_{31}$ |

be the exchange interaction between the n.n. pairs in the triad and $J_2\underline{S}_1\underline{S}_2$ be the interaction between n.n.n. pairs. The only triads of importance are those in which the spins are coupled by n.n. and for n.n.n. interactions. For the f.c.c. arrangement shown in Fig. (7-11) there are six types of triad, which are indicated in table 2. For the first four triads in table 2, the isotropic terms in the Hamiltonian can be written:-

$$\mathcal{H} = J_1(\underline{S}_1\underline{S}_2 + \underline{S}_2\underline{S}_3) + J'\underline{S}_3\cdot\underline{S}_1$$

The terms in $J_1$ correspond to the two n.n. pairs and the term in $J^1$ to the third pair in the triad. From inspection of Fig. (7-11) $J^1 = J_1$ for the equilateral triad, $J^1 = J_2$ for the right angle triad and $J^1 = 0$ for the line and skew triads. If the energies and the state functions for the triad containing two n.n. pairs are calculated[22] then a quadruplet and two doublet states are obtained where $S = \frac{3}{2}$, $\frac{1}{2}$ and $\frac{1}{2}$ respectively ($S = S_1 + S_2 + S_3$). An energy level scheme for several of the types of triad described above is shown in Fig. (7-12), taking into account isotropic and anisotropic exchange. The effect of the anisotropic terms in the Hamiltonian is to produce zero field splittings

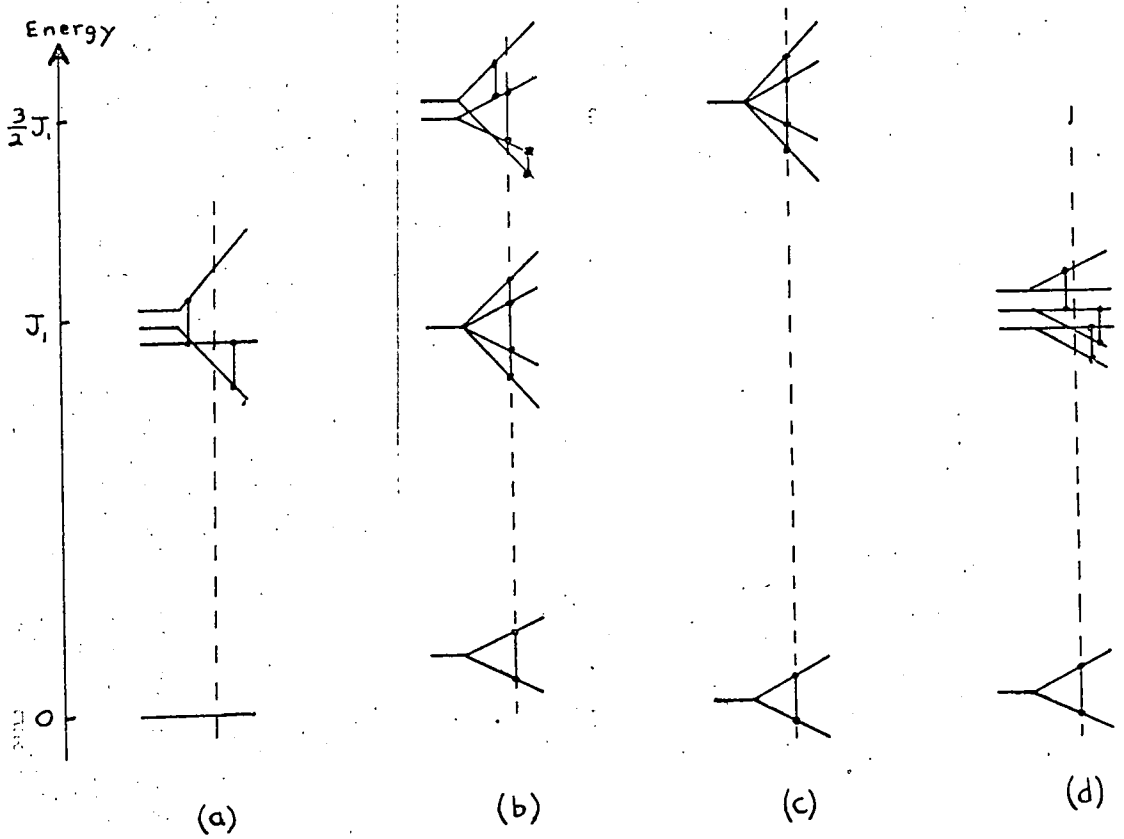


FIG. 7-12. Energy level schemes are shown for the various triads of $Ir^{4+}$ encountered here. (a) n.n. pair (b) line, right angle and skew triad (c) equilateral triad, where the two doublets coincide to form the ground state (d) triads containing one n.n. pair and one n.n.n. pair. Some possible transitions are shown. The only ones which will be observable are those not occurring at or close to the strong line from the isolated ions, which is at the position indicated by the dotted line.

of the $S = \frac{3}{2}$ states as can be seen in Fig. (7-12). The states with $S = \frac{1}{2}$ are not split and the spectra from these fall under the main line of the isolated ions and are not observed. Clearly the triad spectra is very complex, because of the different types of triad and the different zero field splittings for the different types. Harris and Owen[22] were able to identify the lines in their spectra as due to the different triads and showed that their analysis of the Hamiltonian for the triads was correct. It is interesting to note that they concluded that the interaction between n.n. pairs is the same (within experimental error) when the pairs form part of a triad as when they are isolated and they predicted this would be true for the interaction between pairs in higher order associates.

Higher Order Associates

As indicated above the same approach can be applied to a treatment of four or more exchange coupled ions. However the Hamiltonian for such a system will be more complicated than for the triad system. The situation is further complicated by the large number of combinations involved in the system of four, five etc. coupled ions. In principle the treatment should be no more difficult than that for triads but the computation will be far more

tedious. The results obtained on CdS, reported in this thesis, do not warrant the development of such a treatment in detail at present. However it can be stated that a large number of e.s.r. lines due to the quadruples etc. should be observable. It will probably not be possible to resolve all these lines individually because of interference from the lines due to the triads and pairs. In the case of impurity paramagnetic ions in a solid the number of quadruplets and higher associates will be much smaller than the number of triads and so the intensities of these lines will be relatively unimportant compared to the pair and triad spectra. However as indicated at the beginning of this section the formation of the clusters of cadmium vacancies is favoured in CdS for reasons not yet understood and so the intensity of the e.s.r. lines due to clusters may be larger than those due to paired and isolated cadmium vacancies.

7-4.4 Application of exchange coupling to cadmium vacancy clusters in CdS

The possible description of the e.s.r. line A in CdS in terms of a model of exchange coupled associations of cadmium vacancies will now be considered. However, before discussing the effects of exchange coupling, it is necessary

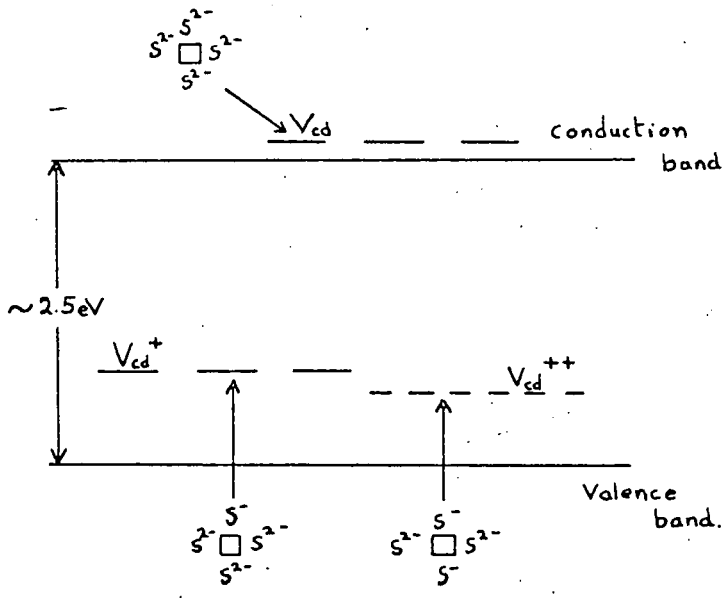


FIG.7-13. Energy level diagram for the various charge states of the cadmium vacancy site in CdS. A schematic representation of the charge distribution in each charge state is also depicted.

first of all to consider the model for the isolated cadmium vacancy. Kroger et al[24] treated the vacancy site as being deficient of two electrons so that it acts as an acceptor centre. It is assumed that the deficiency is shared between the four $sp^3$ hybridised orbitals of the surrounding sulphur ions which are directed into the vacancy. As stated in chapter 2, the concentration of donors always exceeds that of acceptors in CdS with the result that the site will be compensated by electrons from the donor levels. At first sight it might be expected that the vacancy will accept two electrons. However, Kroger et al[24] have concluded that the second energy level lies in the conduction band. The second electron therefore is always ionised and can be ignored. The vacancy, having been compensated by one electron, i.e. containing one trapped hole, can be thought of as having an energy level which lies close to that for the site which is deficient of two electrons. The situation can be represented on an energy band diagram as shown in Fig. (7-13). Consequently the $V_{Cd}^{+}$ configuration describes the state of the vacancy at $4.2^{o}K$, i.e. it is a compensated acceptor site as required by the observations on e.s.r. line A. From the evidence of the red (self activated) emission from undoped CdS which has been heat treated in

a sulphur atmosphere Kroger et al[24] conclude that the $Vcd^{+}$ levels lie about 0.7eV - 1eV above the valence band. If a hydrogenic model for the trapped hole at the cadmium vacancy site is assumed then the hole ionisation energy should be about 0.15eV, assuming the value of effective mass to be 0.81Me from the cyclotron resonance data of Sawamotto[25]. The radius of the orbit of the hole is then approximately 6Å. However the height of the level above the valence band has been estimated to be at least 0.7eV. In this situation the trapped hole is more localised at the vacancy than the predicted 6Å. Clearly it is reasonable to assume that the hole is completely localised at the vacancy site and that the hydrogen model does not apply. The localisation of the hole is one of the central assumptions of the proposed method of treating the e.s.r. spectrum of a cadmium vacancy pair as a pair of exchange coupled paramagnetic vacancy sites. If the hole is localised the value of the g-tensor for the isolated vacancy can be calculated in exactly the same way as the g-tensor was evaluated in section (7-2) for an electron localised at a sulphur vacancy. The g-shift is then given by equation (7-4) as :-

$$\Delta g = - \frac{\lambda}{\Delta E}$$

The trapped hole problem requires the sign of $\lambda$ to be negative. The magnitude of $\lambda$ is estimated to be 0.025eV from the atomic energy levels of the free sulphur ion[8]. The value of $\Delta E$ is approximated to the ionisation energy of the centre, i.e. 0.7eV.

$$\text{Thus } \Delta g \simeq 0.03$$

and an isotropic e.s.r. line with a g-value of approximately 2.03 ($S = \frac{1}{2}$) is predicted for the isolated cadmium vacancy.

Pairs of cadmium vacancies

From the discussion of exchange interactions outlined earlier, the paired system of cadmium vacancies is expected to lead to a spin system consisting of two states of total spin 0 and 1. The ordering and separation of these levels depends on the sign and magnitude of J, the isotropic part of the exchange interaction. No data is available to estimate the value of J. The sign will be assumed to be positive since this was the case for the defect pair centre in KCl[15] and the results obtained for CdS could be understood using this assumption. However the interpretation of the results is not seriously affected if J is assumed to be negative. Some degree of anisotropy in the exchange might be

expected, but this is likely to be small because Ishikawa[26] is of the opinion that exchange coupled pairs of $Mn^{2+}$ ions in CdS are well described by a completely isotropic exchange interaction. However the presence of a pair of cadmium vacancies must introduce local strain and disturb the local symmetry at the site. This would be expected to introduce an anisotropic exchange term, but it is difficult to give any quantitiative estimate of the magnitude of this term. Further strains set up in the sample during cooling following growth, especially after quenching, would prdduce similar effects. Many of our samples are known to be highly strained since they frequently crack or shatter during removal from the growth tube and the dislocation density is very high - see section (5-4). The effect of all these anisotropic terms is to produce two pair lines due to zero field splitting on the triplet state away from the isolated vacancy line. If the sample has a variable stress throughout its volume, then the strain will be different at different vacancy pairs. As a result the zero field splitting could be continuously variable throughout the vacancy pairs in the sample. This would produce an e.s.r. line centred at the position of the isolated vacancy line but somewhat broader. The line may also be broadened because there are two possible types of vacancy

pair in hexagonal CdS. In addition the next nearest neighbour interactions may be important since the ratio of the nearest neighbour pair separation to the next nearest neighbour pair separation is approximately 3:4. Thus further pair lines may result, with a corresponding increase in the complexity of the e.s.r. spectra.

The proposed mechanism for the effect of random strain variations broadening the pair lines is supported indirectly by the work of Bleaney and Bowers[21] on the e.s.r. of exchange coupled pairs of copper ions in copper acetate. The authors postulated that the main contribution to the resonance line width was thermal modulation of the exchange integral J. The lattice vibrations cause a small fluctuation in the separation of the interacting ions. Since the exchange integral is a measure of the overlap of the wave functions, it is very sensitive to such fluctuations. A modulation of the anisotropic exchange terms will contribute to the line width of the pair lines. Clearly strain modulation of the vacancy pair separation would produce a similar effect.

Triads of cadmium vacancies

A system of three nearest neighbour cadmium vacancies is obviously complex and should lead to a complex e.s.r. spectrum. There are three distinct types of triad in the cubic zinc blende lattice, each of which can be subdividied in the hexagonal modification. Referring to Fig. (7-14)

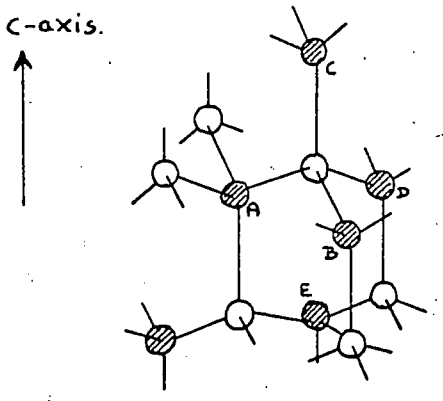


○ ≡ Sulphur ion.

◍ ≡ Cadmium ion.

FIG.7-14. Wurtzite CdS lattice illustrating the different types of cadmium vacancy triads.

the basic types of triad have structures ABC, ABE and CAE respectively. The first two are tetrahedral while the third is a skew chain system. In the hexagonal modification there are two kinds of the triads ABC and ABE. There are seven types of chain triad. When next nearest neighbour interaction is included three of these types must be subdivided twice. Consequently there are 14 different arrangements of cadmium vacancy triads. In line with the treatment of section 7-4.2 for the triads of $Ir^{4+}$ ions, the spin Hamiltonians can in principle be written down for the 14 types of triad, and solutions for the energies and eigenstates of the different triads obtained. However this is not possible since no estimation of the magnitude of the exchange integrals can be made and the importance of the anisotropic terms relative to the isotropic ones is not known. However by comparison with the discussion of the $Ir^{4+}$ ions, it is fairly obvious that an extremely complicated triad spectrum will result. The modulation of the exchange integral necessitated by the randon strains in the crystals would be expected to broaden each of the triad e.s.r. lines by varying the zero field splittings of the $S = \frac{3}{2}$ spin state, producing one broad structureless line similar to that postulated for vacancy pairs. However the triad line

should be broader than that associated with pairs because the triad of vacancies, will produce a greater lattice distortion at the site and hence a larger anisotropic interaction.

Higher order clusters

Clearly the arguments discussed in the previous section can be applied to a quadruplet, quintet, etc. of vacancies, but correspondingly computations will be more tedious and complex. A complicated set of spin energy levels will be formed for each permutation and once again a broad structureless e.s.r. line may be expected. The line width should be greater than for the triads because of the greater lattice distortion at the more complex vacancy cluster site.
It has been suggested [9, 13] that sulphur vacancies might be present at the cadmium vacancy cluster sites. These will not greatly affect the shape or nature of the expected broad line, since this is essentially due to holes localised at cadmium vacancies. The situation where the missing sulphur ion is one linking a cadmium vacancy pair is an exception. In this instance a delocalisation of the holes at the particular cadmium vacancy pair will result but the effect of this cannot be predicted until the wavefunctions of the holes can be estimated. The presence of a sulphur vacancy

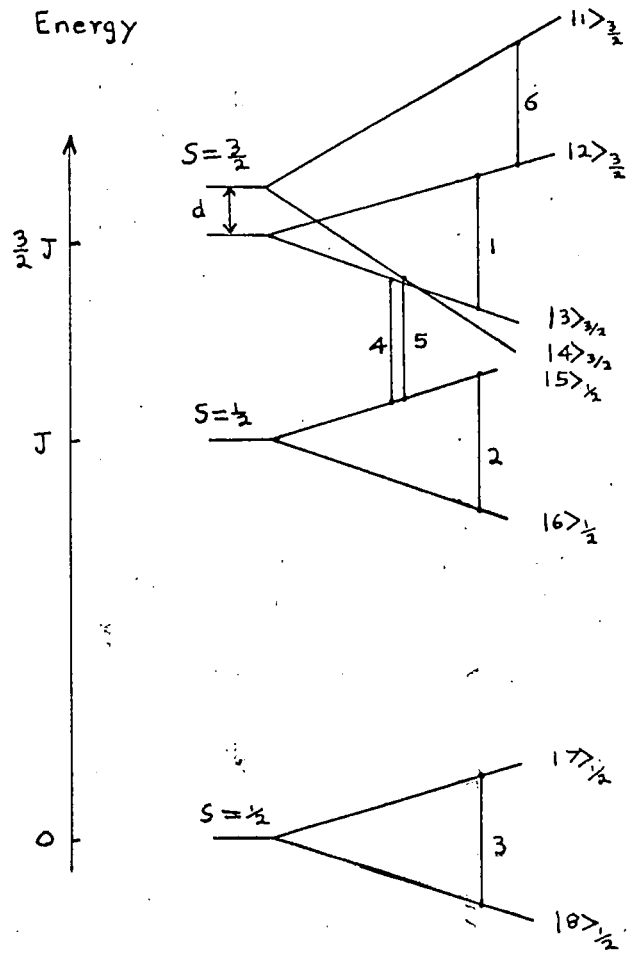


FIG.7-15. Possible energy level scheme for a vacancy triad with some of the possible transitions indicated.

close to a cadmium vacancy cluster should broaden the e.s.r. line due to the cluster alone by increasing the local strain.

7-4.5 Discussion of the e.s.r. results using this model

As indicated in the previous three sections the e.s.r. line A can be explained in terms of the resonance of clusters of exchange coupled cadmium vacancies, each of which has trapped one hole. It has been suggested in section (7-4.1) that the line A is composed of several components and this can be explained in terms of different order clusters contributing to the line.

The general shape of the line A can be understood in terms of the triad of vacancies. By comparison with Fig. (7-12) a possible energy level scheme for a vacancy triad is shown in Fig. (7-15), assuming J is positive.

There will be 14 energy level schemes of this form for the 14 different triads. Since the broadness has been ascribed to strain modulation of the zero field splitting of the levels, then since the only one with such a splitting is the $S = \frac{3}{2}$ level, this level must be populated at $4.2^{o}K$. Therefore the magnitude of the isotropic part of the exchange J must be less than $2cm^{-1}$. To a first approximation therefore let us assume $J = 1cm^{-1}$. The transitions in the $S = \frac{3}{2}$ total spin state, it has been postulated, will give a broad e.s.r. line centred

on the position of isolated vacancy line. The lower lying doublets will give a sharp line centred at this position. For a system in which the exchange is isotropic the 2S + 1 substates of each total spin state are well defined by the $S_z$ component of S so that there are no matrix elements coupling states in different total spin states and no transitions of this type can be observed. However in this triad vacancy system it has been postulated that anisotropic exchange interactions are present. The effect of these is to produce mixing of the other states into any total spin state. Thus the spin states designated $|n\rangle_{3/2}$ and $|n\rangle_{1/2}$ are in fact linear combinations of all the spin states. Consequently the matrix elements between states with different total spin will not be zero. Thus since $\frac{J}{2}$ is of the same order as $h\nu$ at x-band frequencies then transitions between the $S = \frac{3}{2}$ and $S = \frac{1}{2}$ total spin states will be allowed as indicated in Fig. (7-15). The intensities of these transitions will be smaller than those between levels in the states in which total spin is constant, because to a first order approximation they are forbidden.

Fig. (7-16) shows the possible superposition of these different transitions at x-band frequencies, assuming the line broadening is due to strain modulation of the zero field splitting for $J \sim 1 cm^{-1}$ and assuming that the zero field splitting varies

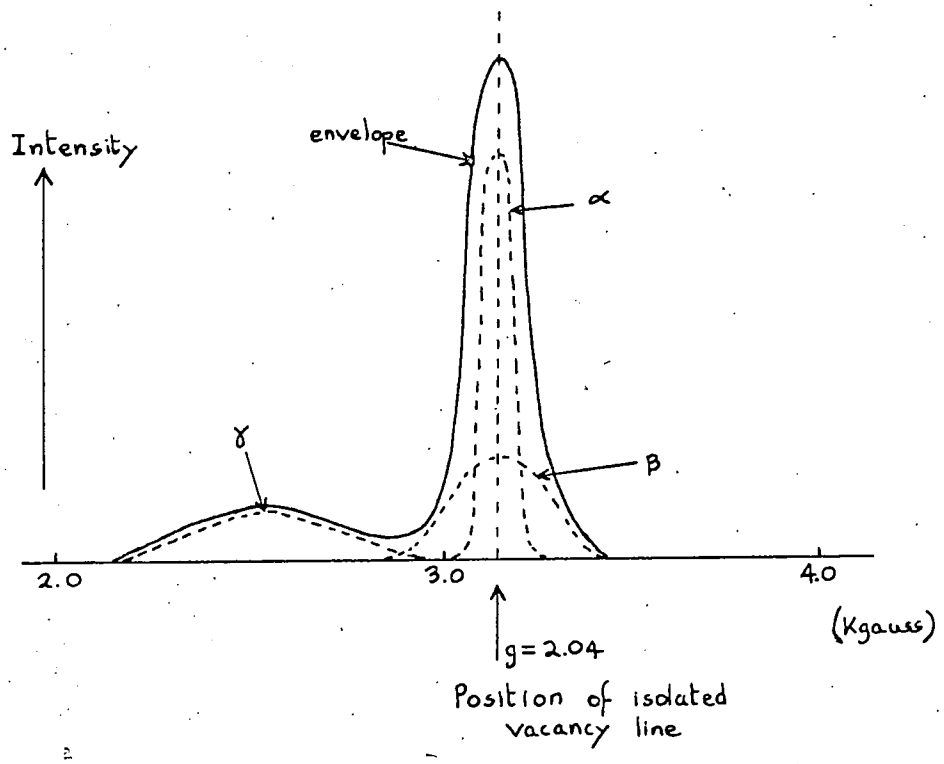


FIG.7-16. Superposition of the e.s.r. lines for the triad system of Fig.7-15. at x-band frequencies.

continuously between 0 and $0.03cm^{-1}$.

The sharp component $\alpha$, corresponds to the transitions 2 and 3 between the levels of the two lower lying doublets of Fig. (7-15). The component $\beta$ is associated with the transitions between the levels of the triplet (1 and 6) which are broadened into one line by the variation of zero field splitting of $S = \frac{3}{2}$ level (d). The component $\gamma$ corresponds to the transitions of the type 4 and 5 between levels in the total spin states $\frac{1}{2}$ and $\frac{3}{2}$, broadened by the variation of d. Clearly the envelope of these components resembles the shape of the observed line A, c.f. Figs. (7-1) to (7-4). However it is too sharply peaked near the position of the isolated vacancy line, because of the magnitude of the component $\alpha$. The contributions to $\alpha$ are from the two lower lying doublets the lower of which will be more important from population considerations. If the centre contained an even number of vacancies, the ground state would be a singlet. At this stage it is not possible to predict the total spin states of such a centre. The simplest centre will be a quadruplet of vacancies, which should have total spin states of 0, 1 and 2, of which the singlet will be lowest. Thus because of zero field splittings of the S = 1 and 2 states, transitions falling on top of the isolated vacancy are not

expected. Thus the component $\alpha$ for a quadruplet will be reduced or even absent. Because of the large increase in the number of levels and the number of ways of arranging the four vacancies the components $\beta$ and $\gamma$ should increase by approximately equal amounts. Thus the line shape associated with a quadruplet for $J \sim 1 cm^{-1}$ and d varying continuously from 0 to $0.03 cm^{-1}$ will closely resemble that observed as the e.s.r. line A. The final conclusion, therefore, is that the shape of the line A can be adequately explained in terms of a quadruplet of cadmium vacancies at nearest neighbour sites. However, there may also be contributions from triads, quintets and higher order clusters.

The model of vacancy clusters can also explain the behaviour of the samples heat treated in atmospheres of cadmium and sulphur vapours. Heating in a sulphur atmosphere will increase the concentration of cadmium vacancies and hence the intensity of the e.s.r. line. The sharpening of the line at the position of the isolated vacancy line which is observed after the sulphur treatment can be understood in terms of a relative increase in the concentration of triads and pairs, both of which are expected to produce a sharp line in this position. With the present data it is impossible to distinguish which type of centre is produced.

The isolated vacancy is ruled out because this would not be observable at 4.2°K where it is expected to be highly saturated. This is deduced from the conclusions reached by Harris and Yngvesson[27] from their measurements of spin lattice relaxation time on $Ir^{4+}$ at concentrations where triads and pairs of $Ir^{4+}$ ions were important. They found the relaxation time for the triads to be shorter than for the pairs and that for the pairs to be shorter than for the isolated ion. It was noted that the line A began to approach saturation at the maximum output of the signal klystron (25mW). Since it is believed that line A is associated with a quadruplet of cadmium vacancies and apparently has quite a long relaxation time, then the spin-lattice relaxation time of the isolated vacancy should be extremely long possibly of the order of 100's of m.secs at 4.2°K and not be observable. This is not unreasonable for a point defect centre. It is interesting to note that in CdS:Al and CdS:B specimens, an isotropic line $g \simeq 2.06 \pm 0.02$ was observed at 77°K. At this temperature this line was saturated at power levels ~ few m. watts and was not observed at 4.2°K presumably because of saturation.

The origin of this line is unknown and it is tempting to ascribe it to the isolated vacancy. However more inform-

ation is required before any identification can be made. The simplest system that can cause the narrow line which appears after heat treatment in a sulphur atmosphere is the pair of cadmium vacancies. Whatever the centre is, it must be unstable as it was noticed that the sharp line decayed in intensity after the sample was left at 300°K for a few days. The possibilities are that the pair dissociate into isolated vacancies which cannot be observed, or that they associate to form higher clusters and add to the broad line A.A similar situation occurs in silver bromide where the 'sub image', which consists of two $Ag^+$ ions at nearby kink sites, is unstable. The pair of $Ag^+$ ions migrate to form an $Ag^+_4$ complex which is the stable 'latent image' in the photographic process which occurs in silver bromide.

Following heat treatment in a cadmium atmosphere the intensity of line A is reduced and no new components can be detected. The heating is expected to reduce the concentration of cadmium vacancies. Since cadmium pairs are thought to be unstable the treatment would not be expected to increase their concentration at the expense of the higher clusters. Thus the decrease in the intensity of line A is expected on the vacancy cluster model and the non-appearance of the sharp line is not surprising.

An experiment was performed to attempt to determine whether the width of the line A was stress dependent as suggested in the discussion of the proposed model. An undoped sample was given an uniaxial stress of approximately 200 Kgm/cm$^2$ while the e.s.r. was investigated at 4.2$^o$K. The line width between the maximum slope positions was found to have increased by approximately 15%. This suggests that the random internal strains can undoubtedly contribute to the line broadening and that the applied stress is considerably less than the internal ones and so adds to these and increases the line width.

Our samples appear to be highly stressed. It has been reported that CdS single crystals fracture at stresses of approximately 1000Kgm/cm$^2$ (26), whereas our samples were found to fracture at about 300-500Kgm/cm$^2$. This lends further support to the postulate of line broadening by strain modulation of the zero field splittings of the spin states. Obviously, however, more quantitative measurements of this type on a variety of samples are required.

The conclusions derived here concerning the nature of the centres responsible for line A are in qualitative agreement with those obtained by Cowell and Woods(9) from their work

on thermally stimulated currents and I.R. emission in CdS. They concluded that the centres responsible for the 1.6/1.85 micron I.R. emission band (see section 2-3.4) lie about 0.7eV above the valence band and are identical with the photoconductivity sensitising centres. Various arguments were used to deduce that the centres were wholly or partly composed of a number of cadmium vacancies. They showed that electron trapping centres 0.63eV and 0.85eV below the conduction band were most prominent in samples heated in 15-30 atmospheres of sulphur vapour and probably consist of various forms of cadmium vacancy. Further it was demonstrated that two 0.85eV traps disappear under illumination at temperatures in excess of 350$^{o}$K to form one 0.63eV trap. Heat treatment at 380$^{o}$K in the dark converts all the 0.63eV traps in sulphur rich crystals to 0.85eV traps. Thus they concluded that the 0.63eV trap consists of at least two cadmium vacancies and can be converted in some crystals to the sensitising centres by a photochemical process. It follows, therefore, that these latter centres are a more complex association of cadmium vacancies. In addition the 0.63eV traps can be created from the 0.85eV traps which are either single cadmium vacancies or pairs of cadmium and sulphur vacancies.

Clearly the sensitising centres can be identified with the centres responsible for the broad line A, which has been ascribed here to quadruplets of cadmium vacancies. The narrow e.s.r. line observed in sulphur rich crystals can be identified with the 0.63eV trap which has been ascribed to pairs of cadmium vacancies from the two independent measurements. The gradual decay of this line at 300°K can be ascribed to the dissociation of 0.63eV traps into those at 0.85eV which Cowell and Woods observed as a rapid process when the sample was heated to 380°K in the dark. Clearly a series of experiments should be carried out to measure the thermally stimulated current, I.R. luminescence and e.s.r. spectra of the same samples to determine whether the centres observed in the three measurements are in fact identical as the present evidence suggests.

7-4.6 Conclusions

The e.s.r. measurements for the line A have been discussed in terms of two models, one an association of cadmium vacancies and donor impurity and the other an association of cadmium vacancies only. The e.s.r. data is best described by the latter model, which is also supported by independent measurements of thermally stimulated current

and I.R. luminescence spectra. However a good deal more experimental evidence is required before the explanation offered can be regarded as conclusive.

7-5 Resonance line B

The nature of the centre responsible for this resonance line is little understood at the present time. As we saw in section (7-2) there is no correlation between its occurrence in the e.s.r. spectra and the other properties of the samples measured in this laboratory. It is unlikely that the line is due to an impurity ion since there is no agreement with the published work on the e.s.r. of commonly occurring impurity ions in CdS.

The resonance line B is observed as a shoulder on the broad line A with $g_{//} = 2.00 \pm 0.01$ and $g_{\perp} = 1.99 \pm 0.01$. It always seems to appear when line D is observed, but its intensity is not related to that of line D. The samples R9 and R11 grown in a high sulphur vapour pressure ($\sim$ 20m.m.) did not show the line B but on the other hand its intensity was not reduced by heating samples in which it occurred at 700°C in 30-40 atmospheres pressure of sulphur vapour. This seems to suggest that the centre is a complex consisting of both sulphur and cadmium vacancies.

The g-value is indicative of an electron trap. Consequently the centre might be associated with one of the deep electron traps, with levels between 0.2eV and 1.0eV below the conduction band, observed by thermally stimulated current measurements. See, for example, references (29) and (30) and section 2-3.3. The line B was completely unaffected by irradiation with light of any wavelength while the sample was maintained at $4.2^{o}K$.

The e.s.r. data at present is insufficient to allow any definite conclusions concerning the nature of the centre responsible for the line to be reached. It is hoped that the thermally stimulated current measurements, which it is planned to make on these samples, will confirm whether the centre is an electron trap or not.

When the samples which showed line B were cooled from $300^{o}K$ to $4.2^{o}K$ under continuous illumination with light of photon energy greater than the band gap, a new resonance line, which we shall designate B', was observed. (The normal procedure was to cool the samples in the dark). This line B' was very close to B and was approximately the same intensity so that it also appeared as a shoulder on the broad line A. The value of $g_{//}$ for B' was exactly the same as for B and the two could not be resolved with ~~the~~

the magnetic field orientated along the crystallographic c-axis. As the magnetic field was moved off the c-axis the two lines could be resolved and with the magnetic field perpendicular to the c-axis the new line B' was approximately 2 gauss higher in field than B. The new line could only be produced when the specimens were illuminated continuously from 300°K to 77°K. If the illumination was not carried out until the samples had cooled to 77°K, the line was not produced. If the specimens in which the line B' was observed were warmed from 4.2°K to 300°K and recooled to 4.2°K in the dark, the line disappeared.

A similar behaviour has been observed by several workers, for example, references (29) and (30), in carrying out thermally stimulated current measurements. It is found that certain traps can be produced photochemically at the expense of others by irradiation of the sample with white light at or above room temperature. Also certain traps have a repulsive barrier around them and can only be filled by irradiation above a certain temperature, which lies somewhere between 77°K and 300°K. Thus line B' may be associated with such a trapping centre and it is hoped that the thermally stimulated current measurements planned will confirm this identification.

## 7-6 Resonance line C

The line C was observed in samples R9, R11, R29 and G.P.O. 17A35. The nature of the centre responsible for this line is not known. All the samples which showed this line had a high n-type conductivity $\sim 10^{-4}$ mho.cm$^{-1}$. Conductivity of samples R9 and R11 did not change on cooling from 300°K to 4.2°K, which suggests that conduction proceeds via a band of overlapping donor levels. In R29 and G.P.O. 17A35 there was an order of magnitude decrease in the conductivity on cooling to 4.2°K. But in these specimens the donor resonance line D was detected and this decrease is probably due to trapping of donor electrons, so that at 4.2°K the donor band conductivity dominates. However it is not understood why these samples should have a large concentration of donor centres, especially since R9 and R11 were grown in high sulphur vapour pressure ($\sim$ 20Torr) which is expected to suppress the concentrations of those lattice defects which behave as donors. There is no evidence to suggest the incorporation of large concentration of donors impurity ions in these samples.

The four samples also exhibit rather different edge luminescence spectra from the typical spectrum shown in

Fig. (7-5). R9 and R11 show only one exciton, which is believed to be $I_5^{(2)}$, an exciton bound to a neutral acceptor, and edge emission is of low intensity and shifted from the position of the X and Y series in Fig. (7-5). Consequently, it is thought that in these samples the acceptor level normally responsible for the edge emission is not present and a new acceptor centre has been formed. This would explain the non-appearance of the exciton $I_1$, the appearance of exciton $I_5$ and the shift in the edge emission peaks. The resonance line C might be due to the new acceptor centre. Samples R29 and G.P.O. 17A35 exhibit a slightly different luminescence spectrum. In both cases $I_1$ and a large exciton which is thought to be a superposition of $I_2$ and $I_5$ was observed. (The resolution of the optical spectrometer is insufficient to resolve the two lines separately). $I_1$ was of much lower intensity compared with the spectrum shown in Fig. (7-5). The edge emission displayed the series X. These features can be understood if there are comparable concentrations of the usual acceptor and the new one but that the edge emission proceeds dominantly via the usual acceptor levels. In this case the edge luminescence series X is to be expected since there is a large concentration of

shallow donor levels as indicated by the observation of the resonance line D and the exciton $I_2$. Unfortunately these observations give no indication of the nature of the new acceptor centre which appears in these four samples. As indicated above, the resonance line C might be associated with the new acceptor which gives rise to the exciton $I_5$ in the luminescence spectra. Since it occurs in samples R9 and R11 which were grown in a high sulphur vapour pressure, the centre responsible may be associated with interstitial sulphur atoms or with cadmium vacancies. But no model can be envisaged at the present time which explains the extremely asymmetric shape of the line, see Fig. (7-3).

In samples R29 and G.P.O. 17A35 there is evidence from the e.s.r. measurements of charge transfer between the centres responsible for line A and those associated with line C (c.f. the change transfer between the centres responsible for line A and the shallow donor levels responsible for line D discussed in section (7-4.1)). The relative intensities of the two lines was initially unaffected by irradiation with light of photon energy greater than the band gap and with light of wavelength 0.6 micron to 0.9 micron. (It was found impossible to measure the absolute intensities of the lines after each irradiation, because the change in sample resistivity

caused by the irradiation was sufficient to require re-stabilisation of the spectrometer and it was not possible to ensure that the overall spectrometer sensitivity was identical each time). However, irradiation with I.R. illumination of wavelength greater than one micron reduced the intensity of line A relative to line C. Subsequent irradiation with light of photon energy greater than the band gap or with red light of wavelength 0.6 to 0.9 microns approximately re-establish the initial intensity ratio of the two lines. So far only qualititative observations have been made but they indicate a direct charge transfer between the two centres. More detailed measurements may reveal a more complex transfer mechanism involving other centres, since at the present time the direct charge transfer cannot be understood in terms of a simple band picture involving only two acceptor levels and a set of shallow donor levels. There is no evidence to suggest that there are any other levels in the forbidden gap.

In view of this uncertainty the possibility that the broad line C is associated with donor centres responsible for the proposed donor band conductivity mechanism cannot be ruled out. The electrons in this band will be very delocalised and it would be inappropriate to consider

the resonance absorption of an electron localised at one donor site. Instead a collective absorption process with the electrons considered as one unit forming a plasma would be more relevant. Absorptions of this type are referred to as magneto-plasma resonances. Cyclotron resonance of the carriers is unlikely since the resistivity of the samples indicates that the density of carriers is too high to observe the cyclotron resonance but is possibly sufficiently high to observe the magneto-plasma resonance (see below).

Calculations predicting the characteristics of magneto-plasma resonances are complex and depend critically on the shape of the specimen considered. Consequently they have only been attempted for specimens with particular geometries and containing carriers which have a single isotropic mass. The reader is referred to the review article of Lax and Mavroides[31]. However the predicted plasma resonance frequencies are often in error by as much as an order of magnitude. The plasma frequently ($\omega_p$) in a semiconductor which is disc shaped and of a thickness which is less than the r.f. skin depth is given by [32]:-

$$\omega_p = \frac{LNe^2}{m^*(1+L\chi)} \qquad (7\text{-}13)$$

where N is the carrier density, L is a geometric depolarisation factor (analogous to demagnetisation factor in ferromagnetism) and $\chi$ is the dielectric susceptibility. Thus we see that the plasma frequency is dependent on carrier density and sample geometry. In CdS the plasma frequency becomes comparable to x-band frequencies at carrier densities of the order of $10^{12} cm^{-3}$. Despite the fact the samples exhibiting the resonance line C are of irregular shape and the effective mass of the carriers is unknown, since they are contained in a band composed of overlapping donor levels, a measurement of the carrier density at $4.2^{o}K$ would be a useful guide to the validity or otherwise of this interpretation of the resonance absorption line C.

The magneto-plasma resonances observed in Ge and Si[32] and InSb[33] are broad, typically of the order of 1 to 2 kgauss half width and are asymmetric peaks. Clearly then this type of magneto-plasma resonance might be expected to give a broad asymmetric absorption peak of the form exhibited by the resonance line. There are, however, several objections to this interpretation. The four samples showing the line C. R9, R11, R29 and G.P.O.17A35 are of different shapes and it is unlikely that they have

identical values of carrier density and yet the resonance line C is of the same shape and occurs at the same value of magnetic field in each sample. The apparent charge transfer between the centres responsible for line A and the proposed band of donor levels giving rise to the absorption peak C is difficult to understand since this would be expected to change the shape and position of line C, unless the charge transferred is negligible to carrier density in the donor band. Clearly more quantitative measurements concerning the exact shape and position and the changes in the spectrum on irradiation with light are required before any definite conclusions can be reached.

Thus it can be seen that from the presently available e.s.r. data no definite model for the nature of the absorption process responsible for the resonance line C can be given. However it is hoped that the tentative suggestions given above will provide the basis for future investigations.

## REFERENCES

(1) J. J. Hopfield and D. G. Thomas - Phys. Rev. 122, 35, 1961.

(2) Clark and Woods - to be published.

(3) H. H. Woodbury and R. Hall - Phys. Rev. Letts. 17, 1093, 1966.

(4) K. A. Müller and J. Schneider - Phys. Letts. 4, 288, 1963.

(5) K. Morigaki - J. Phys. Soc. Japan 19, 1253, 1964.

(6) P. H. Kasai and Y. Otomo - J. Chem. Phys. 37, 1263, 1962.

(7) R. M. Eisberg - 'Fundamentals of Modern Physics' Wiley, New York and London, 1964.

(8) "Atomic Energy Levels" - edited by C. E. Moore, National Bureau of Standards Circular No. 467, 1949.

(9) T. A. T. Cowell and J. Woods - to be published.

(10) H. H. Woodbury - Phys. Rev. A134, 492, 1964.

(11) W. C. Holton, M. DeWitt and J. L. Estle - to be published.

(12) R. S. Title, G. Mandel and F. F. Morehead - Phys. Rev. A136, 300, 1964.

(13) K. W. Boer and C. A. Kennedy - Phys. Stat. Sol. 19, 203, 1967.

(14) W. D. Compton and H. Rabin - Solid State Physics 16, 121, 1964.

(15) H. Seidel - Phys. Letts. 7, 27, 1961.

(16) D. C. Krupka and R. H. Silsbee - Phys. Rev. 152, 816, 1966.

(17) J. J. Markham - Solid State Physics, Supplement 8, 1966.

(18) P. A. M. Dirac - Proc. Phys. Soc. A219. 714, 1929.

(19) J. F. Ollom and J. H. Van Vleck - Physica 17, 205, 1961.

(20) J. Owen - J.A.P. Supplement to Volume 32, 213S 1961.

(21) B. Bleaney and K. D. Bowers - Proc. Roy. Soc. A214, 451, 1952.

(22) E. A. Harris and J. Owen - Proc. Roy. Soc. A289, 122, 1966.

(23) C. P. Slichter - Phys. Rev. 99, 479, 1955.

(24) F. A. Kroger, H. J. Vink and J. Van Den Boomgard - Z. Phys. Chem. 203, 1, 1954.

(25) K. Sawamotto - J. Phys. Soc. Japan 19, 318, 1964.

(26) Y. Ishikawa - J. Phys. Soc. Japan 21, 1473, 1966.

(27) E. A. Harris and K. S. Yngvesson - Phys. Letts. 21, 252, 1966.

(28) B. A. Kulp and K. A. Gale - Phys. Rev. 156, 877, 1967.

(29) J. Woods and K. H. Nicholas - B.J.A.P. 15, 1361, 1964.

(30) J. Woods - Admiralty Contract CP11339/63. Research on cadmium sulphide Rul5-2 Annual Report 1965-66.

(31) B. Lax and J. G. Mavroides - Solid State Physics 11, 261, 1960.

(32) G. Dresselhaus, A. F. Kip and C. Kittel - Phys. Rev. 98, 368, 1955.

(33) G. Dresselhaus, A. F. Kip and C. Kittel - Phys. Rev. 100, 618, 1955.

# CHAPTER 8

# CONCLUSIONS

## 8-1 Summary

It has been clearly demonstrated that electron spin resonance techniques provide a useful tool for studying the defect centres in cadmium sulphide.At the present time the technique has not provided evidence to enable definite models for the defect complexes to be determined unambiguously but several working models for further investigation have been proposed.It is suggested that the criterion for adopting a particular model for a defect centre is it's ability to describe all the experimentally observed data e.g. electron spin resonance spectra, thermally stimulated currents, luminescence spectra etc. more adequately than any other. Consequently attempts have been made to correlate the electron spin resonance results as far as possible with other properties of the samples measured in this laboratory.The work reported in this thesis has been concentrated on undoped single crystal boules of cadmium sulphide grown here.Electron spin resonance spectra have been obtained which cannot be explained in terms of isolated impurity ions in the lattice.The fact that the spectra cannot be related to the impurity content and are unaffected by doping with various donor ions suggests that the resonance

lines are associated with intrinsic lattice defects.The centres responsible for the resonance lines have been shown to be responsible for many of the electrical and optical properties of the samples since the occurrence of the resonance lines can be related to the resistivity and luminescence spectra.The electron spin resonance spectra suggest that there are four paramagnetic defect centres present in the CdS samples investigated.Only one of these centres occurs in every sample.It is proposed that this is a class 2 acceptor centre which is responsible for the photoconductive sensitisation and is also an I.R. recombination centre in CdS.The shape and g-value of the resonance line associated with this centre have been adequately described in terms of a centre consisting of a quadruplet of exchange coupled cadmium vacancies. It is suggested that heat treatment in sulphur vapour favours the formation of pairs of associated cadmium vacancies but these rapidly either dissociate into cadmium vacancies or associate to form more class 2 centres. One of the paramagnetic centres has been shown to be a shallow donor centre giving rise to a level $\sim$0.05eV below the conduction band.The nature of the donor site

cannot be determined from the resonance spectrum.However it is probably a sulphur vacancy.The nature of the centres responsible for the other resonance lines observed is not understood.It is proposed that one of the lines be ascribed to a deep lying trap with an energy level somewhere between 0.1eV and 1.0eV below the conduction band. Two resonance processes have been tentatively proposed to explain the final resonance line.It is suggested that either (a) the electron spin resonance of an acceptor centre which is only found in CdS grown in a high sulphur vapour pressure or (b) the magneto-plasma resonance attributed to electrons free to move in a band of overlapping donor levels is responsible for the line.Work has been reported on the electron spin resonance of the group 3 ions B.,Al.,Ga.,In. and Tl. in CdS.It is concluded that all the ions behave as donor centres giving rise to levels below the conduction band the depth of which follows the series Ga. $<$ In. $<$ Tl. $\sim$ Al. $\lesssim$ B.Where Ga gives a level 0.03eV below the conduction band and B. one approximately 0.1eV below the conduction band.As the donor depth increases the bound electron is in a less de-localised orbit from that for the Ga. ion.This is evident in the shift of g-values from 1.8 for the Ga. ion

towards 2.002 for the other ions.Also the spin-lattice relaxation time increases as the donor depth increases. Both these observations indicate that the trapped electron acquires more s-character as the depth of the donor level increases.It is suggested that a continuation of the work on larger single crystals will eventually lead to a complete understanding of the method of incorporation of the group 3 donor impurity ions in CdS.

8-2 Suggestions for future work

Clearly a good deal of information will be obtained by repeating many of the measurements described in this thesis ina more qualitative and detailed manner in the light of the proposed models for the defect centres.These measurements should also be extended to a larger range of samples as they are grown in this laboratory.In addition several experiments can be carried out to test the proposed models :-

1) Measurements of the Hall effect, thermally stimulated current spectra and the I.R. luminescence spectra of the samples investigated in the work described in this thesis. This should provide information to ascertain whether the identification of the centres responsible for line A as class 2 acceptor centres is correct and whether it is

correct to attribute the line B to deep electron traps.It may also provide information about the centres responsible for lines C and D.

2) A more careful study of the effects of heat treatment on the e.s.r. spectra and on the measurements outlined in 1) above should lead to a better understanding of the atomic composition of the defect centres.

3) A complete investigation of doped single crystals of CdS should enable one to determine whether impurities are important in the composition of the defect centres and if the concentration of the defects is controlled by the impurity content.

4) An increase in sensitivity of the microwave spectrometer would enable the measurements outlined above to be made more accurately.The simplest way of increasing the sensitivity would be to use better quality microwave klystrons and both I.F. and A.F. amplifiers.The possibility of using phase sensitive detection at the I.F. frequency instead of simple diode detection could also be investigated.

5) A study of the changes in the e.s.r. spectrum using monochromatic light would probably lead to a determination of the position of the energy levels of the paramagnetic centres in the forbidden gap.

6) The large width of line A has been attributed to

continuously variable stresses across the samples.A detailed study of the width and shape of line A under applied stress may verify this suggestion.As indicated in chapter 7, preliminary experiments suggest that this is the case.

Clearly the results of research on these lines will suggest further experiments, and it is hoped that eventually an unambiguous determination of the nature of the defect centres responsible for determining the properties of CdS will emerge.If this is achieved the electron spin resonance technique can be used to monitor the concentrations and types of defect centres present in CdS samples. This approach should prove very useful in evaluating different growth methods and in interpreting other properties of the material.